Two-Stage Filtration to Control Manganse and DBPS at the Lantern Hill Water Treatment Plant

TWO-STAGE FILTRATION TO CONTROL MANGANESE AND DBPS AT THE LANTERN HILL WATER TREATMENT PLANT

A Master's Project Presented

By

MINH PHAM

Submitted to the Department of Civil and Environmental Engineering of the University of Massachusetts in partial fulfillment of the requirements for the degree of

MASTER OF SCIENCE IN CIVIL ENGINEERING

September 2010

Department of Civil and Environmental Engineering

TWO-STAGE FILTRATION TO CONTROL MANGANESE AND DBPS AT THE LANTERN HILL WATER TREATMENT PLANT

A MS Report Presented

By

MINH PHAM

Approved as to style and content by:

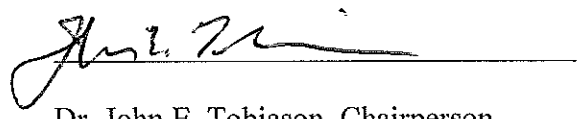

Dr. John E. Tobiason, Chairperson

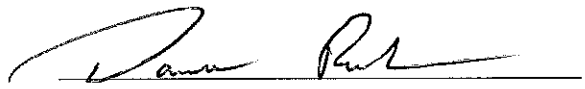

Dr. David Reckhow, Member

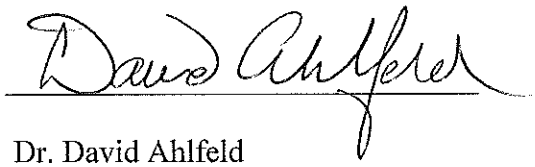

Dr. David Ahlfeld

Graduate Program Director

MS Civil Engineering Program

ACKNOWLEDGMENTS

The author wishes to express his gratitude to all who helped him to adjust to a new environment and make this project possible. The patience, expertise, and support from my advisor Dr. John Tobiason were indispensable. Additionally, I would thank Dr. David Reckhow for sitting in my committee as well as other professors here at the University of Massachusetts Amherst, who have taught me so much about this field.

I am also grateful to the Aquarion Water Company for funding this work. In particular, I would like to express my gratitude to Gary Kaminski for all of his assistance during numerous field trips to the Lantern Hill Water Treatment Plant.

I would like to extend appreciation to fellow students who always found the time to lend a helping hand or share their knowledge and suggestions. A special thanks to Anjuman Islam for helping me so much throughout this project, and to Yesher Larsen and Tom Orszulak for assisting me on multi-day field trips.

Last but not least, I would like to thank all of my friends and family here in US as well as in Vietnam, for their support, patience and love.

ABSTRACT

This research involved full- and pilot-scale studies of treatment of the Aquarion Water Company (AWC) Lantern Hill groundwater source. With elevated levels of both dissolved manganese (~0.19 mg/L), dissolved iron (~1.9 mg/L) and natural organic matter (NOM) (~3 mg/L) the existing treatment plant is having difficulty in achieving required manganese removal while maintaining low concentrations of disinfection by-products (DBPs) in finished water. At full-scale, dissolved manganese in the raw water is removed through pre-filter oxidation and adsorption on iron precipitates via application of free chlorine and permanganate as well as adsorption of dissolved manganese onto $MnO_x(s)$ coated filter media (anthracite and greensand) which is continuously reactivated by free-chlorine oxidation. The addition of pre-filter chlorine to the raw water with high concentration of NOM leads to the formation of elevated levels of regulated DBPs such as trihalomethanes (THMs) and haloacetic acids (HAAs).

To investigate the effect of achieving NOM removal prior to chlorine addition on decreasing DBP formation, a two stage pilot-scale filter system was installed at Lantern Hill. A first-stage filter column (7.5 in diameter) with conventional dual media (anthracite over sand) for NOM and oxidized iron removal is followed by a second stage high-rate coarse media filter for Mn removal. Prior to the first stage filter, permanganate is dosed in the range of 0.5 to 1.25 times the stoichiometric requirement to oxidize most of the reduced iron and a portion of the dissolved manganese to insoluble forms; pH was controlled at 7 to 7.5 by NaOH addition. In addition, synthetic cationic polymer was also applied ahead of the dual media filter to improve particle and NOM removal. Free

chlorine is dosed to the first stage filter effluent prior to the second stage contactor which is operated at a hydraulic loading rate (HLR) of 10 to 20 gpm/ft^2.

The results show a dramatic decrease in DBP formation and excellent removal of Mn, Fe and NOM. After the first stage filtration, NOM levels decreased from 3 mg/L to 2 mg/L prior to any chlorine addition, dissolved manganese was between 0.03 to 0.2 mg/L while very low concentrations of reduced iron (<0.01 mg/L) were recorded. Post-filter chlorine addition and the second-stage contactor routinely decreased dissolved Mn to levels of 0.01 to 0.02 mg/L except at high HLR and shallower bed depths when very low pre-filter $KMnO_4$ dosing caused filter effluent manganese levels to rise to 0.15 to 0.2 mg/L. Resulting DBP analyses showed that contactor effluent levels were only 20 to 30% of full-scale levels in the presence of a similar 1 mg/L free chlorine residual and well below regulatory requirements.

An existing model which simulates manganese removal as a function of bed depth was modified and utilized in simulating the experimental data for the second-stage contactor at the LHWTP. The results show that the modified model can capture well the manganese concentration along the second-stage contactor. The model was later used to simulate manganese removal for different designs of the post-contactor to help the Aquarion Water Company to determine the best design for a Lantern Hill Water Treatment Plant upgrade.

TABLE OF CONTENTS

ABBREVIATIONS

AWC: Aquarion Water Company.

BOD: Biochemical Oxygen Demand

DAF: Dissolved Air Flotation

D/DBPR: Disinfectants and Disinfection Byproducts Rule

DM: Dual Media

EPA: Environmental Protection Agency.

GAC: Granular Activated Carbon

GPM: Gallons per Minute.

HAA: Haloacetic Acid

HLR: Hydraulic Loading Rate

ICR Information Collection Rule

LHWTP: Lantern Hill Water Treatment Plant

NGE: Natural Greensand Effect

OCM: Oxide-Coated Media

PPT: Part Per Trillion

QC: Quality Control

RAA: Running Annual Average

THM: Trihalomethanes

TOC: Total Organic Carbon

WHO: World Health Organization

LIST OF TABLES

LIST OF FIGURES

CHAPTER 1: INTRODUCTION

1.1 Problem Statement

Manganese is a naturally occurring metal and an essential nutrient. In drinking water treatment, elevated manganese concentrations typically cause aesthetic problems rather than human health concerns. In order to prevent manganese aesthetic problems, USEPA set a manganese secondary maximum contaminant level (SMCL) of 0.05 mg/L. However, even below this level, some chronic problems may still occur and it is recommended for water utilities to set their manganese treatment goal at 0.01 to 0.02 mg/L.

To achieve a manganese concentration of 0.01 to 0.02 mg/L in drinking water, many water utilities have used the process of adsorbing dissolved manganese to oxide coated media with continuous reactivation through free-chlorine oxidation. Although this method has been very effective and reliable in dealing with manganese, it also brings a new concern to water systems. A higher concentration of disinfection by products (DBPs), produced through reaction between free chlorine and natural organic matter (NOM), may occur for water treatment plants utilizing the adsorption technique to remove manganese.

According to ongoing research, exposure to trihalomethanes (THMs) and haloacetic acids (HAAs), the two most prevalent of disinfection by products, is suggested to be a potential reproductive and developmental health hazard (Federal Register, 2006). To minimize the health impact of DBPs, in December 1998 the US Environmental Protection Agency (USEPA) promulgated the Stage 1 D/DBPs rule which established

maximum residual disinfectant levels (MDRLs) and maximum contaminant levels (MCLs) of 80 µg/L and 60 µg/L for THMs and five HAA compounds (HAA5), respectively, based on a running annual average (RAA) of quarterly distribution system samples. With the concerns that customers may still be exposed to elevated DBPs even when their system (WTP) is in compliance with the Stage 1 D/DBP rules, in January 2006 the USEPA decided to tighten the control of DBPs by promulgating the Stage 2 D/DBPs rule which will become effective in April 2012 (Federal Register,2006).

The Lantern Hill Water Treatment Plant (LHWTP), belonging to the Aquarion Water Company (AWC) of Connecticut, is the main focus of this research. With an unusually high concentration of NOM for a ground water source (~3 mg/L), LHWTP is among water systems having difficulties to meet the Stage 2 D/DBP rule and maintain a low concentration of manganese in finished water. Along with the Deans Mill Water Treatment Plant, the LHWTP supplies water for the Mystic system which is currently under control of the Aquarion Water Company of Connecticut, an Aquarion subsidiary. Utilizing chemical oxidation and media adsorption to remove manganese, high concentrations of DBPs above 80 µg/L and 60 µg/L for THMs and HAAs, respectively, are often found in LHWTP finished water. To ensure compliance with the Stage 1 D/DBP rule, the LHWTP has been taken out of service periodically to lower the RAA concentration of DBPs in the distribution system. A compressive solution which will ensure adequate removal of manganese while keeping DBP production under control was investigated in this study.

1.2 Objective

The main objectives of this research are to (1) optimize chemical doses at the LHWTP, (2) evaluate the effect of removing NOM prior to chlorine addition on DBP production along with a second-stage contactor for Mn removal, (3) investigate and apply an existing model to simulate Mn removal across a media contactor (4) to determine appropriate values of HLR and bed depth for post contactor design.

1.3 Scope of the work

This research involved field- and pilot-scale studies of treatment of the Lantern Hill groundwater source. Pilot studies included operation of a two–stage filter system which was constructed on-site. By monitoring manganese removal and DBP production, the benefit of reversing chemical addition order of permanganate and chlorine and using the second-stage contactor was evaluated and compared with existing treatment conditions at full-scale. Measurements of manganese, iron, turbidity, ultraviolet absorbance at 254nm wavelength (UV254) were conducted on site while DBP and TOC concentrations were measured at the UMass laboratory. Further development of a model for manganese removal by the second-stage contactor was also undertaken.

CHAPTER 2: BACKGROUND AND LITERATURE REVIEW

This chapter provides fundamental information about manganese and DBPs in drinking water as well as a review of previous research conducted on manganese and DBP associated problems. A significant portion of this chapter is used to discuss manganese removal by adsorption onto oxide-coated media (OCM) and associated DBP concerns which is the main focus of this research

2.1 MANGANESE:

2.1.1 Source:

Manganese is the twelfth most abundant element and the fifth most abundant metal on the earth, making up 0.1% of the earth's crust (US EPA 2004). It is found mainly as oxide carbonates and silicates in over 100 minerals with pyrolucite as the most naturally-occurring form. Although manganese often occurs into surface water and groundwater due to the erosion of rocks and soils, according to the Agency for Toxic Substances and Disease Registry (ATSDR 2008), human activities are also responsible for much of the manganese contamination in water in industrial areas. This report indicates a median manganese level of 16 µg/L in surface water; with 99^{th} percentile concentrations of 400 to 800 µg/L. Higher levels in aerobic waters are usually associated with industrial pollution.

While the manganese levels in groundwater are rather stable during the year, surface water treatment facilities often experience elevated concentrations of manganese

during and after lake turnover happening at the end of the summer. During those events, the anoxic hypolimnion layer, rich in dissolved manganese, is mixed with the aerobic epilimion layer, increasing the ambient manganese in the treatment plant raw water.

According to a USEPA (2004) report, food is the main source for manganese exposure in humans. Manganese can be found in variety of foods such as many nuts, grains, fruits, legumes, tea, leafy vegetables, infant formulas and some meat and fish. An adult can consume between 0.7 and 10.9 mg/day in the diet, with even higher intakes often relating to vegetarian diet or the consumption of large amount of tea. Manganese compounds are also found in air with varying concentrations depending on proximity of point-sources such as ferroalloy production activities, coke ovens and power plants. Average ambient levels near industrial sources are usually in the range from 220 ng/m^3 to 330 ng/m^3, while levels in urban and rural areas without point sources range from 10 to 70 ng/m^3. In the US, EPA estimated an average manganese concentration of 40 ng/m^3 based on measurements in over 102 cities.

2.1.2 Health and Aesthetic Concerns:

It should be noted that at an appropriate level, manganese is an essential nutrient for human and animal health. Several enzyme systems have been reported to interact or depend on manganese for catalytic or regulatory functions. Manganese also plays a critical role in bone mineralization, protein and energy metabolism, metabolic regulation, and so on (ATSDR2008). Table 2-1 shows adequate manganese intake amounts which have been determined by the Food and Nutrition Board of the Institute of Medicine. Although manganese is an essential nutrient, exposure to high manganese levels for an extended period via inhalation or digestion may cause some adverse health effects known

as manganism with symptoms that include tremors, difficulty walking, and facial muscle spasms.

Table 2-1. Adequate manganese intake for men, women and children (Source: ASTDR 2008)

Life stage	Age	Males (mg/day)	Females (mg/day)
Infants	0–6 Months	0.003	0.003
Infants	7–12 Months	0.6	0.6
Children	1–3 Years	1.2	1.2
Children	4–8 Years	1.5	1.5
Children	9–13 Years	1.9	1.6
Adolescents	14–18 Years	2.2	1.6
Adults	19 Years and older	2.3	1.8
Pregnancy	All ages	—	2.0
Lactation	All ages	—	2.6

In the US, manganese concerns in drinking water always relate to aesthetics rather than human health. Soluble manganese in water distribution systems can be oxidized by oxygen or disinfectants such as free chlorine, or chloramines into a brown-black residue which can cause water discoloration, clothes, fixture staining, turbid water, and metallic taste at very high levels. Even at a low concentration of 0.02 mg/L, manganese oxide deposits can develop in pipeline systems, causing a restriction of water flow, and increasing head loss (Sly et al. 1990). Furthermore, when disinfectant levels are not enough to kill manganese-utilizing bacteria, colonies of these organisms can be found on pipeline or toilet tank surfaces, thus clogging pipe systems or creating anesthetic problems. These problems may be controlled by increasing the disinfectant doses and by improved manganese removal at water treatment facilities.

2.1.3 Regulations:

To prevent potential adverse effects on human health, the World Health Organization (WHO) has issued a provisional guideline for manganese of 0.5 mg/L. This guideline is provisional due to the lack of concrete evidences of health effects. As discussed above, manganese in drinking water below the health-based guideline value still can cause taste, odor and other aesthetic problems (U.S. EPA 2004).

Currently there is no USEPA health-based maximum contaminant level (MCL) for manganese; however, USEPA has set a secondary maximum contaminant (SMCL) of 0.05 mg/L for manganese but does not require water facilities to monitor manganese in finished water. The 0.05 mg/L manganese level is solely aimed to protect customers from experiencing manganese-related anesthetic problems. The Food and Drug Administration (FDA) also recommends a limit of 0.05 mg/L in bottled water (U.S. EPA 2004). According to Sly et al. (1990), even at this level, manganese deposition still occurs and can cause anesthetic problems (see Section 2.1.2). For this reason, a manganese treatment goal of 0.01 mg/L is recommended by the author. After conducting a survey of nearly 250 water utilities to assess manganese removal effectiveness, Kohl & Medlar (2006) recommended that water utilities should reduce manganese in their finished water to levels of no more than 0.02 mg/L.

2.1.4 Aquatic Chemistry of Manganese:

As a transitional metal, manganese can exist in eleven oxidation states. In natural water, eight of those oxidation states are found (see Table 2-2). The most important oxidation states of manganese in drinking water treatment are 2+, 4+ and 7+. While manganese with oxidation states of 2+ and 7+ is relatively soluble in water, manganese

with an oxidation state of 4+ is insoluble in water. Manganese at the highest oxidized state, Mn^{7+}, is a very strong oxidant and often used in water treatment in form of permanganate (MnO_4^-). Morgan and Stumm (1964) also reported that manganese can exist in a mixed oxidation state, MnO_x, where x can range from 1.3 to 2.

Table 2-2. Oxidation states of Manganese (Source: Tobiason et al. (2009))

Oxidation State	Mn Compound
0	Mn
2+	Mn^{2+}
2.67+	Mn_3O_4
3+	$Mn_2O_3(s)$
4+	$MnO_2(s)$
5+	$MnO_4^{3-}(s)$
6+	$Mn_2O_4^{2-}(s)$
7+	MnO_4^-

In aquatic systems, the oxidation state of manganese depends highly on the presence of oxygen. For example, manganese species in the upper layer of a lake are often in insoluble form with the oxidation state of 4+ while in groundwater or in the bottom layer of a lake, where aerobic/anoxic conditions exist, soluble forms of manganese often dominate the system. It is understood that aerobic/anoxic conditions favor the existence of manganese-reducing bacteria which utilize manganese as an electron acceptor and reduce oxidized particulate forms to soluble forms, Mn^{2+}. In contrast, manganese-oxidizing bacteria often found in the upper layer of water bodies convert Mn^{2+} to MnO_2 or other insoluble forms (Gabelich et al. 2006).

2.1.5 Mn Control Methods in Drinking Water Treatment

Oxidation of manganese to particulate form and adsorption of manganese onto OCM are the two common approaches to control manganese in drinking water treatment. Depending on specific water quality, one approach may be more effective than the other. For surface waters with high fraction of oxidized manganese, a conventional treatment system may be adequate to control manganese; however, this is not be the case for groundwater treatment with elevated dissolved manganese in water source. For that reason, clearly understanding the advantages and disadvantages of each approach is always required before designing/upgrading treatment processes to control manganese.

In addition, it is also essential to understand the form of manganese in a treatment process as follows:

- Particulate manganese: is manganese that is retained by a 0.2 µm pore size membrane filter.
- Colloidal manganese: is a smaller oxidized form of manganese which can pass through a 0.2 µm pore size membrane filter and be retained by a 30K ultra filter.
- Dissolved manganese: is manganese that can pass through a 30K ultra filter, typically reduced Mn^{2+}, and also MnO_4^-.

2.1.5.1 Manganese Oxidation followed by Particle Removal:

In this approach, a strong chemical oxidant is first added to oxidize dissolved manganese (Mn^{2+}) into an insoluble form ($MnO_{2(s)}$) which can be removed via common solid-liquid separation methods such as flocculation/coagulation, clarification and

filtration. A number of factors can affect required oxidant doses in this method. These factors include total oxidant demand in the water, temperature, pH, alkalinity, and the presence of competitive reduced species (iron, sulfide, nitrate, ammonia, and NOM). It is recommended that water treatment systems should be designed to have adequate detention time for oxidation reactions to be completed (Kohl and Medlar 2006). Also, choosing a suitable oxidant for specific raw water quality is crucial for the success of this process. Table 2-3 presents the theoretical reaction stoichiometry for soluble manganese with common oxidants. The pros and cons for common oxidants which can be used to oxidize manganese are discussed below.

Chlorine has been used as an oxidant and disinfectant for years and can only be used to oxidized dissolved manganese for pH greater than 8.0. The oxidation reaction is much slower than the reaction between chlorine and iron. Knocke (1990) reported that a higher dose than the stoichiometric dose of 1.3 mg Cl_2/mg Mn was required to completely oxidize soluble manganese. Even at four times greater than the stoichiometric dose, a minimum of a 3-hour contact time was needed to oxidize the soluble manganese from 1.0 mg/L to 0.7 mg/L at pH of 7.0. The contact time decreased to one hour only when the pH was increased to 9.0 and the manganese concentration was below the SMCL of 0.05 mg/L. Ambient temperature is also a significant factor in this reaction. When temperature decreased from 25^{o}C to 14^{o}C, manganese oxidation was not possible even if the reaction time was increased by a factor of three or four. Due to these disadvantages, typically, free chlorine cannot be used as a sole chemical to oxidize soluble manganese but rather has been used to oxidize Mn^{2+} absorbed on OCM, also referred to as reactivation.

Table 2-3. Theoretical reaction stoichiometry for soluble manganese (Mn^{2+}) (Sommerfeld 1999)

Oxidant	Oxidation reaction	Stoichiometric ratio (mg oxidant:mg Mn)
O_2 (aq)	$Mn^{2+} + 1/2O_2 + H_2O \rightarrow MnO_{2(s)} + 2H^+$	0.29:1
HOCl	$Mn^{2+} + HOCl + H_2O \rightarrow MnO_{2(s)} + Cl^- + 3H^+$	1.30:1
MnO_4	$Mn^{2+} + HOCl + H_2O \rightarrow MnO_{2(s)} + Cl^- + 3H^+$	1.92:1
O_3	$Mn^{2+} + O_3 + H_2O \rightarrow MnO_{2(s)} + O_2 + 2H^+$	0.88:1
ClO_2	$Mn^{2+} + 2ClO_2 + 2 H_2O \rightarrow MnO_{2(s)} + 2ClO_{2-} + 4H^+$	2.45:1

Chlorine dioxide is usually used in drinking water treatment to control taste and odor problems associated with algae and decaying vegetation. Compared to free chlorine, chlorine dioxide is a much stronger oxidant, leading to rapid reaction with soluble manganese. It is reported to require only 60 seconds for chlorine dioxide to produce effective manganese (2+) oxidation under 4^oC, pH 7.0 conditions (Knocke 1990). An increase in reaction rate was noticed with an increase in pH and temperature, and a decrease in NOM concentration. Although being an effective oxidant, the application of chlorine dioxide in treating water with high manganese concentrations has been limited due to its production of chlorite (ClO_2^-), for which US EPA set as MCL of 1.0 mg/L under the Stage 1 Disinfectant/Disinfection By-Products Rule (D/DBPR).

With its excellence in disinfection and high oxidation capacity, ozone (O_3) has been widely used to remove taste and odor forming compounds, to enhance NOM removal by coupling with bio-filters, and replace chlorine as a disinfectant to decrease DBP production. Ozone is also very effective in oxidizing Mn^{2+}; however, Knocke

(1990) showed that the presence of humic materials significantly inhibited the oxidation of Mn^{2+} by ozone. Since reduced manganese is not well complexed by dissolved organic compounds, this inhabitation can be overcome by adjusting the ozone dose to account for the competitive oxidant demand of the water (Knocke 1990). In addition, Long et al. (1999) indicated that when the total manganese concentration in water exceeded 0.1 mg/L, and excessive ozone doses were used, permanganate would form at concentrations high enough to cause water quality concerns such as "pink water" (the natural color of permanganate) and increasing the turbidity in finished water when the MnO_4^- is reduced to a particulate form ($MnO_{2(s)}$).

With various applications such as taste and odor control, iron and manganese removal, and as a bactericide and algaecide, potassium permanganate is an important chemical used in drinking water treatment (Kohl & Medlar 2006). Knocke (1990) investigated the manganese oxidation capacity of potassium permanganate over a wide range of temperature and pH conditions. The results show that in the pH range of 5.5 to 9.0, at 105 percent of the stoichiometric requirement (temperature 25^{o}C and DOC below 1.0 mg/L), manganese oxidation by permanganate occurred within 60 seconds. When the temperature decreased from 7^{o}C to 2^{o}C under the same experimental conditions (pH 5.5, DOC below 1.0 mg/L), the required retention time for complete oxidation of manganese increased from 60 seconds to 120 seconds. Also, the presence of DOC (up to 10 mg/L) is believed to decrease the rate of manganese oxidation, but overall the required retention time is still rather short (below 1-2 minutes) at 25^{o}C and pH 7.0. An important factor which should be considered for water utilities when choosing potassium permanganate as an oxidant is the precision of the dosing practice. Since potassium permanganate's

natural color is pink, overdosing this chemical can lead to pink color of the finished water and can introduce an undesirable amount of oxidized manganese into the distribution system, and as a result aesthetic problems can occur for customers.

Using strong oxidants such as $KMnO_4$, O_3, and ClO_2 can lead to the formation of stable colloidal manganese which can pass through media filtration. Knocke (1988) showed that approximately 70-90% of Mn^{+2} was oxidized to colloidal form when a strong pre-filter oxidant was applied. Thus, if media filtration is used to remove oxidized manganese, coagulation/flocculation ahead of filter systems is highly recommended.

2.1.5.2 Manganese Adsorption onto Oxidized-Coated Media:

Since being noticed back in the 1950s, manganese adsorption by OCM has been one of the most effective and dependable manganese control technologies in drinking water treatment. When combined with pre-filter oxidation and coagulation, this method can effectively decrease manganese concentrations to levels of 0.01 mg/L or less.

2.1.5.2.1 Oxidation/Adsorption Mechanism:

Adsorption and surface oxidation of manganese is observed at water facilities where free-chlorine is added into the manganese-containing filter influent. Under this condition, manganese deposits or coatings develop onto media surfaces via a two-step process. First, dissolved manganese is absorbed to existing manganese-oxide deposited on media surfaces. Then, adsorbed manganese is oxidized by free chlorine and converted to a solid form ($MnO_{x(s)}$), and becomes new adsorptive sites. Merkle et al. (1997) named

this phenomenon the natural greensand effect (NGE)[1] and proposed a simplified model describing this process based on the work of Coffey et al. (1993):

$$Mn^{2+} + SITE + HOCl \Rightarrow MnO_x\,(s) + SITE^2$$

Since developing a considerable amount of manganese coatings on filter media may take from weeks to months, Knocke (1990) proposed a procedure to facilitate this process. The procedure includes soaking filter media in a 100mg/L potassium permanganate solution for 24 hours with 100 mg/L of chlorine at a pH above 6.

2.1.5.2.2 Process Design Considerations

Type of media

Manganese greensand is a well-known for use in manganese removal, having been used since the 1950s in the United States. Manganese greensand is made from glauconite, an iron, potassium, alumino-silicate material of marine origin. This media, found along the eastern coast of the United States, was first used as natural zeolite to treat hard water, due to its relatively high ion exchange capacity of approximately 3000 grains (of hardness)/cu.ft. To provide adsorption capacity, glauconite is synthetically coated with a thin layer of manganese dioxide. After being coated, the media has a distinct green color, hence the name greensand (Kohl & Medlar 2006). Hungerford & Terry, Inc of Clayton, NJ is one of leading distributors of manganese greensand for the Inversand Company. They further perfected this technology with the development of the Ferrosand

[1] For simplicity, in report, the term "natural greensand effect (NGE)" was used to imply the manganese removal process by adsorption and surface oxidation

[2] Due to the lack of detailed knowledge, "SITE" and MnO_x , representing the adsorptive site structure and oxidation product of dissolved Mn^{2+}, respectively, are used.

Continuous Regeneration Process which was later patented in 2004 (McPeak and Aronovitch, 2004).

A new manganese greensand product developed by the Inversand Company is GreenSandPlus claimed to be a much stronger and more durable media than traditional manganese greensand. The advancement of this new media stems from its silica-based material rather than glauconite which can be crushed under high working pressure. In addition, a stronger base material allows this new product to withstand higher working temperature (over 70^{o}F) and be able to treat water with low dissolved solids and total hardness levels. These working conditions may soften the glauconite-based traditional manganese greensand, reducing the filter running time and eventually causing filter bed failure. GreenSandPlus has an effective size of 0.30 to 0.35 mm, a uniformity coefficient of less than 1.6 and recommended flow rate in ranges of 2-12 gpm/ft^2. Higher service flow rate is achievable when concentrations of influent manganese are very low.

As a filter media, pyrolucite can also been used to remove soluble manganese from water by the NGE. Pyrolucite is a mineral consisting essentially of manganese dioxide and often found in the United States, Australia, Brazil and South Africa (Kohl & Medlar 2006). An advantage of using pyrolucite in treating manganese is that since it is essentially manganese dioxide, there is no need to develop a manganese oxide deposit or worries about the coating levels as can be trouble-causing matters when utilizing this technique. LayneOX^{TM} , the commercial name of pyrolucite media developed by Layne Christensen Company, is claimed to maintain effective manganese removal under a high flow rate of 10-12 gpm/ft^2, hence substantially reducing the filter footprint compared to using traditional manganese greensand. (Layne Christensen Company website)

Influent pH

Without the presence of an oxidant, Morgan and Stumm (1964) evaluated the dependence of Mn^{2+} adsorption on pH (see Figure 2-1). Adsorption capacities of greater than 0.5 mole Mn^{2+} removed/mole MnO_2 were achievable under alkaline conditions and the adsorption process was rapid, happening within the first few minutes of contact. The process was described as ion exchange whereas dissolved manganese (Mn^{2+}) replaced H+ and other surface cations. For that reason, as solution pH increased from 2.8 ±0.3 (zero point of charge) leading to a decrease of competing H^+ concentration, the adsorptive capacity of the oxide-coated media increased accordingly. In another effort, Knocke et al. (1988) conducted a number of experiments in which different operational conditions were tested by varying influent pH, oxidant types and dosing. The results, consistent with Morgan & Stumm (1964), showed that without a pre-filter oxidant and under alkaline conditions (pH >7) removal of Mn^{2+} was very effective compared to acidic conditions (pH <7). When influent pH decreased from 8 to 6, the author estimated an 80% decrease in adsorptive capacity of the manganese-coated media. Therefore, if alum or iron coagulation is utilized to enhance NOM removal and an acidic influent is desired, the effectiveness of the manganese adsorption process can be inhibited. The effect of pH on Mn^{2+} uptake by OCM was confirmed by Tobiason et al. (2008)

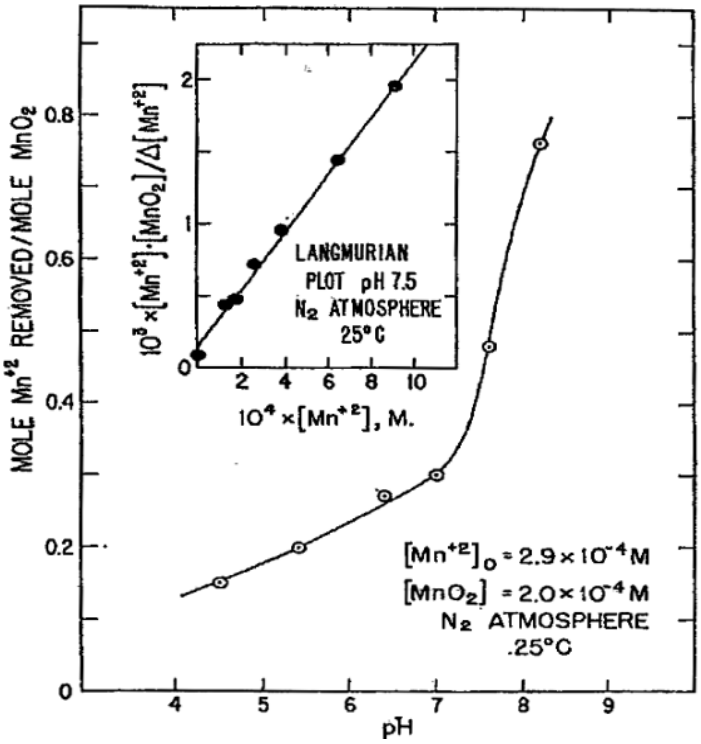

Figure 2-1. pH dependent sorption of manganese (II) on manganese dioxide 25°C. The insert gives a linearized Langmuir plot of sorption equilibrium data at a pH = 7.5(Morgan & Stumm (1964)).

In contrast, when a pre-filter chlorine dose of 2 mg/L was used, manganese adsorption was significant under pH values of 6-6.2 (Knocke et al. (1991b). Figure 2-2 shows experimental breakthrough curves obtained from experiments. The results proved the effectiveness of pre-filter chlorine in enhancing and maintaining the manganese adsorption capacity of oxide-coated media with no breakthrough observed during experimental periods. When pH was adjusted to 7 or greater, a small portion (~5-7%) of dissolved manganese was oxidized by pre-filter chlorine and was present in colloidal form. If not being destabilized via coagulation/flocculation, colloidal manganese contributed to the total manganese in the effluent (Hargette and Knocke 2001). When pH was decreased to 6.0, the oxidation reaction between chlorine and dissolved manganese

was inhibited, resulting in the removal of over 99% influent manganese through NGE process (Knocke et al. (1991b). Again, work by Tobiason et al. (2008) confirmed the role of continuous HOCl addition in maintaining manganese removal by OCM.

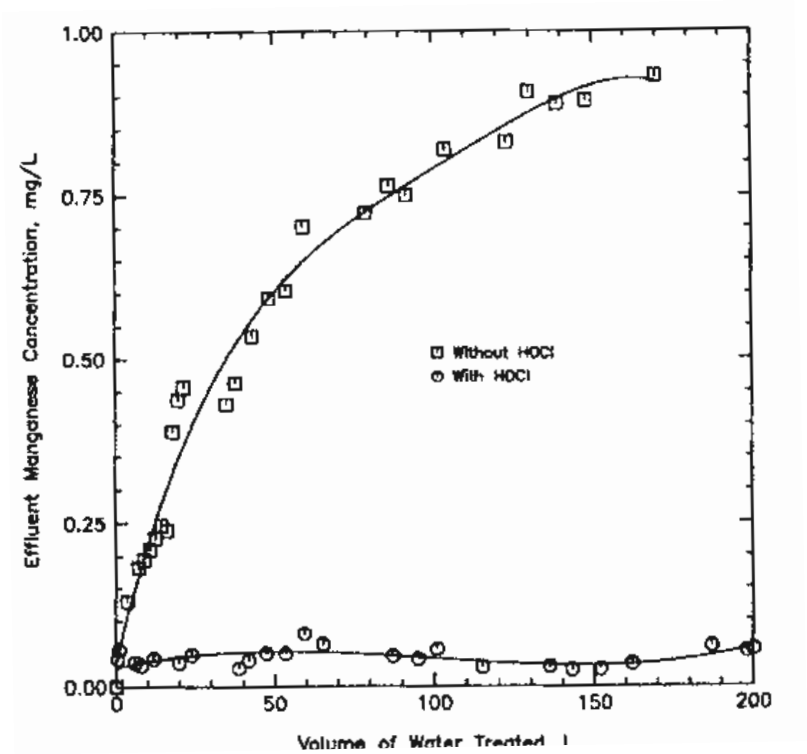

Figure 2-2. Effect of using pre-filter chlorine to enhance adsorption capacity. (Knockle et al. 1991b)

Impact of NOM in water sources

Tobiason et al. (2008) conducted a series of experiments to assess the effect of raw water NOM levels on the manganese uptake capacity of OCM. In the first set of experiments, lab-scale columns with different feed Mn concentrations, NOM levels, and different OCM were tested. The results showed that NOM had an obvious impact on the manganese breakthrough curve; the column with highest feed NOM reached 95% breakthrough the earliest while the column with no feed NOM took the longest time to

breakthrough. However, when pre-filter free-chlorine was dosed, NOM in feed water had no impact on the NGE process with similar effluent manganese levels.

Type of oxidants

Pre-filter application of other strong oxidants such as $KMnO_4$, O_3, and ClO_2 was also tested to assess their impact on manganese uptake by OCM. Knocke et al. (1988) showed that a substantial amount of dissolved manganese was oxidized before reaching the OCM. Therefore, manganese removal was achieved mostly via particle filtration rather than via the NGE process. More importantly, as mentioned above, using strong oxidants can result in stable colloidal manganese oxide which is hard to remove through media filtration unless it is destabilized. In such cases, coagulation is required for better filtration removal performance. Free chlorine is thus the most suitable oxidant for the NGE process. This is because while the solution phase oxidation reaction between free chlorine and dissolved manganese is rather slow at typical pH levels, the reaction between free chlorine and adsorbed manganese is rapid under various testing conditions.

Adsorptive sites and Coating levels:

In general, Knocke et al. (1988,1991) concluded that more manganese adsorption was associated with higher manganese coating levels. Figure 2-3 presents manganese uptake results for different coating levels without continuous addition of free chlorine. However, Knocke et al. (1988) also noticed less-than-expected adsorption capacities of some media which had a large amount of coating. The authors attributed this poor performance to the low oxidation state (2.8 to 3) of the manganese oxide on the media surface. This means that most manganese on the surface was present in reduced form

rather than the oxidized form with an oxidation state of ~4 which had adsorption capacity for dissolved manganese (Mn^{2+}).

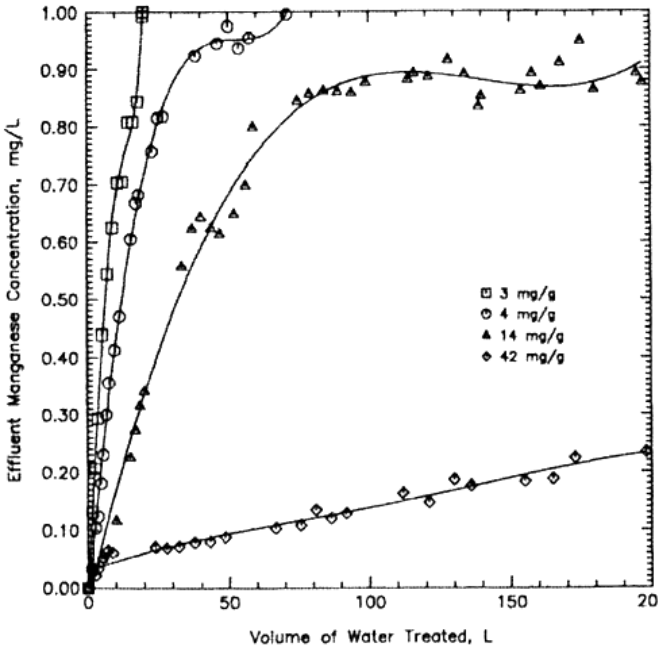

Figure 2-3. Impact of oxide coating levels on manganese uptake capacity of media at pH = 6-6.2 (Knocke et al. 1991).

In another effort, Tobiason et al. (2008) examined the effect of the surface manganese coating level of different media types (anthracite and sand) and different coating levels under the same testing conditions. An inconsistent impact of surface coating level on manganese adsorption to OCM was reported. The authors concluded that manganese coating level alone did not correspond to high manganese uptake capacity of a filter media because not all of the manganese adsorptive sites in the MnOx coating were accessible to dissolved manganese.

2.1.5.2.3 Process Concerns:

Impact of manganese deposits on filter performance:

As use of pre-filter chlorine to regenerate oxide-coated media adds manganese oxide deposits to media grains, research was conducted to investigate effects on the hydraulics of filter operations. Knocke (1990) noted no significant changes in the physical size or density of the oxide-coated media over time with the continuous application of pre-filter chlorine. Also, the oxide coating doesn't have any noticeable impact on filter turbidity removal performance with a slight increase in size (Griffin 1960).

More recent research by Hargette and Knocke (2001) on the effects of backwashing and the long-term fate of manganese on filter media was conducted. The authors concluded that backwashing didn't remove all of the manganese deposits on the media surface and that the remaining coating layer was always enough to ensure a high manganese removal effectiveness after filtration resumed. The results also showed minimal physical changes in effective size or uniformity due to the development of manganese coatings. Consistent with previous experiments conducted by Knocke et al. (1988), manganese profiles across the depth of filter media show that most of the manganese (II) was removed in the upper 6 inches of filter media under loading rates up to 5 gpm/ft^2 (see Figure 2-4).

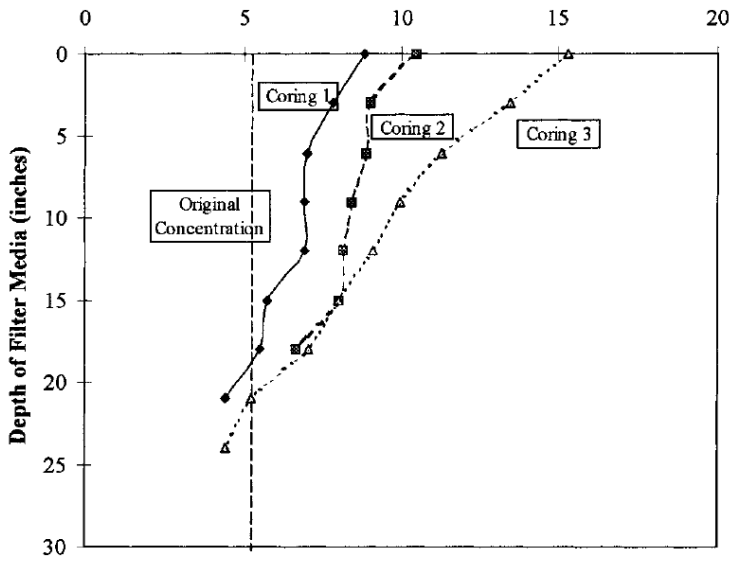

Figure 2-4. Progression of MnOx(s) coating accumulation over time. (Hargette and Knocke 2001)

Release of accumulated manganese from filter column:

As discussed in previous section, under anaerobic conditions, manganese-reducing bacteria may exist and are able to convert solid oxidized forms of manganese (MnO_2) into reduced soluble forms (Mn^{2+}). With the strict control of DBP production by EPA, many water utilities has either removed pre-filter chlorine or delayed chlorine addition after filtration in order to meet the USEPA Stage 1 D/DBP rule. With the absence or lower doses of free chlorine, manganese-reducing bacteria can develop in the media, possibly leading to a higher concentration of manganese in the effluent than in the influent.

Another mechanism for manganese release was reported by Gabelich et al. (2006). The authors investigated manganese release during an upgrade of the Henry J. Mills Filtration Plant in Riverside, CA which switched from pre-filter chlorination to pre-ozonation to comply with the USEPA Stage 1 D/DBP rule. The results showed that the

long-term use of a manganese contaminated ferric chloride coagulant ($FeCl_3$) and pre-filter chlorination had led to manganese deposits on media surfaces. According to the authors, in the absences of free chlorine, Fe(III) or Al(III) displaced Mn(IV)/Mn(III) bound to the anthracite surface through ion exchange. The displaced Mn(III) was then catalytically oxidized to Mn(IV) by the downstream sand layer, producing MnO_2 crystals. This process doesn't result in Mn-surface media coating of the sand, and MnO_2 crystals migrated through the filter via gravity.

DBP concerns

The use of free chlorine as a pre-filter oxidant may cause higher DBP concentrations in finished water compared to post-filter chlorination; especially for water utilities having high NOM in the raw water and the coagulation process downstream of free chlorine inject point. A detailed discussion about this problem is presented in Section 2.3.

2.2 DISINFECTION BYPRODUCTS

After being reported in 1971 by Rook, DBPs have been the focus of extensive research devoted to better understanding their formation in drinking water. The following section briefly reviews some important information about DBPs.

2.2.1 Formation of Disinfection Byproducts

DBPs are groups of organic and inorganic compounds formed during water disinfection. In drinking water, these compounds are created from the reaction between disinfectant and NOM or certain inorganic species. Due to potential health risks,

currently four types of DBPs are regulated under the USEPA Stage 1 D/DBP rules. These four types include trihalomethanes (THMs), haloacetic acids (HAAs), chlorite (ClO_2^-) and bromate (BrO_3^-). Equation 2-1 shows a simplified version of the formation of organic DBPs.

$$NOM + HOCl + Br^- \rightarrow \text{organic DBPs} \qquad \text{Equation 2-1}$$

Names and acronyms for the THM and HAA organic DBPs are presented in Table 2-4. Research data related to regulated and other unregulated DBPs were collected and monitored by the US EPA under the Information Collection Rule (ICR). The collected data were used to evaluate the potential health risks of pathogens, disinfectants, and disinfection byproducts, and guide regulatory and public health decisions (US EPA 2006).

The use of chlorine dioxide as pre-oxidant and disinfectant in drinking water treatment often leads to the existence of chlorite in treated water. In the presence of NOM or other reducing agents in water, chlorine dioxide is reduced to chlorite as shown in Equation 2-2.

$$ClO_2 \rightarrow ClO_2^- \qquad \text{Equation 2-2}$$

Bromate is often found in ozonated water containing inorganic bromide. Ozone can oxide bromide and convert it to bromate as shown in Equation 2-3.

$$O_3 + Br^- \rightarrow BrO_3^- \qquad \text{Equation 2-3}$$

It should be noted that the formation of DBPs is rather complicated, involving many complex reactions and intermediate products rather than the simplified versions presented in Equations 2-1, 2-2, and 2-3.

Table 2-4. Names and Acronyms for common organic DBPs (Xie 2004)

Group	Names	Formula	Acronyms
Trihalomethanes	Trichloromethane	$CHCl_3$	TCM
	Bromodichloromethane	$CHBrCl_2$	BDCM
	Chlorodibromomethane	$CHBr_2Cl$	CDBM
	Tribromomethane	$CHBr_3$	TBM
Haloacetic acids	Monochloroacetic acid	$CH_2ClCOOH$	MCAA
	Monobromoacetic acid	$CH_2BrCOOH$	MBAA
	Dichloroacetic acid	$CHCl_2COOH$	MCAA
	Bromochloroacetic acid	$CHBrClCOOH$	BCAA
	Dibromoacetic acid	$CHBr_2COOH$	DBAA
	Trichloroacetic acid	CCl_3COOH	TCAA
	Bromodichloroacetic acid	$CBrClCOOH$	BCAA
	Chlorodibromoacetic acid	$CBr_2ClCOOH$	CDBAA
	Tribromoacetic acid	CBr_3COOH	TBAA

2.2.2 Health Concerns:

Since the mid 1980's, a number of epidemiological studies have supported potential health risks of chlorinated water. Many of them indicated an association between bladder, colon and rectal cancers with water chlorination. By conducting a meta-analysis of previous epidemiological studies, Morris et al. (1992) showed that approximately 9% of bladder cancer cases and 15% of the rectal cancer cases could be due to DBPs in chlorinated water.

In addition, more recent research on the health impacts of DBPs has suggested potential links between DBPs and reproductive and developmental health effects. Although data at this time do not show concrete proof of these effects on humans, the potential impacts cannot be eliminated (US EPA 2006).

2.2.3 Regulations:

In November, 1979, US EPA promulgated the first DBP regulation, the Total Trihalomethanes rule. Community water systems using surface water and/or ground water that served at least 10,000 people and injected a disinfectant to their drinking water treatment system were required to achieve a MCL of 0.10 mg/L for total Trihalomethanes (TTHM). Compliance data were based on running annual averages of quarterly samples (RAAs).

With increasing health concerns related to HAAs and THMs, the Stage 1 Disinfectants and Disinfection Byproducts Rule (Stage 1 D/DBPR) was issued in 1998 and became effective in January 2002. This rule established enforceable maximum residual disinfection levels (MRDL) and maximum residual disinfection level goals (MRDLGs) for three chemical disinfectants –chlorine, chloramines and chlorine dioxide; maximum contaminant level goals for three THMs, two HAAs, bromate, and chlorite, and enforceable maximum contaminant levels (MCLs) for TTHM, five haloacetic acids (HAA5), bromate and chlorite (see Table 2-5). While THM, HAA5 and bromate compliance is based on RAAs, chlorite is based on daily sampling. Furthermore, under the Stage 1 D/DBPR, water facilities that use surface water or groundwater under the direct influence of surface water and the use conventional treatment are also required to remove specified percentages of organic matter depending on the level of NOM and

alkalinity in their source water. At the same time, to address the tradeoff of decreasing disinfectant as well as DBP eliminating approaches, US EPA finalized the Interim Enhanced Surface Water Treatment Rule (IESWTR) at the same time as the Stage 1 DBPR.

Table 2-5. Stage 1 DBPR regulated contaminants (US EPA 2001)

Regulated Contaminants/Disinfectants					
Regulated Contaminants	MCL (mg/L)	MCLG (mg/L)	Regulated Disinfectants	MRDL* (mg/L)	MRDLG* (mg/L)
Total Trihalomethanes (TTHM)	**0.080**				
Chloroform		-	**Chlorine**	**4.0 as Cl_2**	**4**
Bromodichloromethane		zero			
Dibromochloromethane		0.06			
Bromoform		zero			
Five Haloacetic Acids (HAA5)	**0.060**		**Chloramines**	**4.0 as Cl_2**	**4**
Monochloroacetic acid		-			
Dichloroacetic acid		zero			
Trichloroacetic acid		0.3	**Chlorine dioxide**	**0.8**	**0.8**
Bromoacetic acid		-			
Dibromoacetic acid		-			
Bromate (plants that use ozone)	**0.010**	**zero**	***Stage 1 DBPR includes maximum residual disinfectant levels (MRDLs) and maximum residual disinfectant level goals (MRDLGs) which are similar to MCLs and MCLGs, but for disinfectants.**		
Chlorite (plants that use chlorine dioxide)	**1.0**	**0.8**			

Although the Stage 1 DBPR provided a major decrease in DBP exposure, a national survey conducted by US EPA suggested that some customers are still likely to receive drinking water with elevated DBP concentration even when their water providers are in compliance with the Stage 1 DBPR. To prevent these situations, US EPA further tightened the DBP regulation by issuing the Stage 2 D/DBPR in January 2006 which will become effective in April 2012. While maintaining the same MCL levels for the regulated DBP compounds, compliance will be based on the locational running annual average (LRAA) at several locations rather than a system-wide RAA calculation. To

indentify the Stage 2 DBPR compliance monitoring sites, USEPA requires water systems to conduct an initial distribution system evaluation (IDSE) to locate sampling locations at which DBP concentrations are the highest.

Table 2-6. Stage 2 DBPR regulated contaminants (US EPA 2006)

Stage 2 DBPR Regulated Contaminants			
Regulated Contaminants		MCLG (mg/L)	MCL (mg/L)
Total Trihalomethanes (TTHM)			**0.080 LRAA**
	Chloroform Bromodichloromethane Dibromochloromethane Bromoform	0.07 zero 0.06 zero	
Five Haloacetic Acids (HAA5)			**0.060 LRAA**
	Monochloroacetic acid Dichloroacetic acid Trichloroacetic acid Bromoacetic acid Dibromoacetic acid	0.07 zero 0.02 - -	

2.2.4 Factors affecting DBP formation:

2.2.4.1 Effects of NOM:

The concentration and characteristics of NOM play a crucial role in DBP formation. In drinking water treatment, higher concentrations of NOM lead to higher concentrations of DBPs. This is because a higher level of NOM means a higher level of DBP precursors in water, possibly resulting in higher concentrations of DBPs. Moreover, for water utilities using free chlorine as a pre-oxidant, increasing the NOM level in the raw water increases the chlorine demand, requiring a higher chlorine dose, which leads to higher concentrations of DBPs.

2.2.4.2 Effects of pH

DBP formation is affected by pH in different ways. In general, increasing pH results in higher concentrations of THMs but a lower concentration of HAAs and other halogenated DBPs including total organic halide (TOX) (see Figure 2-5).

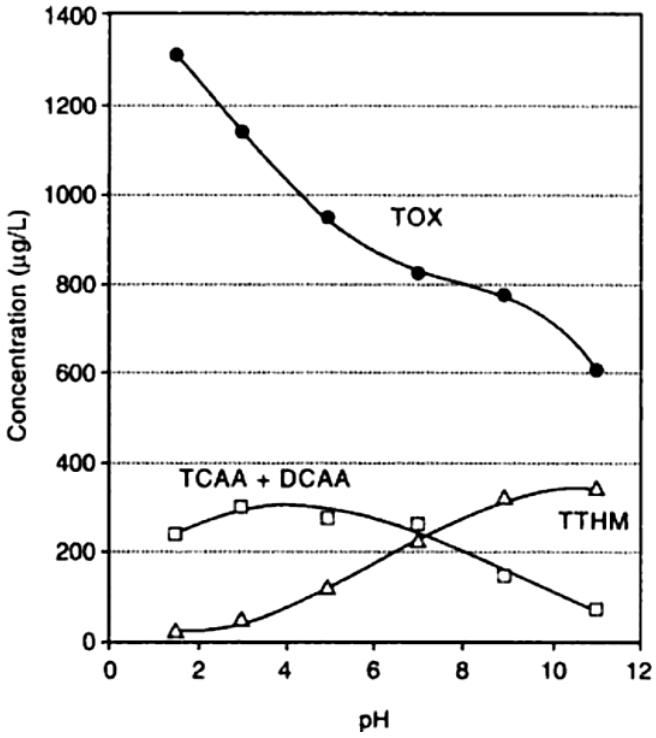

Figure 2-5. Impact of pH on DBP formation (Reckhow and Singer 1986)

2.2.4.3 Effects of chlorine dose and chlorination time:

Similar to NOM, chlorine is a key factor affecting DBP concentrations in drinking water. In general, in drinking water treatment, increasing or decreasing the chlorine dose can directly increase or decrease DBP concentrations. For that reason, many water utilities have decreased or eliminated the use of chlorine to control DBP production.

Many DBP compounds are the results of reactions in series. Since THMs and HAAs are end products, increasing chlorination time will increase the concentration of these compounds. However, if DBPs are intermediate products, increasing the reaction time may decrease the formation of a DBP. Also, if the chlorine residuals are low, biodegradation may decrease the concentration of some DBPs, except for THMs (Xie 2004)

2.2.5 DBP control methods:

Controlling DBPs requires either decreasing the level of DBP precursors ahead of the disinfection point or changing the disinfection practice. This section discusses in detail the methods in each approach in detail.

2.2.5.1 DBP precursor removal:

A conventional method to remove DBP precursors is coagulation/flocculation followed by particle removal. US EPA defined the optimized coagulation process to remove DBP precursors as enhanced coagulation and consider it as one of two best available technologies (BATs) for controlling DBPs; the second BAT is granular activated carbon (GAC) adsorption (US EPA 2001). Aluminum and iron salts are the most commonly used coagulants. NOM substances with high molecular weight are most likely removed during coagulation and flocculation.

In the Stage 1 D/DBPR, in addition to setting the MCLs for DBPs, US EPA also required water systems that treat surface water, or ground water, under direct influence of

surface water through conventional treatment to remove specific percentages of total organic carbon (TOC) depending on water quality as shown in Table 2-7.

Table 2-7. Required Removal of Total Organic Carbon by Conventional Treatment (Adapted from US EPA (2001))

Source Water TOC (mg/L)	Source Water Alkalinity (mg/L as $CaCO_3$)		
	0-60	>60-120	$>120_2$
>2.0-4.0	35.0%	25.0%	15.0%
>4.0-8.0	45.0%	35.0%	25.0%
>8.0	50.0%	40.0%	30.0%

GAC adsorption is also a proven technology to decrease NOM levels in treated water. One study showed that by removing 40% of the TOC in a water source, GAC adsorption resulted in approximately a 15% decrease of THM formation potential (Jodellah and Weber Jr., 1985). GAC can also be used as biologically active carbon (BAC). Through biological activity on the media surface, BAC can remove biodegradable DBP precursors, decreasing DBP production. This process often utilizes pre-filter ozonation to convert non-biodegradable into biodegradable NOM, enhancing DBP precursor removal. Other methods such as ion exchange, and reverse osmosis, and nanofiltration and membrane filtration are also effective in removing NOM in water sources.

2.2.5.2 Disinfection Practice Alternatives:

For water systems with limited funds for a major technology upgrade to meet the Stage 1/2 D/DBPRs, changing disinfection practice could be an effective method to decrease DBPs in finished water. Disinfection parameters which can be changed to

reduce DBP formation include type of disinfectant, and chlorination point. Alternative disinfectants such as ozone, ultraviolet (UV) light, or chlorine dioxide can be used to replace free chlorine in the disinfection process. It is also common for water treatment plants to use a combination of two or three alternative disinfectants such as chlorine/chloramines or ozone/chloramines with chloramines as a secondary disinfectant.

In addition, many water systems have eliminated pre-oxidation with free chlorine and delayed the chlorination point to intermediate or post chlorination to reduce the contact time between free chlorine and DBP precursors, limiting the DBP production. In these cases, pre-oxidation with potassium permanganate or chlorine dioxide is commonly used to control taste and order as well as iron and manganese problems.

2.3 LANTERN HILL DRINKING WATER TREATMENT PLANT

Along with Deans Mill water treatment plant, the Lantern Hill Water Treatment Plant (LHWTP) belongs to the Mystic, Connecticut water system owned by the Aquarion Water Company of Connecticut (AWC), an Aquarion subsidiary. AWC is a private water supply company providing water for more than 580,000 people in 39 cities and towns throughout Connecticut and claims to be the largest investor-owned water utility in New England.

2.3.1 Water Quality

Built in the 1960's, the LHWTP is a groundwater treatment plant. The concentrations of total manganese, iron and NOM are relatively unchanged throughout

the year. Table 2-8 presents the average raw water quality at the Lantern Hill water treatment plant.

Table 2-8. Typical water quality of the LH water source

pH	Mn (mg/L)		Fe (mg/L)		TOC (mg/L)	
	Total	Dissolved	Total	Dissolved	Total	Dissolved
6.36.5	0.15-0.19	0.14-0.18	1.6-1.9	1.5-1.7	2.6-3.0	2.2-2.5

2.3.2 Treatment Process Description

With a design capacity of 1.0 MGD, the LHWTP is currently utilizing pre-filter oxidation, coagulation and filtration, and the OCM process to simultaneously remove manganese, iron and NOM from the raw water. Figure 2-6 presents a process flow diagram for the LHWTP before and after April 09, 2007. Raw water was dosed with HOCl, KOH, $KMnO_4$ and cationic polymer (Superfloc C572). Within seconds, the water enters the three parallel pressurized filters. Each consists of 21 inches of anthracite over 24 inches of greensand. Filter effluent is then dosed with fluoride and PO_4^{-3} before entering the distribution system. In the original design, only pre-filter chlorine was added to oxidize reduced metals, to reactive the manganese adsorption capacity of the filter media, and to generate adequate chlorine residual entering the distribution system. Dissolved manganese and iron in the raw water was converted to solids via oxidation reactions with HOCl and $KMnO_4$; the particulate forms were removed via media filtration. Manganese removal was completed by adsorption and surface oxidation process on the anthracite and greensand media. Also, C572 was added ahead of the filter to facilitate the removal of particulates.

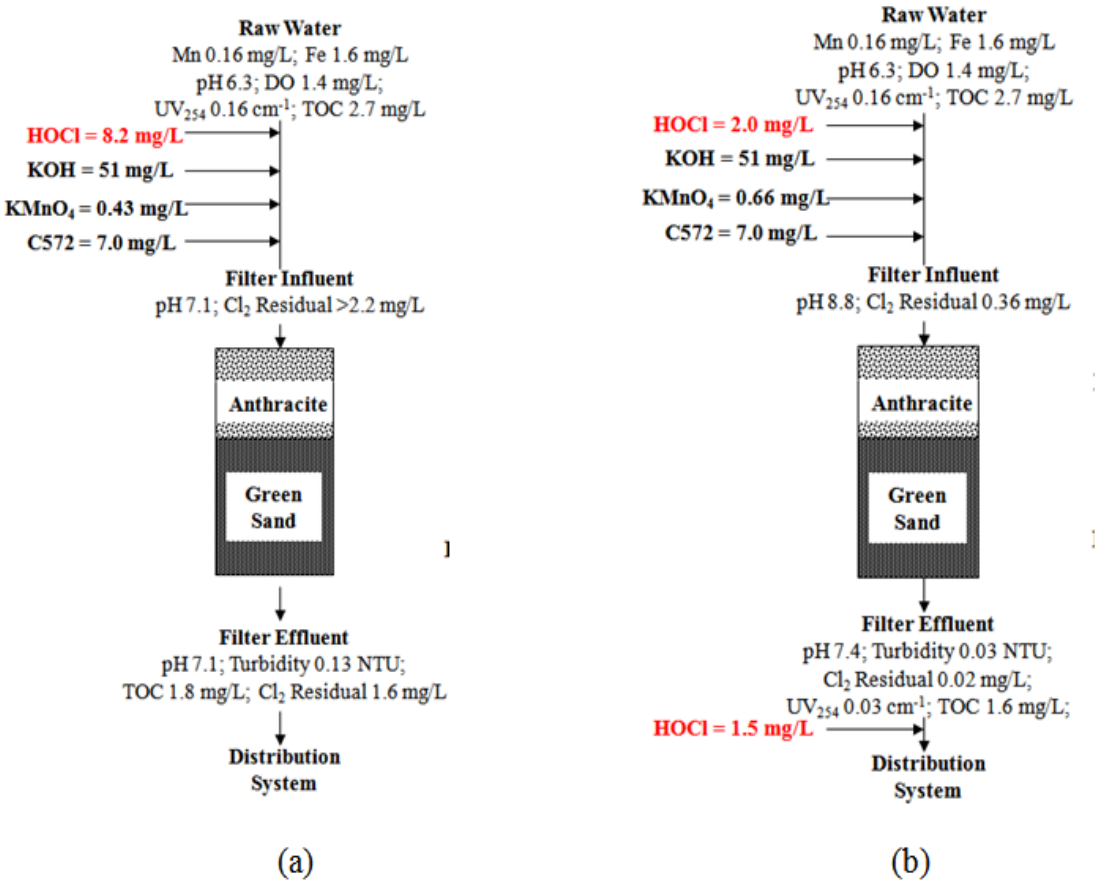

Figure 2-6. The Lantern Hill Water Treatment Plant Flow Diagram: a) Prior 4/9/2007, b) After 4/9/2007 (Russell 2008).

2.3.3 Summaries of Previous Research

With relatively high concentrations of NOM in the raw water throughout the year (~3 mg/L), and high doses of pre-filter HOCl (~8 mg/L), the AWC was having difficulties to meet the Stage 1 D/DBPR and future Stage 2 D/DBPR for the Mystic Water System. To solve the problem, UMass researchers recommended that AWC change the LH treatment process from only pre-chlorination to having both pre-filter chlorination and post-filter chlorination. The idea was that by installing a post-chlorination point and using it to provide the desired chlorine residual entering the

distribution system, the dose of pre-filter free chlorine could be significantly decreased, resulting in lower concentrations of DBPs. On April 09, 2007, LH began to be operated under this new configuration (see Figure 2-6b). The pre-filter chlorine dose was adjusted from 8 mg/L to 2 mg/L and a post-filter chlorination dose of 1.5 mg/L was added to supply the desired chlorine residual concentration.

DBP data showed that decreasing the pre-filter chlorine dose from 8 to 2 mg/L resulted in a 70-90% decrease in plant effluent DBP concentrations. However, 35 to 55 days after decreasing the pre-filter chlorine, the filter effluent dissolved manganese concentrations started to increase, exceeding the filter influent levels, suggesting that the filter media might have started to release manganese, probably due to low concentrations of filter influent and effluent chlorine (see Figure 2-7) (Russell 2008). To deal with this problem, a higher pre-filter chlorine dose of approximately 5 to 6 mg/L has been applied to suppress the manganese release from media; however, this also increased the DBP levels in the finished water. Therefore, further research of different approaches to control both manganese and DBP for the LHWTP has been undertaken.

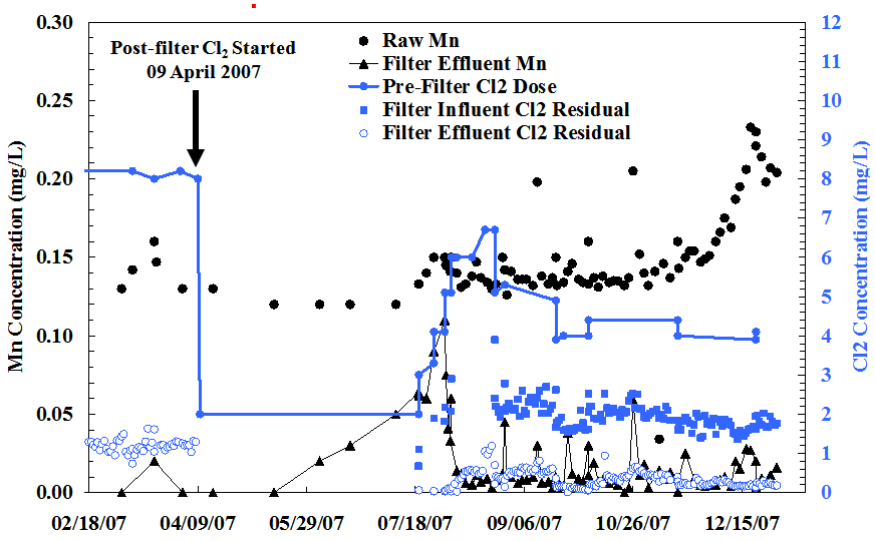

Figure 2-7. Lantern Hill Manganese and Chlorine historical data

CHAPTER 3: MATERIALS &METHODS

This chapter provides detailed information about the Lantern Hill pilot-scale system for treatment process assessment. The analytical methods used to measure water quality are also discussed.

3.1 THE LANTERN HILL PILOT-SYSTEM

The pilot-scale system constructed on-site at the LHWTP was the main focus of this research.

3.1.1 Pilot-Scale System Description:

The pilot-scale system includes a dual-media (DM) filter and a second-stage contactor for manganese removal. The 7.5 inch diameter dual media filter has 24 inches of anthracite (~1mm in diameter) over 12 inches of sand media (~0.06 mm in diameter). The anthracite media was initially new with no manganese coating on its surface, but later was intentionally coated with manganese oxide for experimental purposes. The sand media was standard silica sand rather than the greensand used in the full-scale filtration.

The 3 inch diameter second-stage contactor was originally made by Dr. Knocke's research group at Virginia Tech University and shipped to UMass for further modification before installing at the LHWTP. New pyrolucite media with mesh size 8x20 obtained from Layne Christensen Company was used for the second-stage contactor. To achieve a desired media diameter of greater than 2 mm, the media was furthered sieved to achieve a 8x10 mesh seize yielding media diameters in the range of 2.36 to 2 mm. A nozzle from a full-scale filter underdrain was installed at the bottom of the column to prevent media from being washed out with the filter effluent and to allow the backwashing of the media. Initially, only five sampling ports with a total distance of 20 inches between these ports were placed along the column. Later, to test the second-stage contactor with a deeper bed depth, four more sampling ports were placed on top and

increasing the total distance between these ports to 39 inches (total media depth of approximately 42 inch). The distances between these ports from top to bottom were as follows: 6, 6, 6, 4, 3, 3, 6, and 5 inches.

3.1.2 Pilot System Operation and Maintenance

Raw water for the pilot system was supplied at a flow rate of 1 gallon per minute (gpm) by either diverting from the main supply for the full-scale plant when it was operated or by a submersible pump when the LHWTP was taken out of service. The pilot-plant flow rate was measured using a flow meter installed ahead of the DM filter. At a flow rate of 1 gpm, the hydraulic loading rates were 3 gpm/ft^2 and 20 gpm/ft^2 for the DM filter and the second-stage contactor column, respectively. Chemical stock solutions were prepared fresh at the beginning of each experiment and delivered to the main stream by using manually controlled chemical-feed pumps in which flow rate can be controlled by either adjusting stroke rate or stroke length.

The pilot experiments can be divided into two phases. In Phase I, only the DM filter was used (see Figure 3-1). The valve and piping system was installed to allow for different orders of chemical addition. Sodium hypochlorite (NaOCl) could be added either ahead of NaOH, $KMnO_4$, and Superfloc C572 to mimic the full-scale plant or added in between $KMnO_4$ and Superfloc C572. The impact of increasing contact time between $KMnO_4$ and raw water was tested by inserting a 25-foot long, 1-inch diameter, pipe loop after the $KMnO_4$ addition point. In Phase II, the second-stage contactor was connected in series with the dual-media filter (see Figure 3-2). The NaOCl addition point was moved downstream to a point between the two columns. The flow rate into the second-stage contactor could be decreased from 1 gpm by wasting part of the DM filter effluent after the NaOCl addition point.

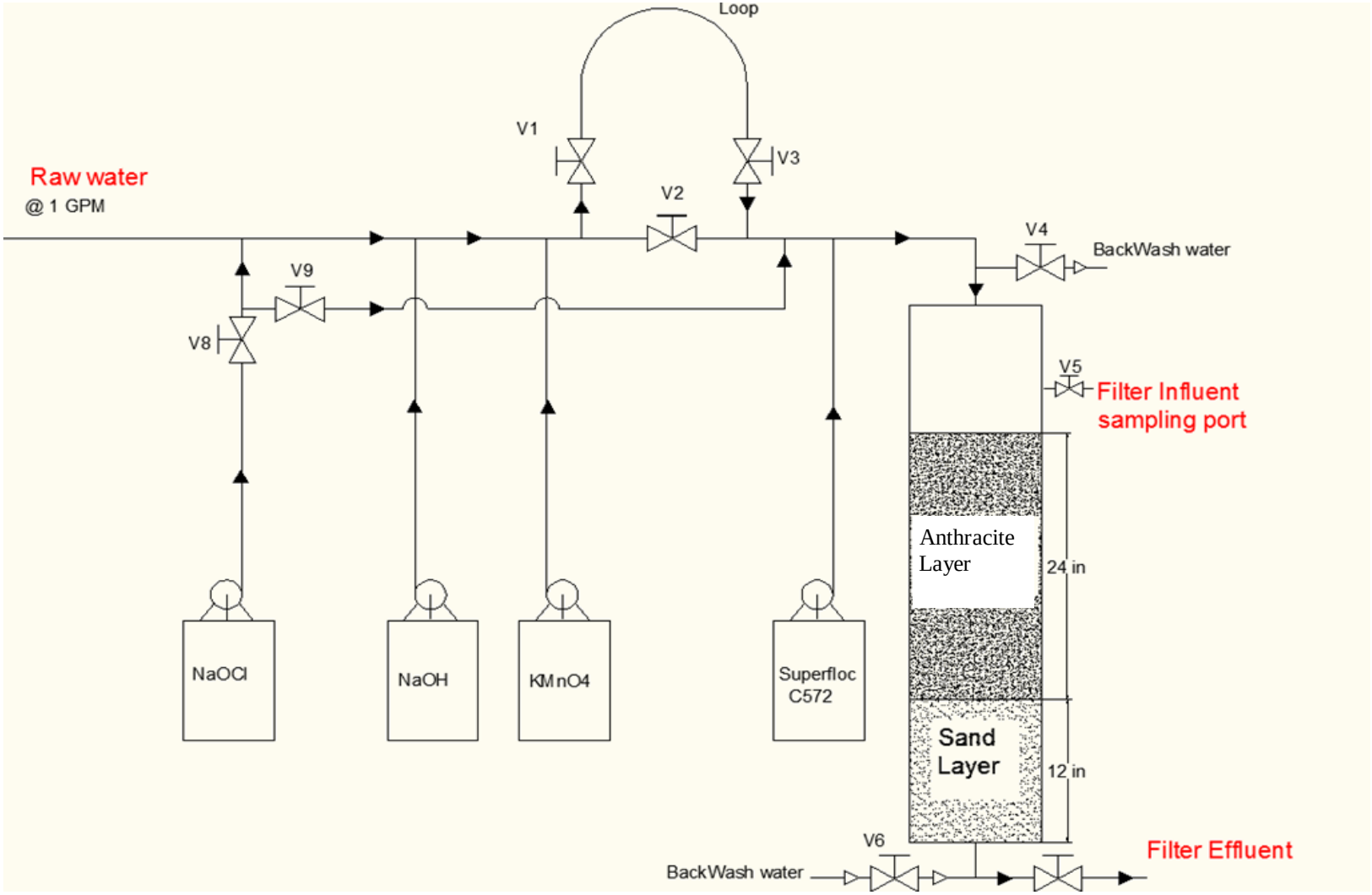

Figure 3-1. LHWTP Pilot system during Phase I

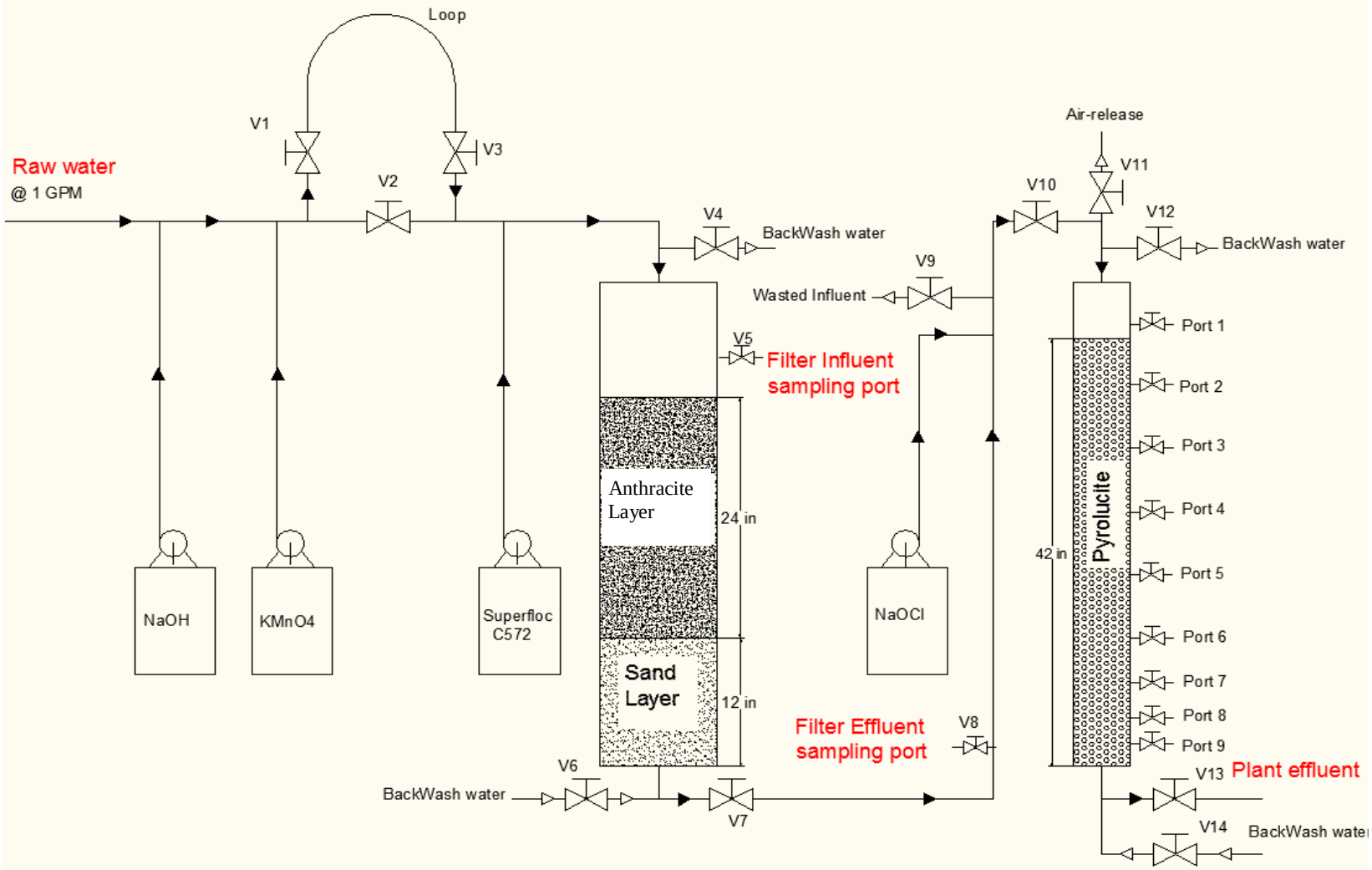

Figure 3-2. LHWTP Pilot system during Phase II

Water quality was monitored at various sampling locations to assess performance of the pilot-system.

Table 3-1 presents monitored water quality parameters at different sampling points. The pilot system was kept running continuously for approximately 24 hours before backwashing; this operating cycle is similar to that of the full-scale filters. Periodically, samples were also collected for analysis of TOC and DBPs. Profiles of manganese concentration along the contactor depth were also measured occasionally.

Table 3-1 Monitored water quality at different sampling locations during pilot experiments.

Sample types	Total & dissolved Mn	Total & dissolved Fe	UV_{254}	Turbidity	Chlorine residual	pH
Raw water	X	X	X			X
DM influent	X	X			X[1]	X
DM effluent	X		X	X	X	
Contactor effluent	X	X		X	X	

[1] Dual media influent chlorine residual was only measured during the Phase I while dual media effluent chlorine residual was only measured during the Phase II.

3.2 Experimental Methods

3.2.1 Fractionation Procedure for Iron, Manganese and TOC

Water quality analysis for this project was used to determine chemical doses as well as the effectiveness of the treatment processes. Manganese, iron and TOC were usually classified into particulate, colloidal and dissolved fractions through two different filtration processes. Colloidal plus dissolved fractions were determined by filtering water samples through 0.2 μm pore size Millipore membrane filter to remove particulate metal

and organic carbon. The metal and organic carbon in the filtrate was considered the colloidal and dissolved fractions for the water samples. To indentify the dissolved fractions, water samples were filtered through a Millipore YM30 ultrafilter using nitrogen gas and an Amicon 8200 200 mL ultrafilter cell to remove particle and colloidal fractions. Nitrogen gas was used to for pressure, and also to prevent oxidation of Mn^{2+} and Fe^{2+} during the filtration process. For most of the LH water samples, no considerable difference in manganese, iron and TOC concentrations in filtrates from these two filtration processes was observed (i.e. no significant colloidal fractions were formed). Due to its simple procedure, filtration through the 0.2 μm membrane was considered to separate particulate and dissolved fractions of manganese, iron and TOC in this research.

3.2.2 Measurement of Manganese Oxide Coatings on Filter Media Surface

Anthracite media samples in the dual media were collected after backwash and placed in plastic containers and filled with chlorinated filter effluent. The samples were then transported to the University of Massachusetts Amherst Environmental Engineering Laboratory to store in a $4^{o}C$ constant temperature room.

A hydroxylamine sulfate (HAS) extraction procedure was employed to quantify the manganese coating level on filter media surfaces. To reduce the manganese oxide to dissolved form Mn^{2+}, the media was soaked in a 0.5% nitric acid, hydroxylamine sulfate solution. The concentration of manganese in filtered extraction solution was measured using inductively coupled plasma mass spectroscopy (ICP-MS).

The detailed extraction procedure is described as follows (Russel 2008):

1. The media samples were first gently rinsed with DI water to remove manganese oxide particles which were not physically attached to the surface of the media.
2. A wet media sub-sample was weighed and then dried in an oven at 105^{o}C. The amount of wet media dried was selected to yield a desired dry media mass of approximately one gram for extraction.
3. After 24 hours, the dried media was removed from the oven and placed in a desiccator to cool to room temperature. Once cooled, the sample was reweighed and placed in an Erlenmeyer flask containing 250 mL of 0.5% nitric acid.
4. Approximately one gram of HAS was added to the solution to increase the rate of dissolution of the metal oxide coating.
5. After at least two hours of reaction time, the liquid phase of the solution was filtered through a 0.7 µm Whatman fine, glass-fiber filter (GF/F) and analyzed for manganese, iron, aluminum and calcium content using an ICP-MS.
6. Once the concentrations of the various metals in solutions were measured, the media surface manganese contents were calculated using the following expression:

$$\text{Media Surface Metal Content, mg-Mn/g-media} = \frac{[Mn].V}{Media\ Mass} \qquad \text{Equation 3.1}$$

Where:

[Mn]: concentration of manganese in the extraction solution, mg/L

V: volume of extraction solution utilized (e.g., 0.25 L), L

Media Mass: dried weight of media extracted in the procedure, g

3.3 DBP Sampling Procedure

DBP data were an important factor in this research; therefore, a precise and consistent sampling technique was required. Two types of DBP data were used to assess DBP levels in the pilot-scale and full-scale effluents. The first type, called instantaneous DBP, was used to assess the amount of DBPs in the filter or plant effluent. Pilot-scale and full-scale effluent samples were quenched immediately with sodium sulfite (Na_2SO_3) to prevent further reaction between free-chlorine and NOM. The second type of DBP data, called 24hour DBPs, simulated the distribution system levels of DBPs. In this method, pilot-scale and full-scale effluent samples were collected in 300 mL biochemical oxygen demand (BOD) bottles, headspace free, and held for a period of 24 hours, in a dark room, at a constant temperature of 20^{o}C. For both types of DBP samples, in order to compare full-scale and pilot-scale effluent DBP levels, it was crucial to have similar chlorine residuals of approximately 1.00-1.05 mg/L at the time of DBP sampling.

3.4 Analytical Methods

3.4.1 Plastic and Glassware Preparation

Following the University of Massachusetts Amherst, Environmental Engineering Research Laboratory Procedures, all plastic and glassware were properly prepared before experiments. Depending on their intended use, the plastic and glassware were cleaned following various protocols. First, they were soaked for 10-15 minutes in a warm detergent solution. They were then rinse three times with tap water, followed by three

rinses with distilled water. After that, they were placed overnight in 10-15% sulfuric acid bath before final rinse with DI water. The plastics vials used for ICP-MS measurement were placed in 2% nitric acid overnight instead of sulfuric acid bath. All BOD bottles used for DBP test were then placed in a 100 mg/L chlorine bath until use. The chlorine bath was prepared fresh weekly. Non-volumetric glassware was later dried in a 110^{o}C oven, while plastic and volumetric glassware were placed in a lower temperature (~ 50^{o}C) convection drying oven.

3.4.2 Metal Concentration Measurements

Since most of experiments were conducted on-site at the LHWTP, iron and manganese concentrations were measured using HACH pocket colorimeter test kits. The ICP-MS measurement was mostly utilized to measure samples for assessing manganese profiles along the second-stage contactor and extracted manganese from filter media sampling.

3.4.2.1 HACH Low Range Total Manganese Pocket Colorimeter Test Kit Method

On-site total manganese concentrations were measured using a HACH low range manganese pocket colorimeter test kit with measurement range from 0.01 to 0.7 mg/L (Method 8149). First, 10 mL of sample was transferred into a HACH sample cell using an Eppendorf pipette. Then, one Ascorbic Acid Powder Pillow, 12 drops of alkaline-cyanide reagent, and 12 drops of Pan Indicator were added to the sample cell. After waiting for 2 minutes, the sample vial was inserted in a colorimeter to measure concentration. Prior to measuring the manganese concentration of the sample, the

instrument was zeroed using a blank sample. The blank sample preparation was similar to sample preparation described above except that 10 mL of DI water was used instead of 10 mL of sample. In order to measure dissolved manganese, the samples was first filtered through a 0.2 µm membrane filter; then the concentration of dissolved manganese in filtrate was measured.

3.4.2.2 HACH Total Iron (FerroVer) Pocket Colorimeter Test Kit Method

Total iron concentrations were also measured on-site using a HACH total iron (FerroVer) pocket colorimeter test kit with the measurement range from 0.02 mg/L to 5.00 mg/L (Method 8008). First, 10 mL of sample was transferred into a HACH sample cell by using an Eppendorf pipette. Then, one FerroVer Iron Reagent Powder Pillow was added to the sample cell. After waiting for 3 minutes, the sample was inserted in the colorimeter to measure concentration. Prior to measuring the iron concentration of the sample, the instrument was zeroed using a blank sample. The blank sample preparation was similar to sample preparation described above except that 10 mL of DI water was used instead of 10 mL of sample. In order to measure dissolved iron, the samples was first filtered through a 0.2 µm membrane filter; then the concentration of dissolved iron in filtrate was measured.

3.4.2.3 Inductively Coupled Plasma Mass Spectroscopy (ICP-MS)

ICP-MS was periodically used to measure manganese in samples collected to determine profiles of manganese along the second-stage contactor as the manganese concentration can be below the detection limit of the colorimeter method (described in

Section 3.4.2.1 above). Samples were stored in a $4^{o}C$ constant temperature room and acidified with 2% HNO_3 before being analyzed. A set of five calibration manganese standard solutions with concentrations of 0.001, 0.05, 0.1, 0.15, and 0.25 mg/L as Mn^{2+} were prepared from $MnSO_4$. A daily performance solution including analytes at different masses across the periodic table was measured to check the instrument performance at different masses and intensities of interferences (oxides, double-charged negative ions). The estimated detection limit for manganese is approximately 0.1-1 part per trillion (ppt). For quality control (QC), the instrument also recorded relative standard deviation (RSD) data for each example. An RSD value greater than 10 was the signal of the instrument performance degradation. In these cases, a specific optimization and cleaning procedures described in instrument's manuals was followed to recover instrument sensitivity.

3.4.3 pH

A Thermo Electron Corp. Orion 520A or 410 A^{+} bench-top pH meter in conjunction with a Thermo Orion pH probe was used for pH measurement. The instrument was periodically calibrated using certified buffer solutions of pH 4, 7, 10.

3.4.4 Turbidity

Filter effluent turbidity was determined using a HACH 2100N turbidimeter. A primary Formazin standard was used to calibrate the instrument and before each use the calibration was checked using secondary standards.

3.4.5 Ultraviolet Absorbance (UV)

UV absorbance was measured using a HACH DR/4000 laboratory spectrophotometer set at a wavelength of 254 nm. Before each measurement, samples were filtered through either a GF/F or 0.2 µm Millipore membrane filter into 1 cm-path length quartz glass cuvette. The instrument was zeroed with DI water before each use.

3.4.6 Total Organic Carbon (TOC)

The Shimadzu TOC/V at the UMass Amherst laboratory was used for this measurement. Samples were collected, acidified to pH of 2 by adding 50µL of HCl 6N, and stored in a 4^{o}C constant temperature room. The instrument was calibrated periodically using four calibration standards which have concentrations as follows: 0, 2, 5, and 10 mg/L. To prepare the standard solutions, a 1000 mg/L carbon stock solution was made by dissolving 2.125 g of reagent grade potassium hydrogen phthalate, previously dried at 105-120^{o}C for 1 hour and cooled in a desiccators, in 1 L of DI water. The stock solution was then diluted with DI water to achieve desired concentrations.

3.4.7 HACH Free Chlorine Pocket Colorimeter Test Kit Method

An on-site test kit method was used to measure chlorine residual during experiments at the LHWTP. The measurement range from 0.02 mg/L to 2 mg/L. 10 mL of water sample was first transferred to each of two HACH sample cells. The colorimeter was then zeroed with one of the sample cells. A DPD Free Chlorine Powder pillow was added to the other sample cell, and within one minute the sample was measured.

3.4.8 DBP Measurements

DBP measurements, including THM and HAA5, measurement were conducted at the University of Massachusetts Amherst Laboratory according to Standard Operating Procedures: Analysis of Haloacetic Acids and Trihalomethanes (Reckhow 2006). These methods are closely aligned with US EPA Method 551.1 and 552.2.

3.4.8.1 Trihalomethane Extraction

Water samples were filled headspace-free into 40 ml amber vials containing 1 mL of 1g/L sodium sulfide (Na_2SO_3) and approximately 1 gram of phosphate buffer. Phosphate buffer was used to adjust pH to 4.5-5.5 while sodium sulfide was used as a quench to reduce free chlorine residual to chloride. After the above procedure, samples can be stored in a 4^oC constant temperature room for no more than 14 days before being extracted.

When performing the extraction, it was necessary to bring the analytical samples to room temperature. In the mean time, calibration standards and QC samples were prepared. For the LH effluent water, standards of 0, 5, 10, 20, 30, 50, 80, 100 and 150 µg/L were prepared. Using an Eppendorf pipette, 20 mL of Mili-Q water was added to 40 mL amber vial. Next, a THM standard stock II solution of 20 mg/L was added using suitable glass syringes to yield desired standard concentration.

The extraction procedure for THMs in analytical samples and standard solutions is described as follows:

1. Using Eppendorf pipette, place 20 mL of sample to be analyzed into vial

2. Using repeater pipet, add 4 mL of the pre-mixed Pentane plus internal standard.
3. 15 g of anhydrous Na_sSO_4 was added to each vial using a handmade glass dispenser.
4. Samples were capped and shaken for 15 minutes in a modified sieve shaker.
5. Using Pasteur pipet, transfer top organic layer to 2 mL autosampler vials. This step must be done under the hood.
6. Autosampler vials were stored in a freezer for at least 3 hours. Each sample was then inspected for ice. Any sample containing obvious ice particles was transferred into a new autosampler vial.
7. Samples were analyzed using a Hewlett-Packard 5890 Series II Gas Chromatograph (GC) within 14 days from extraction. The output data was processed in conjunction with the calibration curve obtained from the calibration standards.

3.4.8.2 HAA Extraction:

Using Eppendorf pipette, 30 mL of water sample was placed into 40 mL clear vial containing 1mL of 1g/L Na_2SO_3. The vials were placed in a 4^oC constant temperature room for less than 14 days until extraction.

When performing an extraction, it was necessary to bring the analytical samples to room temperature. In the mean time, calibration standards and QC samples were prepared. For the LH effluent water, standards of 0, 5, 10, 20, 30, 50, 80, 100 and 150

µg/L were prepared. Using an Eppendorf pipette, 30 mL of Mili-Q water was added to 40 mL clear vials. Next, the THM standard stock II solution of 20 mg/L was added using suitable glass syringes to yield desired standard concentration.

The extraction procedure for HAA in analytical samples and standard solutions is described as follows:

1. Using a 10 mL glass pipette, 1.5 mL of concentrated sulfuric acid (H_2SO_4) was added to each vial.
2. Using 25 µL glass syringe, 20 µL of surrogate (2,3-dibromopropionic acid) stock solution was added to each vial.
3. Using a repeater pipette, 3 mL of pre-mixed methyl tertiary-butyl ether (MTBE) plus internal standard (1,2,3-trichloropropane) was added to each vial.
4. Using the glass dispenser, 15 g of anhydrous Na_2SO_4 was added to each vial.
5. Samples were capped and shaken for 15 minutes in a sieve shaker.
6. While the samples were being shaken, 2 mL of acidic methanol + 5% H_2SO_4 was placed into labeled, 20 mL, clear vials using a repeater pipette.
7. The vials were then placed in a 50^{o}C water bath for 2 hours.
8. After removing from the water bath, 5 mL of $NaHCO_3$ solution was added to each vial using a repeater pipette.
9. 1 mL of pure MTBE was then added to each vial using a repeater pipette.
10. Samples were then capped and shaken for 2 minutes at 400 rpm using a rotary table shaker.
11. The top organic layer of each sample was placed into a 2 mL autosampler vial using Pasteur pipettes.

12. Similar to THM extraction procedure, autosampler vials were stored in a freezer for at least 3 hours to inspect for ice. Liquid portion of any sample containing observable ice was transferred to a new autosampler vial.
13. Samples were analyzed using a Hewlett-Packard 5890 Series II Gas Chromatograph (GC) within 14 days from extraction. The output data was processed in conjunction with the calibration curve obtained from the calibration standards.

3.4.8.3 Quality Assurance/Quality Control Procedures

The following QA/QC procedure was completed for each set of samples to ensure the quality of DBP measurement:

1. To ensure no interference in solvent as well as internal standard solutions, two solvent blanks and two solvent blank plus internal standards were inserted at the beginning positions of each run and between standard and analytical samples.
2. One out of every 12 analytical samples was spiked with 50 µL of HAA stock II solution. The spiked samples were always a duplicate of an analytical sample and was extracted, analyzed concurrently with the samples. The analyte recovery percentages were then evaluated.
3. When new stock solution was made, an old standard solution of 50 µL was extracted, analyzed concurrently with new standard solution to verify/compare the accuracy between old and new stock solutions.
4. Slopes of standard curves were also recorded to check the accuracy of the experimental procedure and accuracy of the instruments.

CHAPTER 4: FIELD EXPERIMENT RESULTS

This chapter provides results of different field experiments for different pilot designs to determine a suitable method to simultaneously control manganese and DBPs at the LHWTP. These experiments can be classified into two phases. In Phase I, experiments involved optimizing the first-stage filter operation to maximize the removal of iron, manganese, and NOM while minimizing DBP formation with or without pre-filter chlorine. In Phase II, experiments were conducted to verify the effectiveness of separating NOM and manganese removal into two different steps with intermediate free-chlorine dosing. The experiments were conducted on the two-stage pilot system built on-site at the LHWTP.

4.1 Phase I: Optimization of the First-stage Dual-Media Filter

Previous research conducted in 2008 at the LHWTP suggested that soluble manganese entering the filter was more likely adsorbed by the top anthracite media rather than the bottom greensand media, and that a higher dose of free chlorine (~5-8mg/L) was required to suppress manganese release which was the result of manganese-reducing bacteria activity (Russel (2008), Islam (2010)). To evaluate the feasibility of changing the full-scale plant filter media to standard anthracite and sand to allow for lower pre-filter chlorine dose without manganese release from the media, new anthracite media with no manganese oxide coating over a layer of silica sand were placed in the first-stage filter pilot column.

4.1.1 Without pre-filter chlorine:

The objective of this experiment was to achieve desired manganese removal through oxidation by permanganate only followed by coagulation and filtration. Permanganate dose and influent pH were optimized based on manganese removal criteria. These experiments were conducted over five days between 12/4/08 and 1/06/09.

By adjusting flow rate of the NaOH and $KMnO_4$ pumps, pH was adjusted to vary from 7.0 and 8.0 while permanganate dosing ranged from about 0.75 to 1.5 times the calculated stoichiometric dose to oxidize iron and manganese in the raw water. The polymer dose was kept at ~4.5 mg/L similar to that at full-scale. At each combination of pH and permanganate dose, the concentration of dissolved manganese along with turbidity and UV were measured. It should be noted that the stoichiometric dose in these experiments was calculated based on dissolved manganese and total iron in raw water rather than dissolved iron. This might have led to an overdose of $KMnO_4$ when the LHWTP was shut down. Under normal operation, the raw water was supplied from a tap on the main feed, and a low concentration of dissolved oxygen (~1 mg/L) was present in the raw water, causing a minimal difference between total and dissolved iron. However, this situation changed when the LHWTP was shut down and a submersible pump was placed in the well and utilized to supply the raw water for pilot work, causing higher concentrations of oxygen (~3-4 mg/L) and increases in the particulate fraction of iron in the raw water.

Figure 4-1 summarizes the concentration of influent/effluent manganese at different combinations of pH and $KMnO_4$. As expected, essentially, all effluent iron and manganese was in the dissolved form. The effluent data show that for all tested

conditions, iron was easily removed through oxidation followed by filtration; the effluent concentrations were mostly below the detection level. In contrast, only 83% manganese removal was achieved at the optimized testing condition with the lowest concentration recorded at 0.05 mg/L which barely meets the SMCL and is higher than the recommended level of 0.01 mg/L. Table 4-1 summarizes manganese and iron results for three different runs. The raw water quality was rather consistent during the experiments with the concentration of total manganese ranging from 0.15 to 0.19 mg/L while the concentration of total iron varied from 1.5 to 1.8 mg/L.

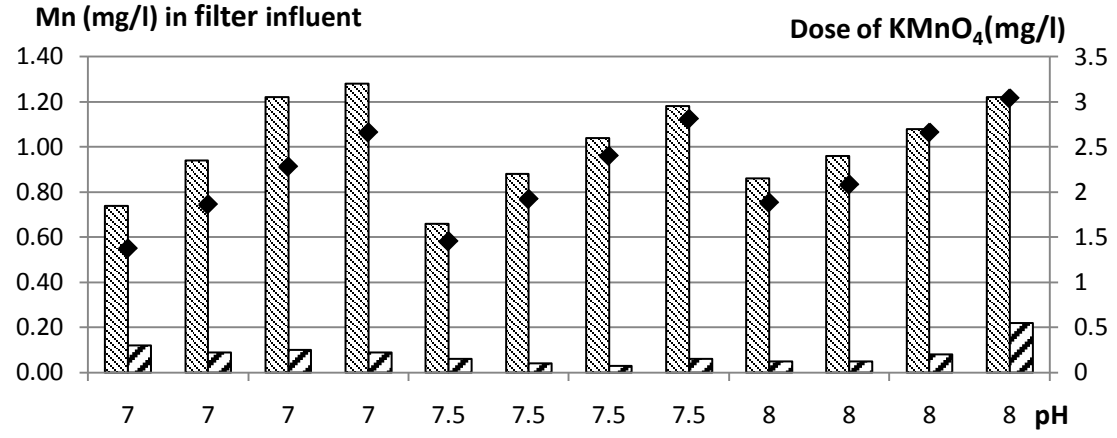

a)

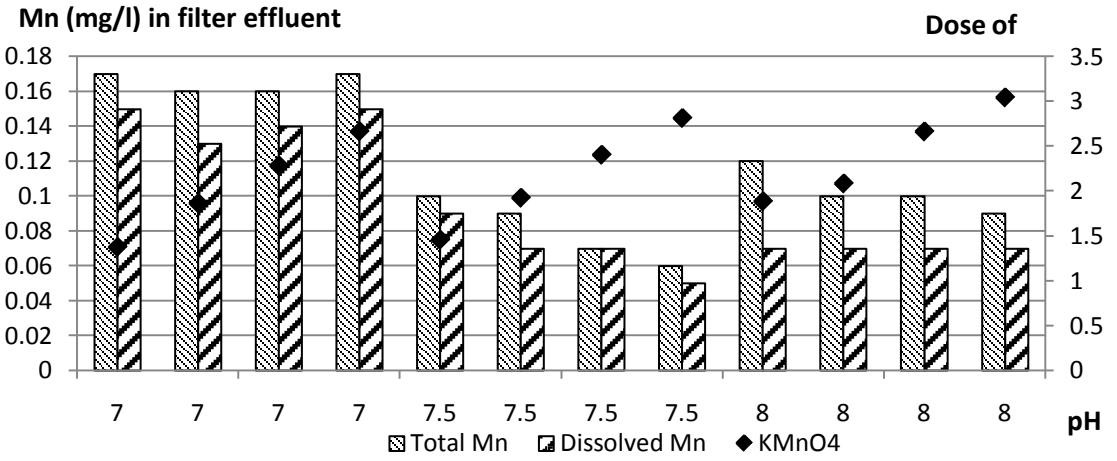

b)

Figure 4-1. The LHWTP pilot system: Impact of $KMnO_4$ dosing and pH on: a) Filter Influent. b) Filter Effluent.

Table 4-1. Summary data for experiments from 12/16/08 to 01/06/09

Date	pH	$KMnO_4$	Sample Location	Mn			Fe		
		mg/L		mg/L			mg/L		
		mg/L		Total	Colloidal	Dissolved	Total	Colloidal	Dissolved
12/16/2008	7	1.37	Raw	0.19			1.80		
		1.37	Filter Influent	0.74	0.12		1.70	0.13	
		1.37	Filter Effluent	0.17	0.15		0.22	0.06	
		1.86	Raw						
		1.86	Filter Influent	0.94	0.09		1.76	0.08	
		1.86	Filter Effluent	0.16	0.13				
		2.28	Raw						
		2.28	Filter Influent	1.22	0.10		1.75	0.00	
		2.28	Filter Effluent	0.16	0.14		0.18	0.11	
		2.66	Raw						
		2.66	Filter Influent	1.28	0.09			0.00	
		2.66	Filter Effluent	0.17	0.15		0.18	0.11	
12/30/2008	7.5	1.45	Raw	0.18	0.17	0.17	1.71	1.63	1.40
		1.45	Filter Influent	0.66	0.06	0.06	1.72	0.00	0.00
		1.45	Filter Effluent	0.10	0.09	0.10	0.00	0.00	0.00
		1.92	Raw						
		1.92	Filter Influent	0.88	0.04	0.06	1.67	0.00	0.00
		1.92	Filter Effluent	0.09	0.07	0.08	0.00	0.00	0.00
		2.4	Raw						
		2.4	Filter Influent	1.04	0.03	0.04	1.78	0.00	0.00
		2.4	Filter Effluent	0.07	0.07	0.07	0.00	0.00	0.00
		2.81	Raw						
		2.81	Filter Influent	1.18	0.06	0.03	1.65	0.00	0.00
		2.81	Filter Effluent	0.06	0.05	0.05	0.00	0.00	0.00
1/6/2009	8	1.88	Raw	0.16	0.16	0.16	1.54	1.26	1.27
		1.88	Filter Influent	0.86	0.05	0.03	1.46	0.00	0.00
		1.88	Filter Effluent	0.12	0.07	0.05	0.00	0.00	0.02
		2.08	Raw						
		2.08	Filter Influent	0.96	0.05	0.03	1.56	0.01	0.01
		2.08	Filter Effluent	0.10	0.07	0.05	0.06	0.02	0.00
		2.66	Raw						
		2.66	Filter Influent	1.08	0.08	0.03	1.47	0.01	0.02
		2.66	Filter Effluent	0.10	0.07	0.05	0.02	0.03	0.00
		3.04	Raw						
		3.04	Filter Influent	1.22	0.22	0.06	1.41	0.00	0.01
		3.04	Filter Effluent	0.09	0.07	0.05	0.05	0.04	0.02

In theory, increasing pH will help to increase the rate of manganese oxidation to particulate MnO_2, and thus lead to better manganese removal during the filtration step. But in fact, the benefit of increasing pH in these experiments is more noticeable at a pH of 7.5 rather than a pH of 8.0. Also, changing the $KMnO_4$ dosing had a different effect at each pH value. At a pH of 7, the dissolved manganese concentrations in the effluent were maintained in the range of 0.09 mg/L to 0.12 mg/L with no clear trend following the increase of $KMnO_4$ dosing from 0.75 to 1.75 times the stoichiometric dose. At a pH of 7.5, however, the effect of increase dosing was more noticeable with the concentration of dissolved manganese decreasing from 0.06 to 0.03 mg/L. At a pH of 8.0, the dissolved manganese started to increase at the permanganate dose of 1.25 times the stoichiometric dose (from 0.05 to 0.08 mg/L) and eventually a pink color on the membrane filter was observed at the highest dose (1.75 times the stoichiometric dose), which was an indication of $KMnO_4$ overdosing. Based on these results, a pH of 7.5 and a $KMnO_4$ dose of 1.25 times the stoichiometric dose were chosen for the next experiments.

The new data, along with previous data collected in 2007, suggested that pre-filter permanganate addition followed by coagulation and filtration cannot achieve the 0.01 mg/L targeted level of dissolved manganese in the dual-media filter effluent. The low concentration of dissolved manganese (<0.02 mg/L) in the full-scale finished water at the LHWTP was due to adsorption of manganese by manganese oxide coated media with continuous addition of pre-filter chlorine to regenerate adsorptive sites. The next logical step was to coat only the anthracite media with manganese oxide and apply a low pre-filter chlorine dose to enhance manganese removal in the pilot filter.

4.1.2 With pre-filter chlorine:

In these experiments, the anthracite media was pre-coated with manganese oxide and the pre-filter chlorine dose was maintained at a low level of 2 mg/L resulting in a filter influent chlorine residual of 0.3-0.6 mg/L and a filter effluent chlorine residual of 0.2 mg/L. The goal was to avoid a manganese coating from developing in the sand layer, minimizing the possibility of manganese release from the dual media column. Samples of media were taken back to UMass for coating level analysis. Due to constraints from both the LHWTP and UMass teams, these experiments were not conducted continuously and stretched over the summer of 2009. The full-scale LHWTP was shut down from January 15, 2009 to July, 2009; thus, some experiments were conducted with raw water supplied by a submersible pump inserted into the well casing that fed a small diameter pipe to the pilot column during the LH shut-down period. Due to low flow of the pilot pump, the concentration of dissolved oxygen in the raw water was higher than normal (~3 mg/L compared to ~1 mg/L). As a result of oxidation by dissolved oxygen, only about 25% of total iron existed as the dissolved form in the raw water prior to treatment.

Another change in this experiment was the increase of contact time between $KMnO_4$ and raw water by inserting a 25-foot long, 1-inch diameter, pipe loop ahead of the DM filter which provided an additional 1 minute of contact time at a flow rate of 1 gpm. The design originated from the possibility of moving the $KMnO_4$ and NaOH addition points from the main building to the well house which would create an additional one minute contact time prior to chlorine and polymer addition. This also represented a reversed order of oxidant addition compared to the full-scale which for the last few years has been free chlorine prior to $KMnO_4$. It was hoped that by providing

additional contact time, reactions between $KMnO_4$ and dissolved manganese and iron will be more complete, possibly reducing the pre-filter chlorine demand, and allowing for a lower pre-filter chlorine dose to establish desired chlorine residual entering the column.

To assess this idea, the chemical addition order of the pilot work was first set up in reverse order to that of the full-scale plant with the pipe loop inserted between oxidant addition points. After collecting DBP and TOC samples, the pilot plant was then switched back to mimic the chemical order of the full-scale plant (the loop was removed in this case) and another set of TOC and DBP samples were collected for comparison purposes. TOC and DBPs were measured at UMass. Timing of the work was crucial for this experiment. These two pilot conditions were tested using the same water quality, so either the raw water supply was diverted from the full-scale supply as occurred prior to January 6, 2009 or from the submersible pump to the pilot plant, but not a mixture of these two conditions.

4.1.2.1 Manganese removal:

Anthracite media were coated by soaking in a 100 mg/L permanganate solution. The media was then backwashed and allowed to soak in free-chlorine solution until use for experiments. An initial coating effort was conducted at the end of January 2009, resulting in a rather low coating level of 0.07 mg Mn/mg media. On February 10, 2009, the concentration of manganese across the filter was assessed to test the adsorption capacity of the newly-coated media. The results in Figure 4-2a show that the effluent dissolved manganese was higher than the influent (0.1 mg/L compared to 0.03 mg/L); this was unexpected as the media had a low coating level of manganese oxide and pre-

filter chlorine was used during the experiment. One possibility leading to this situation was a significant deposit of filter influent components such as NOM and particulate iron and manganese oxide on the GFC 0.2 µm membrane filter; these deposits may have acted as an additional filter, causing less manganese to pass through the membrane filter, thus inducing a lower filter influent dissolved manganese than actually occurred

To evaluate this possibility, samples were first filtered through a GF/F 0.45 µm filter to remove "coarse" components; the filtrate was then filtered through a GFC 0.2 µm filter and an ultra-filter. As shown in Figure 4-2b, the dissolved manganese concentration in the filter influent was still the same; no obvious cake filtration effect was recorded. So far it is not clear why the manganese concentration in the effluent was higher than that in the influent, given a low oxide coating level and the presence of pre-filter chlorine. A more obvious conclusion drawn from this experiment is that there was not manganese removal across the filter column, possibly due to the low coating level of manganese oxide on the anthracite surface.

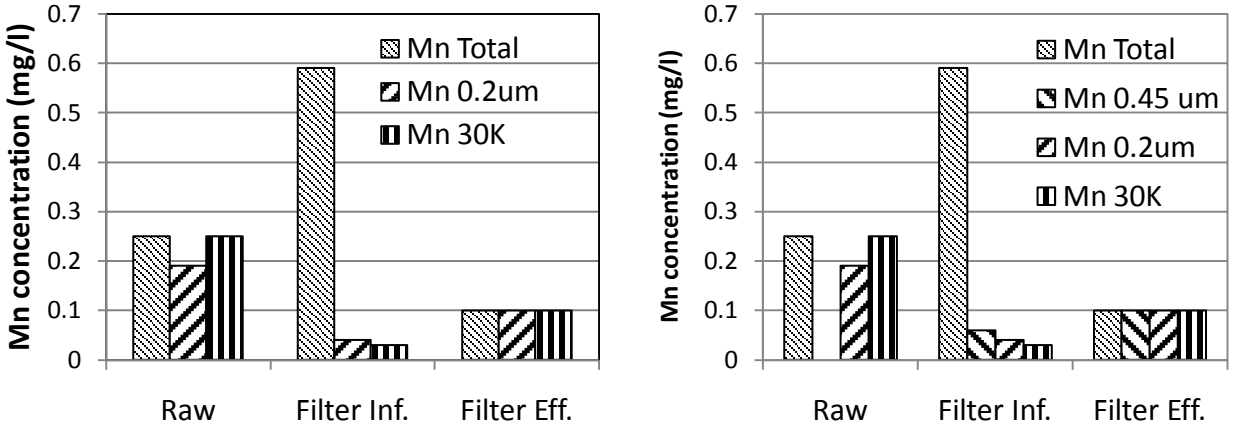

Figure 4-2. Dual media experiments with pre-filter chlorine: Manganese fractions at different locations. a) Without filtering through GF/F 0.45µm. b) Filtering through GF/F 0.45µm. pH =7.5, $KMnO_4$ = 1.25 times the stoichiometric dose.

On March 30, 2009, the anthracite media was recoated and sent to UMass for analysis. Extraction results showed that the coating increased from 0.12 mg Mn/g media to 0.22 mg Mn/g media. On April 15, 2009, a set of experiments to test the adsorption capacity of the recoated media was conducted. Testing conditions for these experiments are presented in Table 4-2, and the results are presented in Figure 4-3. The data suggest that the coated media had an obvious adsorption capacity, decreasing the dissolved influent manganese of 0.05 mg/L to 0.01 mg/L in the effluent. These results are consistent with previous research which proves that manganese adsorption combined with pre-filter oxidation, coagulation and filtration was able to decrease the manganese levels in the LH raw water to the desired level of 0.01 mg/L.

Table 4-2. The pilot-scale testing condition on 04/15/2009

Location/Conditions	**Parameters**	**Unit**	**Values**
$KMnO_4$ dose	--	mg/L	0.66
NaOCl dose	--	mg/L	2.9
Superfloc C572	--	mg/L	2.42
Raw Water	pH	---	6.5
	Total/dissolved Mn	mg/L	0.19/0.18
	UV_{254}	--	0.144
Filter Influent	pH	--	7.55
	Chlorine residual	mg as Cl_2/L	1.26
	Total/dissolved Mn	mg/L	0.41/0.05
Filter Effluent	Chlorine Residual	mg as Cl_2/L	0.2
	Total/dissolved Mn	mg/L	0.02/0.01

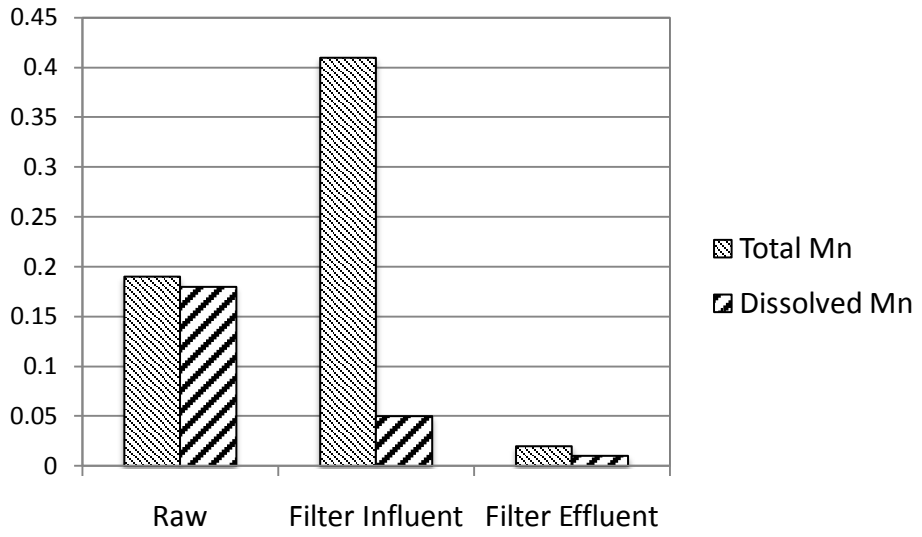

Figure 4-3. Dual media experiments: Manganese fractions at different locations on 4/15/2009.

4.1.2.2 DBP production:

This section summarizes results from three field trips to the LHWTP on 10/01/09, 10/22/09 and 11/03/09 to test the impact on DBPs of reversing the $KMnO_4$ and HOCl addition order and increasing the contact time between $KMnO_4$ and components in the raw water. On two days, 10/01/09 and 10/22/09, the chemical addition order was the same as at full-scale with HOCl added prior to $KMnO_4$. The order was reversed on 11/03/09 by switching $KMnO_4$ and NaOH addition to ahead of the NaOCl addition point.

For unknown reasons, on 10/01/09, no sign of manganese being removed across the pilot filter was recorded but since DBP production was not affected by the manganese adsorption process, the experimental data on 10/01/09 is still included and discussed here. Unfortunately, due to sample contamination during DBP extraction, the HAA5 data on 10/22/09 is not available here. The working conditions of the pilot system for each field trip are presented in Table 4-3.

Table 4-3. Working conditions of the pilot-system for each field trip.

Location/Conditions	Parameters	Unit	10/1/2009	10/22/2009	11/3/2009
Chemical addition order	---	---	Same	Same[1]	Reversed[2]
Raw Water	TOC	mg/L	3.85	NA	3.9
	Total/dissolved Mn	mg/L	0.18/0.17	0.21/0.19	0.20/0.19
	Total/dissolved iron	mg/L	2.11/1.92	2.03/1.72	2.16/1.69
	UV254	--	0.144	0.172	0.15
Filter Influent	Free Chlorine dose	mg as Cl_2/L	5	6.4	4.6
Filter Effluent	Chlorine Residual	mg as Cl_2/L	1.04	1.05	1.04
	TOC	mg/L	2.45	NA	2.55

[1] The pilot-scale chemical order was the same as full-scale with free-chlorine addition point ahead of $KMnO_4$ and NaOH addition points.

[2] The pilot-scale chemical order was the reverse of full-scale with $KMnO_4$ and NaOH addition points ahead of free-chlorine addition point.

Figure 4-4 presents the DBP data across the pilot-scale and full-scale plant on 10/1/2009. The results show rather similar DBP concentrations across the systems. For both systems, while the effluent instantaneous THM concentrations were lower than MCL of 80 µg/L, the 24hr THM and HAA5 were 116 and 131 µg/L, respectively, much higher than the MCLs for these components.

On 10/22/2009 and 11/03/2009, $KMnO_4$ and free chlorine addition points were switched to test the impact of increasing contact time between $KMnO_4$ and raw water on DBP production. The instantaneous DBP results on these days are presented in Figure 4-5. The results show no obvious impact of reversing the chemical addition order as well as increasing contact time on DBP production in the finished water. The HAA5 and THM are almost the same for the two different chemical addition orders; the differences in

DBPs for each test can be attributed to changes in chlorine dose or more likely sample extraction and data analysis. Based on these results, a different treatment technology is needed to control manganese and DBP at the LHWTP.

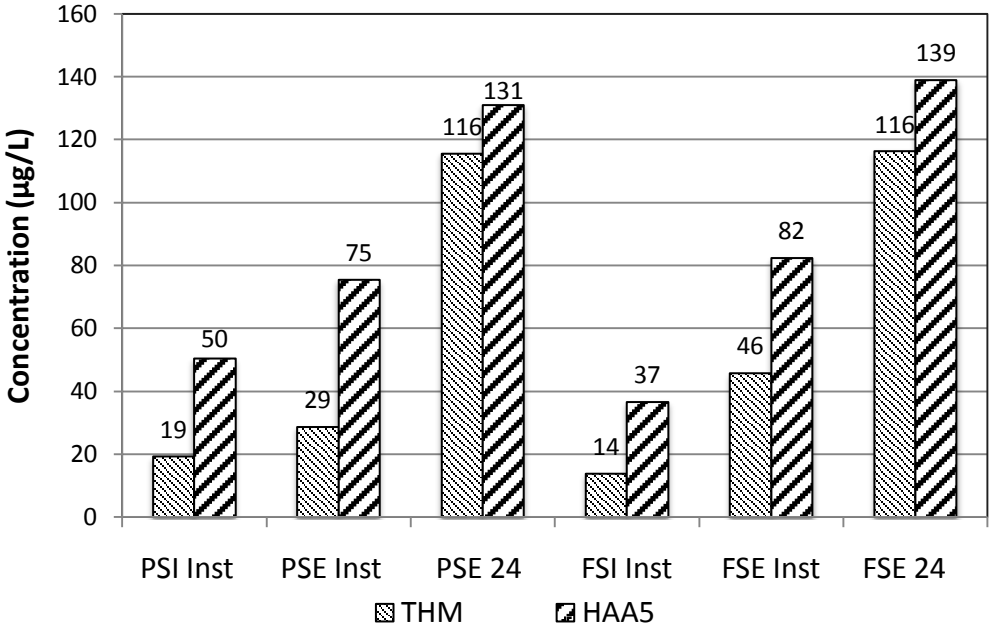

Figure 4-4.DBP concentrations across the pilot-scale and full-scale on 10/01/2009.

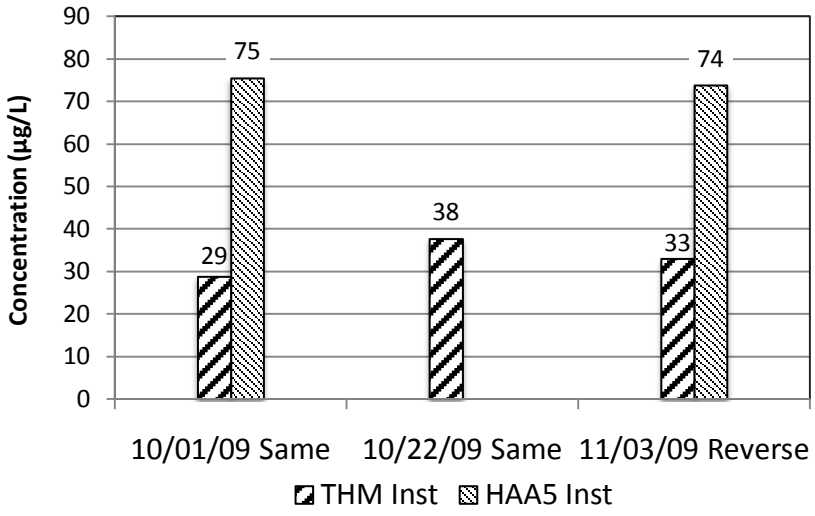

Figure 4-5. LH pilot-scale filter effluent instantaneous DBP data from different configurations. Same: the chemical order is the same as full-scale. Reversed: the chemical order is the reverse of full-scale with $KMnO_4$, NaOH ahead of free chlorine addition.

4.2 Phase II: Second-stage contactor

This section presents experimental data from the two-stage pilot-scale filter system with emphasis on decreasing DBP production. These experiments were conducted during three different field trips (12/21-12/22/09, 01/05-01/07/10, 01/12-01/13/10). Data for an experiment on 7/15/2010 which evaluated the impact of HLR variation on manganese removal are also included.

The pilot system ran continuously and was backwashed after an approximately 24-hour run consistent with the full-scale filter running cycle. A free chlorine dose of 2 mg/L which generated ~1mg/L chlorine residual was added in front of the second-stage contactor. The flow rate to the second-stage contactor was adjusted by wasting part of the first-stage effluent. The chemical addition order for the two-stage pilot-scale system followed the reversed order of the full-scale in which $KMnO_4$ and NaOH were added to the raw water in front of the pipe loop followed by cationic polymer (Superfloc C572). DBP and TOC samples were collected when the pilot system achieved desired performance based on UV and turbidity data. Manganese samples for concentrations at different second-stage bed depths were also collected and used for manganese removal model calibration. The objectives of these experiments were to (1) assess DBP formation when removing some NOM prior to free chlorine addition (2) assess the impact of second-stage contactor hydraulic loading rate (HLR) and bed depth on manganese removal.

4.2.1 Impact of NOM removal on DBP production

The $KMnO_4$ dose was initially set at 1.25 times the stoichiometric dose for the experiment on 12/21-12/22/09. Figure 4-6 summarizes manganese concentrations across

the two-stage pilot system during these experiments. At the beginning of the experiment when the $KMnO_4$ dose was set at 1.25 times the stoichiometric doses (equal to 0.70 mg as Mn/L), low concentrations of dissolved filter influent manganese (~0.02 mg/L) were recorded, leading to almost no manganese coming out of the first-stage filter (<0.01 mg/L). This was expected since the dual media must have had a some manganese coating developed from previous experiments.

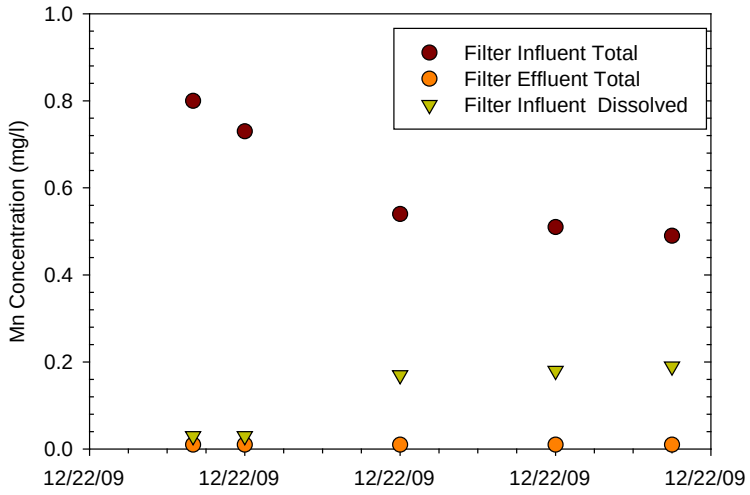

Figure 4-6. Manganese results across pilot-scale filter system on 12/22/09

In order to generate more dissolved manganese from the first-stage filter, the $KMnO_4$ dose was decreased to 1.0, 0.75 and then 0.5 times the stoichiometric dose. The results show that only at 0.5 times the stoichiometric dose (0.33 mg as Mn/L), about 0.18 mg/L of dissolved manganese entered the DM filter; since this value was equal to the dissolved manganese in the raw water, it was believed that the $KMnO_4$ was consumed only through reactions with dissolved iron and NOM. However, even with the high concentration of dissolved manganese entering the column, very low concentrations of DM filter effluent dissolved manganese were recorded.

The manganese data for the next two field trips on 1/5-1/7 and 1/12-1/13/2010 are summarized in Figure 4-7 below. The results from the prior field trip suggested that a longer run of the pilot system might be required to exhaust the unwanted adsorption capacity in the DM filter. In order to do that, the $KMnO_4$ dose was maintained at 0.5 times the stoichiometric dose, just enough to oxidize the dissolved iron in the raw water. After achieving good performance, the pilot system was operated for 24 hours. During the first run on 1/5/2010, obvious manganese removal occurred in the DM filter, resulting in dual-media effluent manganese concentrations of 0.02-0.04 mg/L. However, during the second run on 1/6/2010, after the first few hours, the adsorption capacity in the first-stage filter showed signs of exhaustion with an effluent manganese concentration of greater than 0.05 mg/L. Near the end of this run, the effluent manganese concentration went up to 0.19 mg/L, equal to the raw water manganese concentration on that day. A similar pattern of manganese concentration across pilot system was observed on 1/12-13/2010.

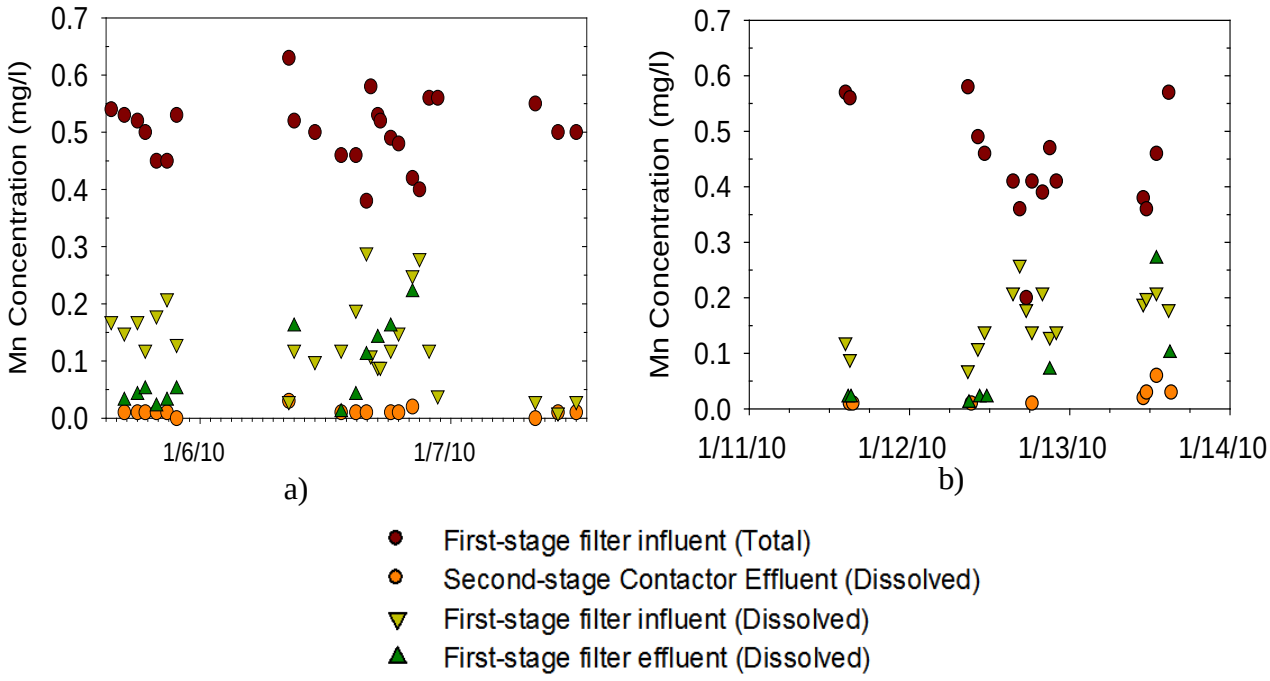

Figure 4-7. Manganese results across pilot-scale filter system on: a) 1/5-1/7. b) 12-1/13/2010

The full-scale and pilot-scale conditions at the time of collection of DBP samples are presented in Table 4-4. Similar TOC removal results (~1 mg/L) for the dual-media pilot-scale and the full-scale filters were observed for each field trip corresponding to UV_{254} decreases from 0.153 cm^{-1} to 0.038 cm^{-1}. The pilot-scale pre-filter chlorine dose was adjusted to produce a chlorine residual of 1.05 mg/L similar to the full-scale plant effluent.

Table 4-4. DBP testing conditions of the full-scale and pilot-scale plants

Date	Sampling Location	Two-Stage Pilot System			Full-Scale		
		TOC	Chlorine Residual	UV_{254}	TOC	Chlorine Residual	UV_{254}
		mg/L	mg/L as Cl_2	cm^{-1}	mg/L	mg/L as Cl_2	cm^{-1}
12.22.09	Raw	3.63	--	0.153	3.63	--	0.153
	DM[1]/FS Inf[2].	--	--	--	--	2.03	--
	DM Eff[3]	2.09	1.09	0.04	--	--	--
	Contactor/FS[4] Eff	2.21	1.08	--	2.28	1.05	0.038
01.06.10	Raw	3.33	--	0.159	3.33	--	0.159
	DM/FS Inf.	--	--	--	--	2.03	--
	DM Eff	2.17	0.79	0.04	--	--	--
	Contactor/FS Eff	2.11	0.80	--	2.26	1.06	--
01.13.10	Raw	2.87	--	0.157	2.87	--	0.157
	DM/FS Inf.	--	--	--	--	2.03	--
	DM Eff	1.98	1.04	0.039	--	--	--
	Contactor/FS Eff	1.88	0.85	--	2.2	1.06	0.039

[1]DM: First -stage dual-media column .
[2]Inf.: Influent.
[3]Eff: Effluent.
[4]FS: Full-Scale

The DBP data for each field trip are presented in Figure 4-8. The results show that both instantaneous and 24 hr DBP levels in the pilot-scale effluent were 80% less than DBP levels for the full-scale effluent and were in the range of 30-45 µg/L for HAA5 and 15-55 µg/L for THMs. It was obvious that removing 1 mg/L of NOM before dosing with free-chlorine helped to significantly decrease DBP levels in the filter effluent.

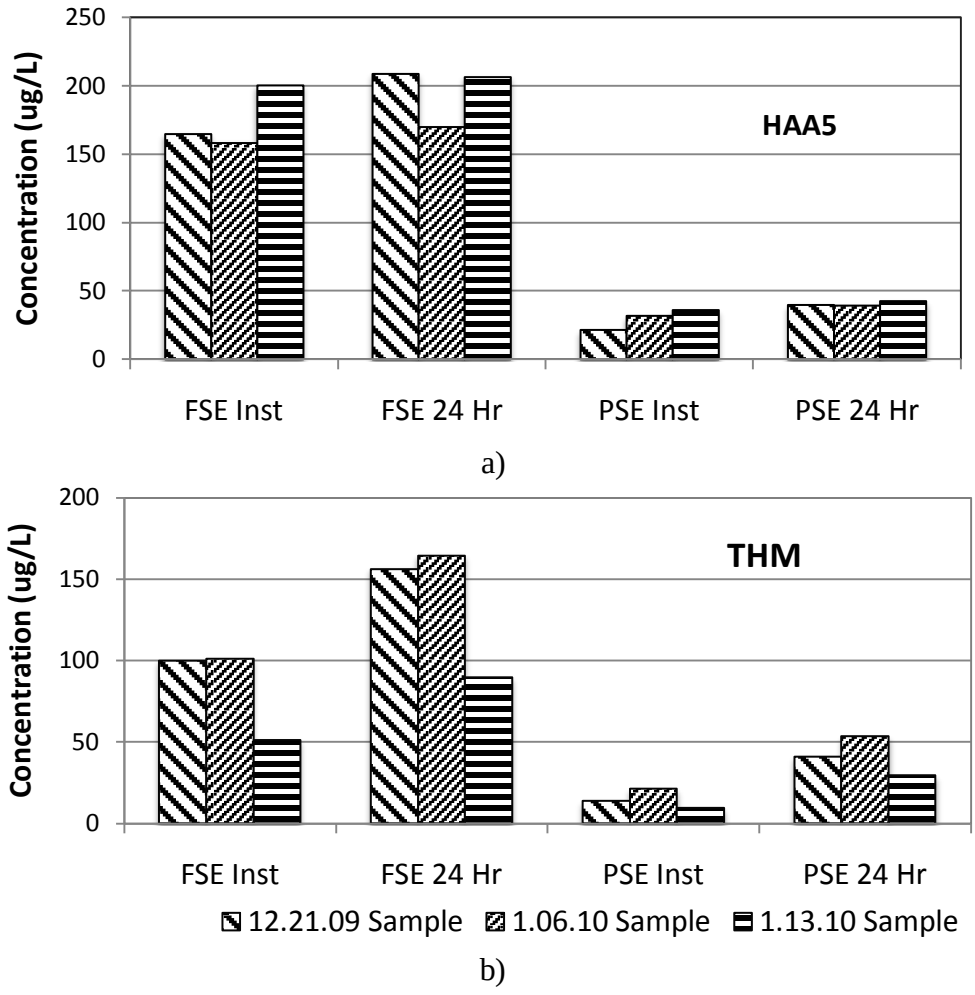

Figure 4-8.Comparison between the LHWTP Full-Scale and Pilot-Scale a) Instantaneous and 24 hours HAA5 results. b) Instantaneous and 24 hours THM results.

DBP impact is very large in this case. This could be due to the fact that pre-filter $KMnO_4$ reacted with NOM, converting NOM into different forms with lower DBP formation potential. Also, note that adding pre-filter chlorine for direct filtration maybe

the worst case for DBP impact, since beside NOM in the raw water, pre-filter chlorine can also react with deposited NOM in the full-scale filters. In conclusion, the two-stage filtration system is a suitable technology for the LHWTP to simultaneously control manganese and DBPs in the finished water.

4.2.2 Impact of HLR on manganese removal

To test the manganese removal capacity of the second-stage contactor, combinations of different HLR and influent manganese concentrations for the second-stage contactor were tested; the results are summarized in Figure 4-9. The manganese concentration in the second-stage contactor influent was adjusted by varying the $KMnO_4$ dose ahead of the DM filter.

The pre-filter chlorine of 1.33 mg/L was essentially unchanged for each testing condition. Decreasing the HLR leads to a decrease of dissolved manganese concentration along the bed depth. At an HLR of 20 gpm/ft^2, for all testing conditions, the dissolved manganese concentration in the filter effluent reached the SMCL of 0.05 mg/L at a bed depth of 30 inches, and decreased to as low as 0.02 at a bed depth of 40 inches. A manganese treatment goal of 0.01 mg/L could not be achieved until the HLR was decreased to 5 or 2 gpm/ft^2 at bed depth of 25 inch and 16 inch, respectively.

In conclusion, the DBP and manganese results prove that the two-stage filtration approach in which NOM and manganese were removed separately by different filters with intermediate chlorine addition is an effective technology for simultaneous control of manganese and DBPs at the LHWTP.

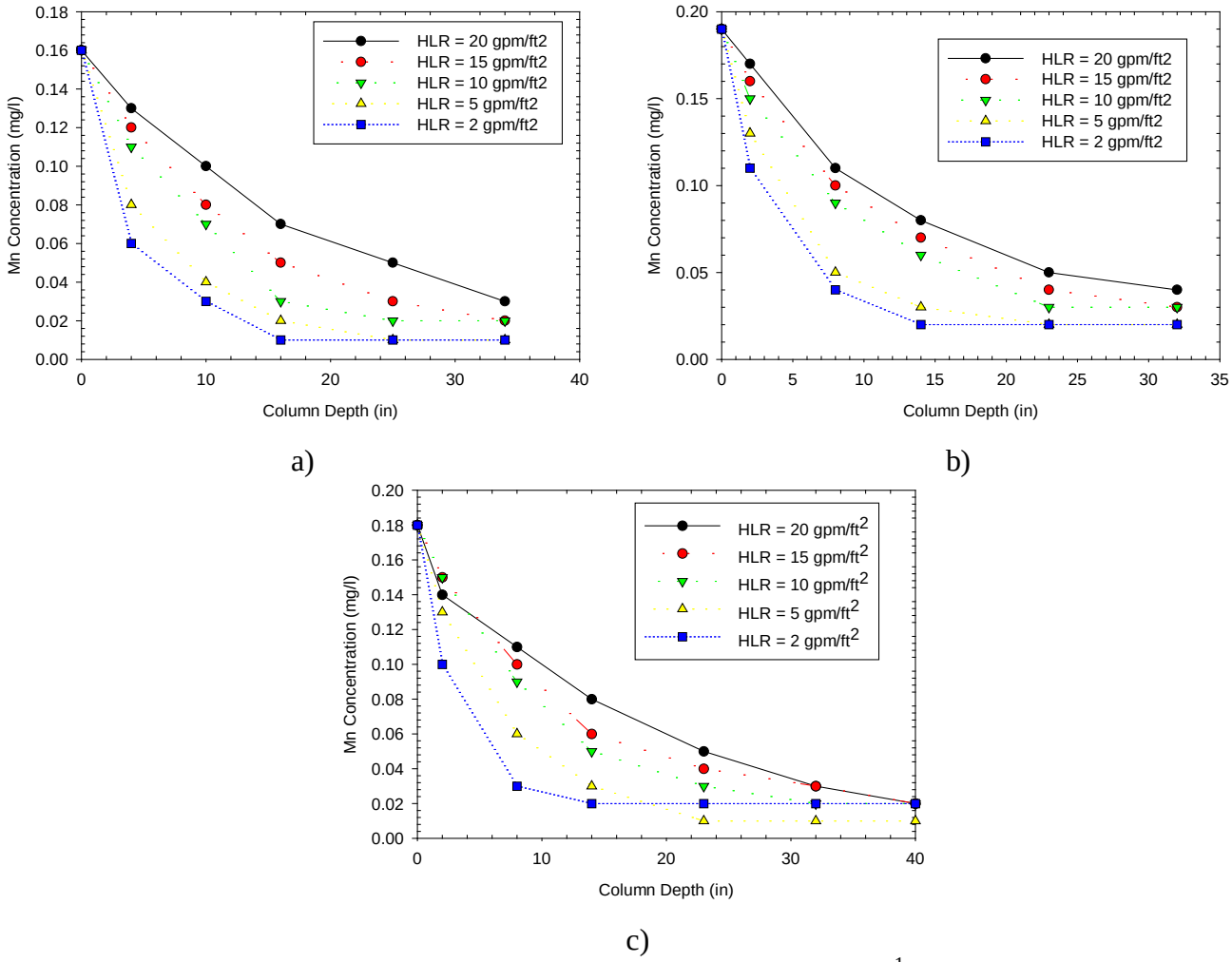

Figure 4-9. The LH Two-Stage Pilot System: Manganese profile[1] of the second-stage contactor at different HLRs on 7/15/2010 with pre-filter chlorine doses of 1.3 mg/L. a) Influent [Mn] = 0.16 mg/L, pH = 6.7, b) Influent [Mn] = 0.19 mg/L, pH = 7, c) Influent [Mn] = 0.18 mg/L, pH = 7.

[1] Manganese concentrations were measured by the low range HACH pocket kit method

CHAPTER 5: MODEL DEVELOPMENT AND RESULTS

The two-stage filtration approach has proved to be effective in removing manganese at high HLR. The next logical step is to determine design parameters for the second-stage contactor, including hydraulic loading rate and bed depth, to achieve the desired manganese removal. An existing mathematical model which simulates manganese removal via adsorption and oxidation onto the surface of OCM was modified and used to guide the determination of design parameters. A thorough review of this model as well as model results for the LHWTP are provided in this chapter.

5.1 MODELING BACKGROUND

5.1.1 Initial Model Efforts

A number of researchers have modeled the removal of dissolved manganese by oxide coated media over the past several decades. After the initial effort of Nakansiki (1967), Coffey (1993) characterized steady-state manganese removal by OCM based on the following equations:

$$Mn^{2+} + MnO(OH)_{2s} = MnO_2.MnO_{2(s)} + 2H^+ \qquad \text{(Equation 5-1)}$$

$$MnO_2.MnO_{2(s)} + HOCl = 2MnO_2 + H^+ + Cl^- \qquad \text{(Equation 5-2)}$$

A fixed number of potential adsorption sites that were continuously regenerated through the addition of free chlorine was assumed in this model. Based on these early efforts, a dynamic model for soluble Mn^{2+} removal by oxide coated filter media was developed by Merkle et al. (1997). This model incorporated a modified Gnielinski mass transfer correlation for the liquid film boundary layer, the Freundlich isotherm, modified

Keinath correlation for intracoating surface diffusion and hydrodynamic dispersion to describe the following overall process:

$$Mn^{2+} + SITE + HOCl \Rightarrow MnO_x\,(s) + SITE \qquad \text{(Equation 5-3)}$$

Equation (5-3), a simplified version of Coffey's equations, was the core of the Merkle (1997) model. Due to the lack of detailed knowledge, "SITE" and MnO_x , representing the adsorptive site and the product of oxidation of dissolved Mn^{2+}, respectively, are used. Intermittent and continuous regeneration models corresponding to two working modes were developed. To construct these mathematical models, Merkle et al. (1997) conducted a series of experiments to investigate the chemical makeup and composition of the natural and synthetic oxide coating on the filter media surface. Based on the similarity between coated media and GAC characteristics, internal transport kinetics could be a factor in dissolved manganese adsorption and so were included in the model. Merkle et al. (1997) divided the total adsorption capacity into kinetically "available" and "unavailable" pools relating to external adsorption sites and internal sites, respectively. The transport processes in the Merkle model can be summarized by following equations:

$$Mn^{2+} + Site_{AV} \overset{k_1}{\leftrightarrow} Mn^{2+}(Ads_{Av}) + Site_{Un} \overset{k_2}{\leftrightarrow} Mn^{2+}(Ads_{Uv}) + Site_{Av} \qquad \text{(Equation 5-4)}$$

$$Sites_{total} = Site_{Av} + Site_{Un} = K\,[Mn^{2+}]^{1/n} \qquad \text{(Equation 5-5)}$$

$$Mn^{2+}(Ads_{Av}) + HOCl\ (fluid) \overset{k_r}{\leftrightarrow} MnO_x + Site_{Av} \qquad \text{(Equation 5-6)}$$

Where:

k_1: fluid to surface transfer rate coefficient, m/s

k_2 : internal transport rate coefficient, m/s

k_r: apparent surface oxidation rate constant, $L^2\ mol^{-1}\ min^{-1}$.

$Site_{Av}$: sorption site kinetically "available" by film transport.

$Mn^{2+}(Ads_{Av})$: Mn^{2+} adsorbed to "available" sites.

$Site_{Un}$: adsorption site kinetically "unavailable"

$Mn^{2+}(Ads_{Uv})$: Mn^{2+} adsorbed to "unavailable" sites.

$Sites_{total}$: total sorption sites specified by a Freundlich isotherm

K, n: Freundlich isotherm constants.

In order to simplify the mathematical complexity, the authors assumed that the number of adsorption sites was fixed and independent of the amount of deposited manganese oxide; this assumption, as discussed in Chapter 2, may not be valid over time. Also, changes in pH near the media surface due to the sorption and oxidation were not taken into account in these models.

Mass balance equations describing the transport processes in the Merkle model are presented in Equation 5-7 to Equation 5-11.

$$\frac{\partial C_{1b}}{\partial t} = u\frac{\partial C_{1b}}{\partial z} + D_L\frac{\partial^2 C_{1b}}{\partial z^2} - k_f A_V\left[\rho_b X_a\left(\frac{1-\varepsilon}{\varepsilon}\right) - C_{1b}\right] \quad \text{(Equation 5-7)}$$

$$\frac{\partial C_{1sa}}{\partial t} = k_f A_V(X_a - \varepsilon\rho_b^{-1}C_{1b}) - \frac{\partial C_{1sa}}{\partial t} \quad \text{(Equation 5-8)}$$

$$\frac{\partial C_{1sa}}{\partial t} = k_s A_V(X_u - C_{1sa}) \quad \text{(Equation 5-9)}$$

$$X_a + X_u = KC_{1b}^{1/n} \quad \text{(Equation 5-10)}$$

$$X_a = AFR(X_a + X_u) \quad \text{(Equation 5-11)}$$

Where:

ε: bed porosity

u: pore velocity (L/T)

D_L: dispersion coefficient (L^2/T)

A_v: specific surface area (L^2/L^3)

P_b: bulk density of filter media (M/L^3)

K: fluid to solid mass transfer coefficient (L/T)

AFR: available fraction of adsorption sites. AFR = $Site_{Av}/Site_{Total}$.

C_{1b}: bulk aqueous-phase manganese concentration (mol/m^3)

C_{2b}: bulk aqueous-phase of HOCl concentration[1] (mol/m^3)

C_{1sa}: concentration of absorbed manganese (mol/kg media)

X_a: mass or available sorption sites per mass of filter media.

X_u: mass of unavailable sorption sites per mass of filter media

kf: mass transport coefficient (m/s)

For the continuous mode, the author simultaneously fitted AFR and k_r to experimental data. Since k_r should be constant for all tested conditions, the fitted value of k_r was then used for other experiments and AFR was the only fitting parameter (Merkle et al. 1997).

The results presented by Merkle et al. (1997) showed that the model could consistently simulate manganese removal in the lab-scale system. However, the model failed to simulate field data; the authors suggested that the variation in composition between the lab and field media may contribute to this problem. In addition, the model didn't succeed in simulating both field and lab data under extreme testing conditions of low sorption capacity and high flow rate. For that, the authors did not provide an explanation.

[1] HOCl concentrations were used in the model since HOCl is much stronger oxidant compared to OCl^-

5.1.2 Recent Model Efforts

Zuravnsky (2006) and Knocke et al. (2010) conducted experiments to investigate the potential use of a $MnO_{x(s)}$-coated media process in a water treatment train as a post-filtration adsorptive contactor. The results showed an effective manganese removal for HLR up to 24 gpm/ft^2. With the proven effectiveness of a post-filter contactor for manganese control, a mathematical model to simulate manganese removal by a post contactor at high HLR would be very useful. Based on the research of Merkle et al. (1997), Zuravnsky (2006) and Subramaniam (2010), former students of Dr. Knocke at Virginia Tech, were successful in developing a model to simulate manganese removal as a function of bed depth under high loading rate (16-24 gpm/ft^2) for the continuous regeneration mode. The field sites in their research were the tap water at the Virginia Tech laboratory, the Blacksburg Christiansburg-VPI Water Authority water treatment facility, and the Newport New water treatment plant (NNWTP). A post-contactor was constructed on-site and used pyrolucite as filter media and the full-scale combined filter effluent as the pilot influent. In general, the design allowed the operator to vary HLR, pH, temperature, manganese concentration, and chlorine residuals in the influent.

To overcome the failure of Merkle model under high flow rate, Zuravnsky (2006) removed the internal transport phenomenon (represented by the AFR parameter) and focused solely on steady-state conditions rather than non steady-state as in the Merkle model. In the Zuravnsky model, manganese transport processes include:

- Advection and dispersion (represented by the pore velocity (U) and dispersion coefficient D_L)
- Film diffusion (represented by mass transfer coefficient (k_f))

- Adsorption (represented by Freundlich constants (K,1/n))
- Second-order surface oxidation (represented by the oxidation constant k_r)

The processes are illustrated in Figure 5-1.

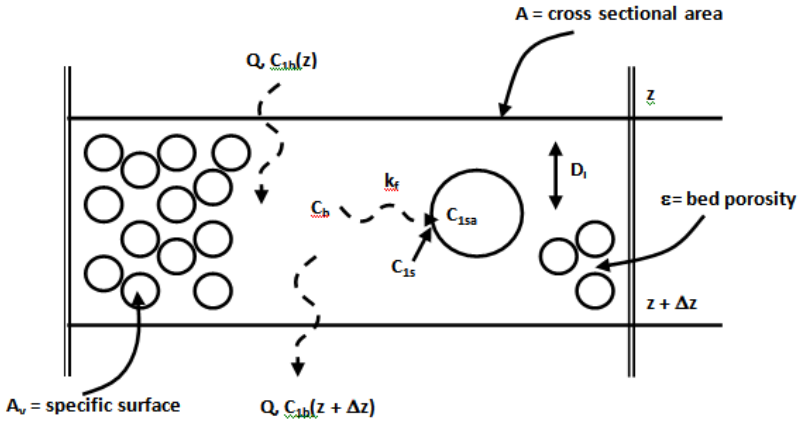

Figure 5-1. Transport processes for manganese in an incremental depth of media (Zuravnsky 2006)

The mass balance equations for manganese and free chlorine in the Zuravnsky (2006) model are as follows:

$$0 = -U\frac{\partial C_{1b}}{\partial z} + D_L\frac{\partial^2 C_{1b}}{\partial z^2} - k_f A_v\left(\frac{1-\varepsilon}{\varepsilon}\right)\left[C_{1b} - \left[\frac{C_{1sa}}{K}\right]^n\right] \quad \text{(Equation 5-13)}$$

$$0 = -U\frac{\partial C_{2b}}{\partial z} + D_L\frac{\partial^2 C_{2b}}{\partial z^2} - \rho_b k_r C_{1sa} C_{2b} \quad \text{(Equation 5-14)}$$

$$0 = \frac{k_f A_v}{\rho_b}(1-\varepsilon)\left[C_{1b} - \left[\frac{C_{1sa}}{K}\right]^n\right] - k_r \varepsilon C_{1sa} C_{2b} \quad \text{(Equation 5-15)}$$

$$C_{1b(in)} - C_{1b(out)} = C_{2b(in)} - C_{2b(out)} \quad \text{(Equation 5-16)}$$

Where

k_r: oxidation rate constant (m^3/ mol.s)

A numerical method utilizing Taylor series and Newton method was coded in the Matlab 7.0 environment to solve the above equations. To calibrate the model, Zuravnsky (2006) used k_f as a fitting parameter and adopted a value for kr, the rate of oxidation of adsorbed Mn^{2+} and free chlorine, from the Merkle et al. (1997) model. To support this

idea, the author also conducted a model analysis which showed no significant impact of k_r and K (Freundlich constant) on the model results (see Figure 5-2). The results in Zuravnsky (2006) showed that the model captured manganese removal in a post-contactor at different bed depths under a high loading rate of 24 gpm/ft^2 (see Figure 5-3).

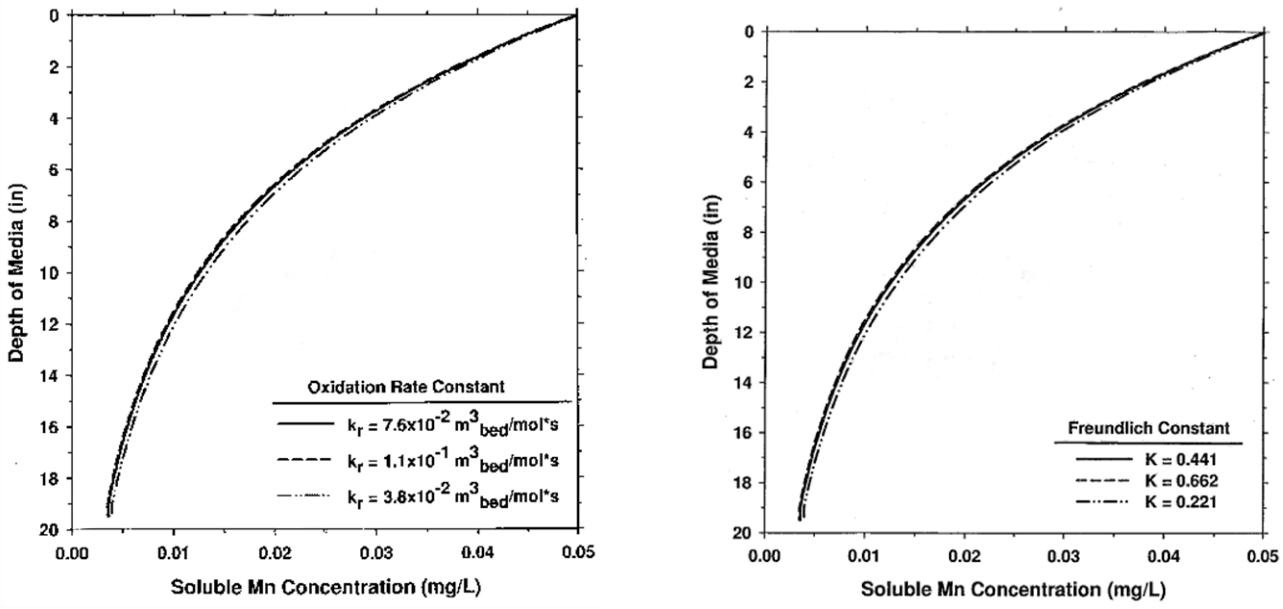

a) b)

Figure 5-2. Zuravnsky model analysis: a) Impact of surface oxidation rate: k_r. b) Impact of Freundlich: K (Zuravnsky 2006)

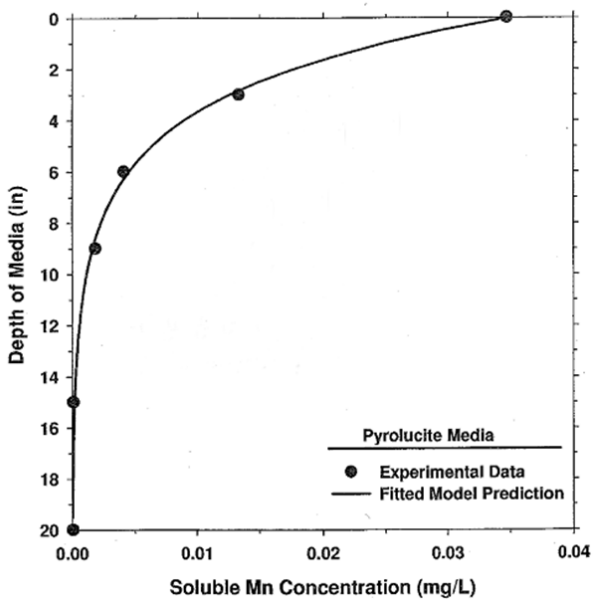

Figure 5-3. Post-contactor data and model results. Influent water: HLR = 24 gpm/ft^2, pH = 7.5, HOCl = 1.9 mg/L, Mn^{2+}= 0.035 mg/L (Zuravnsky 2006)

5.2 MODEL DEVELOPMENTS:

Because of its simplicity and effectiveness under high flow rates, the model developed by Zuravnsky (2006) was chosen to simulate manganese adsorption and oxidation for the second-stage contactor at the LHWTP as part of the contactor design for the AWC. Upon analyzing the Matlab code for the model received from Virginia Tech, errors in the Zuravnsky (2006) model were found. Modifications from the Zuravnsky (2006) model to fix these errors as well as a sensitivity analysis are presented in this section.

5.2.1 Modifications from Zuravnsky Model

5.2.1.1 Model Fitting

A complete analysis of the Zuravnsky model was conducted. The results are consistent with the Zuravnsky (2006) analysis except for impacts of the oxidation rate (k_r) and Freundlich constant (K) (see Figure 5-4). Compared to the Zuravnsky (2006) results (Figure 5-2), Figure 5-4 shows that k_r and K do have significant impacts on model output.

According to Zuravnsky (2006), one of the reasons for using k_f as a fitting parameter rather than k_r was that the k_r value, taken from Merkle et al. (1997), should be constant and unchanged under all testing conditions. While this notion is correct for the

data in Merkle et al. (1997), it is not generally correct. In Merkle's model, the internal transport of adsorbed Mn^{2+} was taken into account and represented by the AFR parameter. To determine kr, Merkle et al. (1997) first simultaneously fitted AFR and k_r. The best-fit k_r was used to simulate the remaining data with AFR being fitted. Because of this fitting practice, the k_r value from the Merkle et al. (1997) model should have not been used in the Zuravnsky (2006) model which didn't include the impact of the internal transport phenomenon. Put in another way, compared to the k_r value in Merkle's model, the k_r parameter in Zuravnsky (2006) does not represent the oxidation rate but rather is a lumped parameter which represents the impact of both oxidation and internal transport processes.

In addition, the value of the external mass transfer coefficient (k_f) can be calculated from first principles and should not be a function of water quality or media type. In the Merkle et al. (1997) model, a simplified form of Gnielinski's correlation was used to calculate kf.

$$Sh = (2 + 0.644R^{1/2}Sc^{1/3})[1+1.5(1-\varepsilon)] \qquad \text{Equation (5-17)}$$

Where:

Sh: Sherwood number. $Sh = k_f.d/D_{ff}$

R: Reynolds number. $R = u.d/\upsilon$

d: hydraulic diameter (m).

Sc: Schmidt number. $Sc= \upsilon/D_{ff}$

υ : Kinematic viscosity (m^2/s)

D_{ff}: molecular diffusion coefficient (m^2/s)

Based on this discussion, k_r should be used as a fitting parameter in the model rather than k_f which can be calculated by a generalized correlation such as Gnielinski. A calibration algorithm, using the least-squares method and k_r as a fitting parameter, was integrated into the Zuravnsky (2006) code.

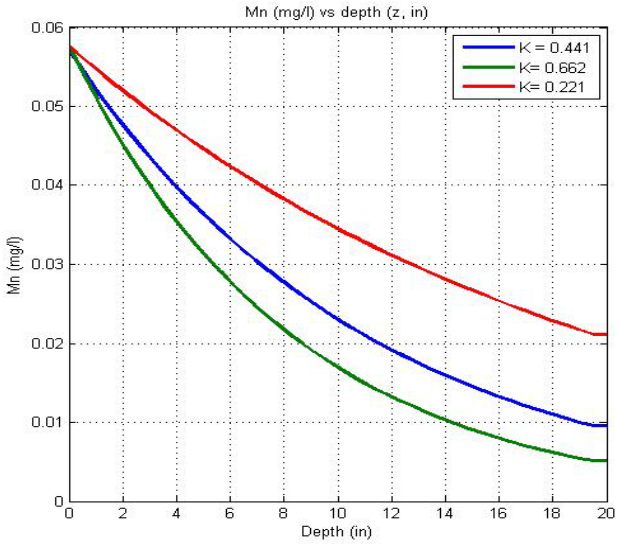

a)

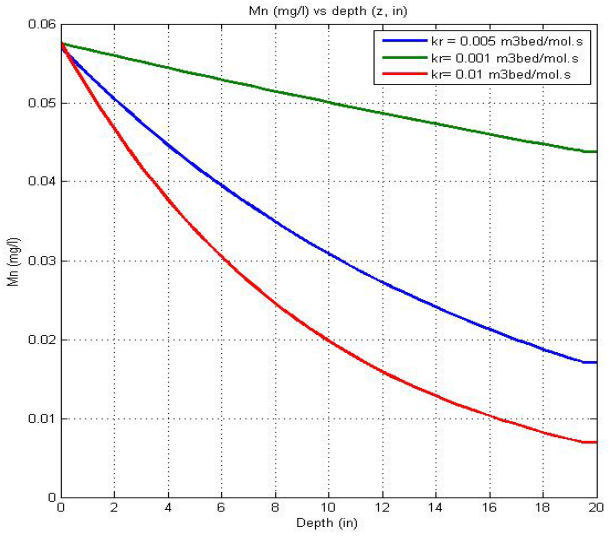

b)

Figure 5-4. Zuravnsky model sensitivity analysis: a) Impact of Freundlich constant (K) on model output. b) Impact of oxidation rate constant (k_r) on model output. (Other model parameters were kept the same as in the Zuravnsky (2006) sensitivity analysis)

5.2.1.2 Role of Free Chlorine in the Model

In the Zuravnsky (2006) model, the oxidation of adsorbed manganese by free chlorine was assumed to be a second-order reaction as follows:

$$r = -k_r \varepsilon C_{1sa} C_{2b} \qquad \text{Equation (5-18)}$$

Pilot-scale post-contactor data collected at the NNWTP by Virginia Tech researchers was used to test the simulating ability of the modified model which used k_r as the fitting parameter. Testing conditions at the NNWTP are presented in Table 5-1.

Table 5-1. The NNWTP post-contactor testing conditions (Subramaniam 2010)

HLR	pH	Total Cl_2	HOCl
gpm/ft^2	--	(mol/m^3)	(mol/m^3)
16	6.5	0.0210	0.0188
16	7.5	0.0248	0.0115
20	6.5	0.0229	0.0205
20	7.5	0.0229	0.0106
24	6.5	0.0248	0.0222
24	7.5	0.0248	0.0115
24	6.5	0.0972	0.0871
24	7.5	0.0991	0.0459

Figure 5-5 shows fitted k_r values as a function of HOCl concentration based on manganese data collected at the NNWTP. It should be noted that the model also accounted for changes in manganese adsorption capacity at different pH by selecting appropriate Freundlich constants obtained from manganese uptake experiments (see Section 5.2.3). Overall, the fitted k_r decreases with the increasing HOCl concentration and varies in a relatively wide range from 0.05×10^{-4} m^3bed/mol.s to 4.5×10^{-4} m^3bed/mol.s.

For example, at pH = 7.5, a four-fold increase of influent HOCl concentration results in a decrease of fitted k_r by factor of five. These results suggest that the model does not capture all of the manganese transport processes or their dependence on water quality and testing conditions, or both, leading to different fitted k_r values which in theory should be constant.

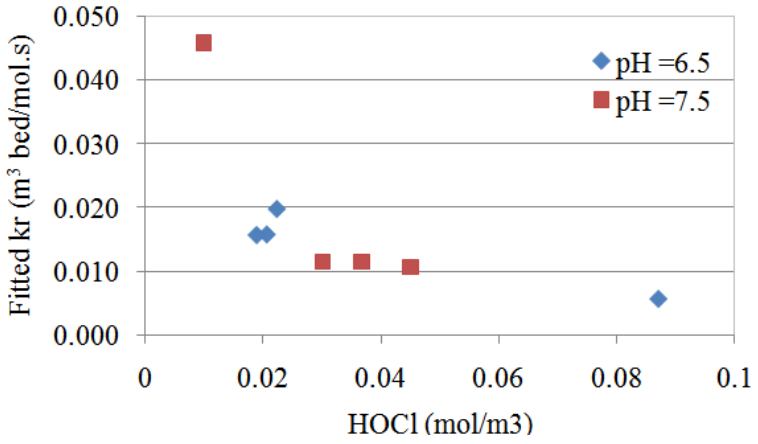

Figure 5-5. Model results for the NNWTP pilot-scale data: fitted k_r vs. influent HOCl at different pH.

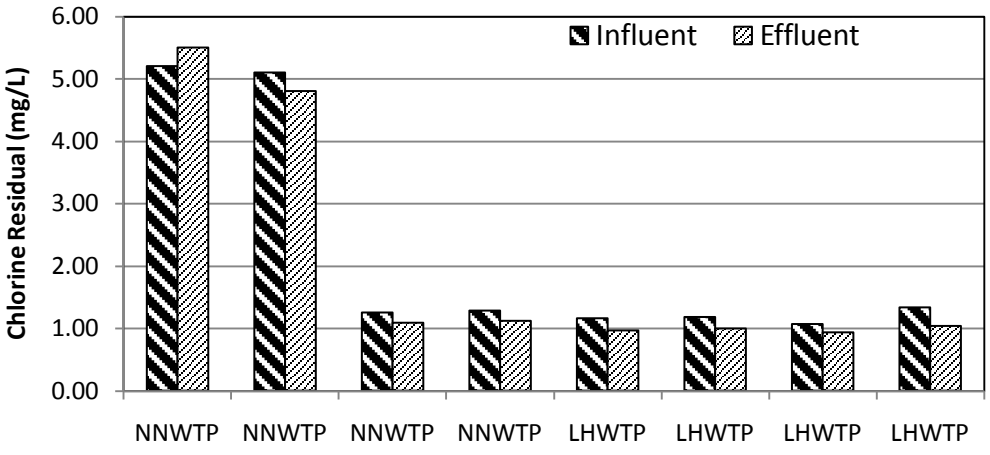

Figure 5-6. Chlorine residual concentrations in the pilot-scale contactor influent and effluent at the LHWTP and NNWTP pilot plant.

Moreover, during experiments at both LHWTP and NNWTP, chlorine residuals were relatively constant along the post-contactors (see Figure 5-6). The results suggest that free-chlorine concentrations were much higher than free chlorine demand for surface oxidation on the pyrolucite media; thus, the surface oxidation rate possibly did not depend on free chlorine concentration in these cases or only require that a minimum level of chlorine be present. Based on this discussion, free chlorine concentration was removed from Equation 5-18, making the surface oxidation a "pseudo" first-order reaction as described below:

$$r = -k_r' \varepsilon C_{1sa} \qquad \text{Equation (5-18)}$$

Where:

k_r': surface oxidation rate constant, s^{-1}.

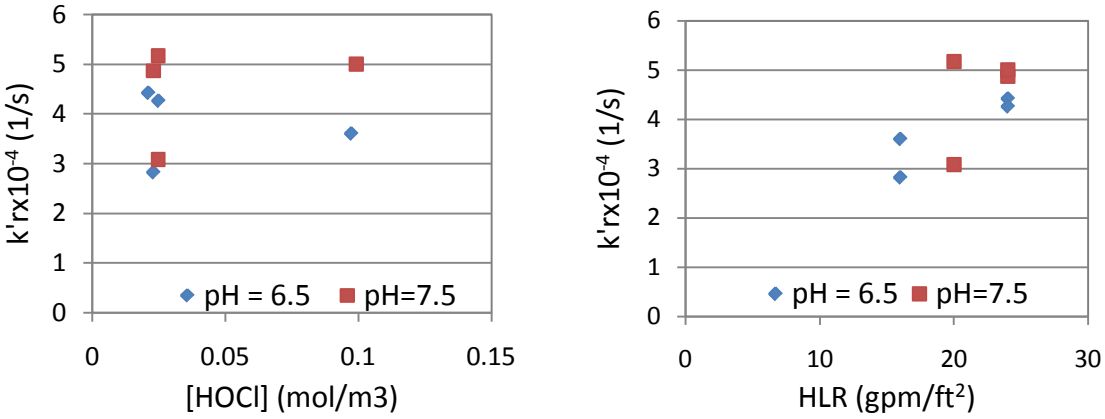

Figure 5-7. Model results for the NNWTP pilot-scale data: a) Fitted k_r' vs. influent HOCl at different pH (Subramaniam 2010); b) Fitted k_r' vs. HLR.

As shown in Figure 5-7a, by removing the HOCl concentration from the surface reaction, for all testing conditions, the fitted values of k_r' vary in a relatively narrow range of 2.9×10^{-4} s^{-1} to 5.5×10^{-4} s^{-1} compared to the k_r range of 0.05×10^{-4} m^3bed/mol.s to 4.5×10^{-4} m^3bed/mol.s. Figure 5-7b shows a plot of k_r' vs HLR. The results suggest a possible dependence of k_r' on HLR; an increase in HLR leads to an increase in k_r'. In principle, k_r' should not depend on HLR, the impact of HLR on k_r' is likely due to a

relationship between k_f, which depends highly on HLR, and k'_r. To avoid confusion later, the modified Zuravnsky (2006)model is called UM-model and used to simulate the performance of the second-stage contactor at the LHWTP

In conclusion, modifications in the UM-model compared to the Zuravnsky (2006) model are listed below:

1. The modified oxidation rate (k'_r) is used as a fitting parameter instead of the mass transfer coefficient (k_f).
2. An algorithm to calibrate the model based on least-square method was incorporated.
3. The free chlorine concentration was removed from the surface reaction equation.

5.2.2 UM-model Values:

As in Zuravnsky model, parameters used in UM-model can be classified into three groups: (1) initial values, (2) test conditions, and (3) calculated values. Most of data presented in Table 5-2 was taken from the Zuravnsky (2006) model since the LH second-stage contactor has the same design and pyrolucite media (8x10 mesh size).

In the UM-model, k_f was calculated using the Ohashi correlation which was claimed to be valid for Reynolds (Re) in the ranges of 5.8 to 500 (Roberts et al. 1985).

$$Sh \approx \frac{k_f d_p}{D_{ff}} \approx \left(2 + 1.21 R^{1/2} Sc^{1/3} \right) \qquad \text{(Equation 5-19)}$$

Where:

Sh = Sherwood number
k_f = liquid to solid mass transfer coefficient (m/s)
d_p = particle diameter (m)
D_{ff}= bulk liquid diffusivity (m^2/s) = $1x10^{-9}$ m^2/s @ 10°C
Re = Reynolds number. $Re = ud_p/\upsilon$)
Sc = Schmidt number. $Sc = \upsilon/D_{ff}$
υ = kinematic viscosity = $1.0006x10^{-6}$ m^2/s @ 10°C

Table 5-2. Summary of model parameters used in the sensitivity analysis of UM-model.

Type	Model Parameter	Symbol used in model	Value	Unit	Source/Comment
Initial values	Porosity	ε	0.52	m^3 water/ m^3 bed	Zuravnsky (2006)
	Bulk density	R_o	1992	kg media/ m3 bed	Zuravnsky (2006)
	Media diameter	d_p	2.20E-03	m	Zuravnsky (2006)
	Kinematic viscosity	k_{visc}	1.00E-06	m^2/s	Value at 10^oC
	HOCl acidity constant	k_{const}	2.51E-08	--	Benjamin (2010)
	Diffusion coefficient	D_{ff}	1.00E-09	m^2/s	Zuravnsky (2006)
	Freundlich isotherm constants	K	0.88	$[(mol/kg)/(mol/m3)]^{(1/n)}$	Value at pH =7.5 –(Subramaniam 2010)
		nn	1/1.19	--	
Testing Condition	Total bed depth	L	20	inch	
	Hyraulic loading rate	HLR	10	gpm/ft	
	Initial manganese concentration	C10	0.28	mg/L	
	pH	pH	7.5	---	
	Contactor column diameter	d_{ia}	0.075	m	
	Free chlorine in	C_2	1.33	mg/L as Cl_2	
Calculated values	Specific surface area	Av	7260	m^2 media /m^3 media	$Av = 6x(dp)^{-1.16}$ - Zuravnsky (2006)
	Mass transfer coefficient	k_f	3.08E-5	m/s	Ohashi relationship
	Axial dispersion coeffcient	D_L	2.17E-04	m2/s	D_L= u(m/s)/1.2/100 - Merkel et.al, 1997
	Pore Velocity	U	0.0131	m/s	u= Q/A/ε

Subramaniam (2010) estimated the Freundlich constants based on manganese uptake capacity experiments for pyrolucite media used in the NN pilot-plant. The full-scale combined influent from the NN water treatment plant was used in these experiments. The NN pyrolucite media had been used for several months and one might expect a considerable amount of MnO_x deposits on media surface. To model the LHWTP pilot-plant data, the Freundlich constants were interpolated from the NN results, as shown in Table 5-3.

Table 5-3. Freundlich isotherm constants for "used" pyrolucite media from NN pilot-plant (Subramaniam (2010))

pH	Temperature ranges	K (mg Mn/g media)	1/n
	°C	[(mol/kg)/(mol/m3)] $^{(1/n}$	
6.5	20-25	0.72	1.20
7.5	20-25	0.88	1.19

5.3 Sensitivity Analysis Using the UM-Model:

A sensitivity analysis was conducted to investigate the impacts of each model parameter on the model results. Each model parameter chosen in this analysis was increased and decreased from the baseline value presented in Table 5-2. A column depth of 20 inches was used.

Figure 5-8a show the dependence of the model results on specific surface area (Av) of filter media. Doubling the value of Av can result in a 0.015 mg/L decrease in the model effluent manganese. The independence of model output on D_L, presented in Figure

5-8b is expected since at the high HLR, the flow pattern in the second-stage media contactor is similar to plug-flow with relatively low amount of dispersion.

The impact of adsorption capacity on the NGE process is characterized through the Freundlich constants (K, n) (see Figure 5-8c and Figure 5-8d). For the Freundlich constant K, by doubling its baseline value (K = 0.88), the model effluent manganese concentration decreases from 0.03 mg/L to 0.015 mg/L. The impact of the Freundlich constant n is even more significant. At the value of 1/2.28, the model results show no manganese removal across the bed depth, i.e., the influent manganese concentration is equal to effluent manganese in this case due to very slow adsorption rate. The impact of the advection process on manganese removal is shown through the HLR in Figure 5-8e. An increase of HLR from 10 gpm/ft^2 to 20 gpm/ft^2 leads to an increase in the model effluent manganese from 0.03 mg/L to 0.08 mg/L.

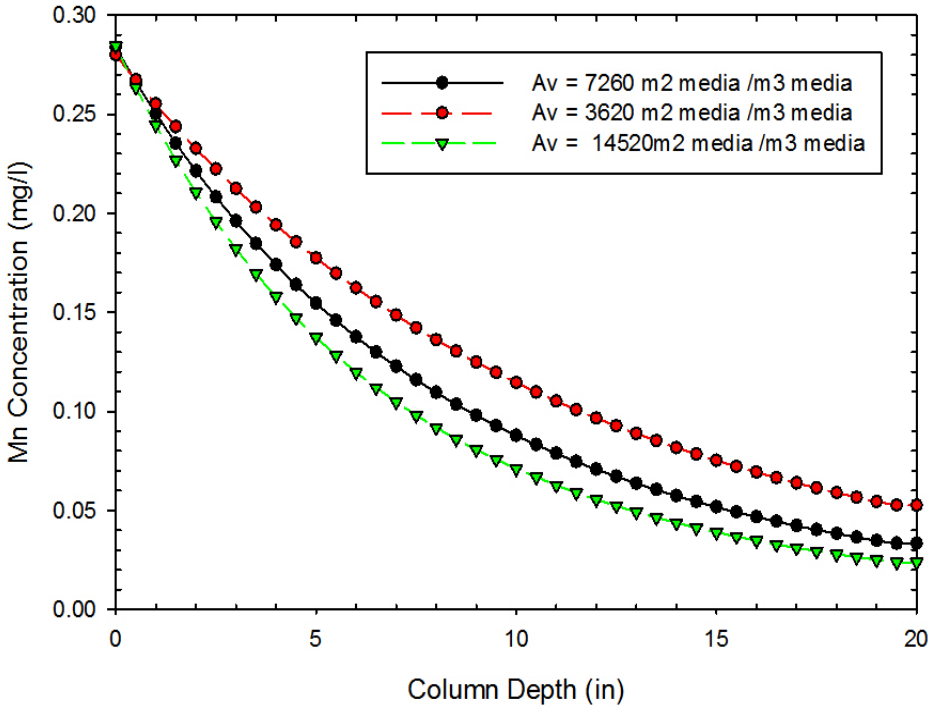

a)

Figure 5-8a. Impact of specific area: A_v

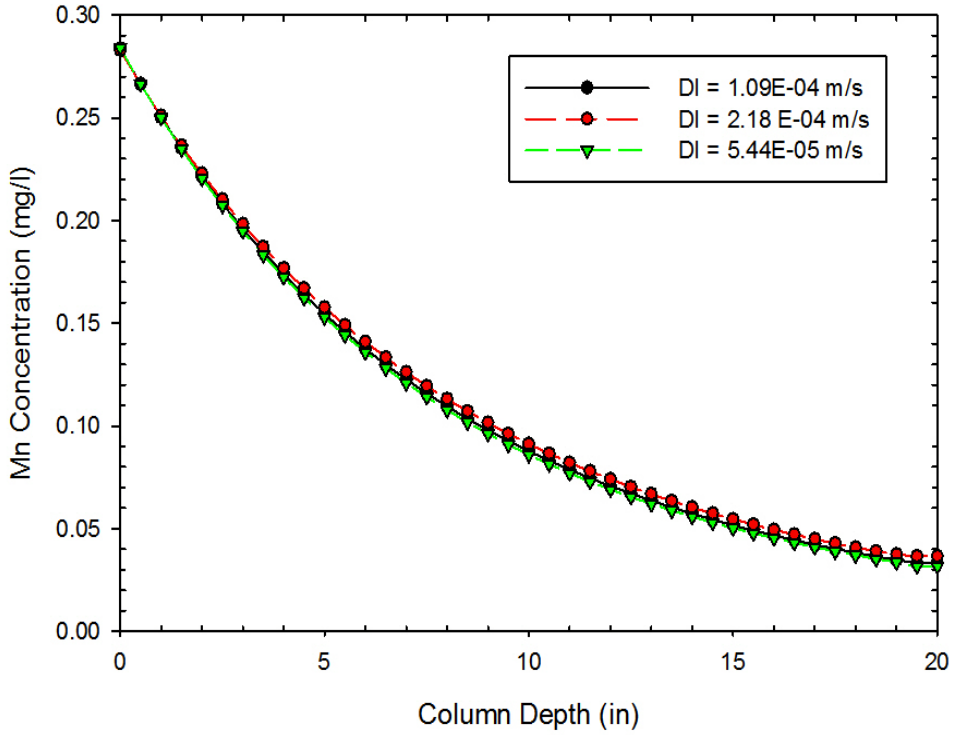

Figure 5-8b.Impact of D_L on model output.

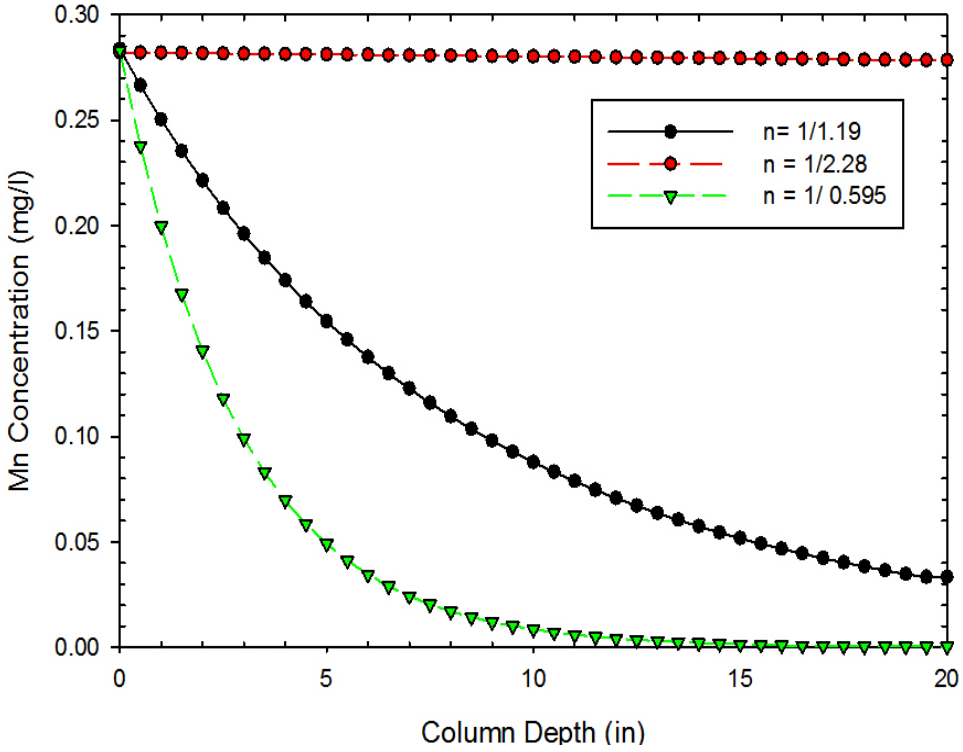

Figure 5-8c.Impact of Freundlich constants: n.

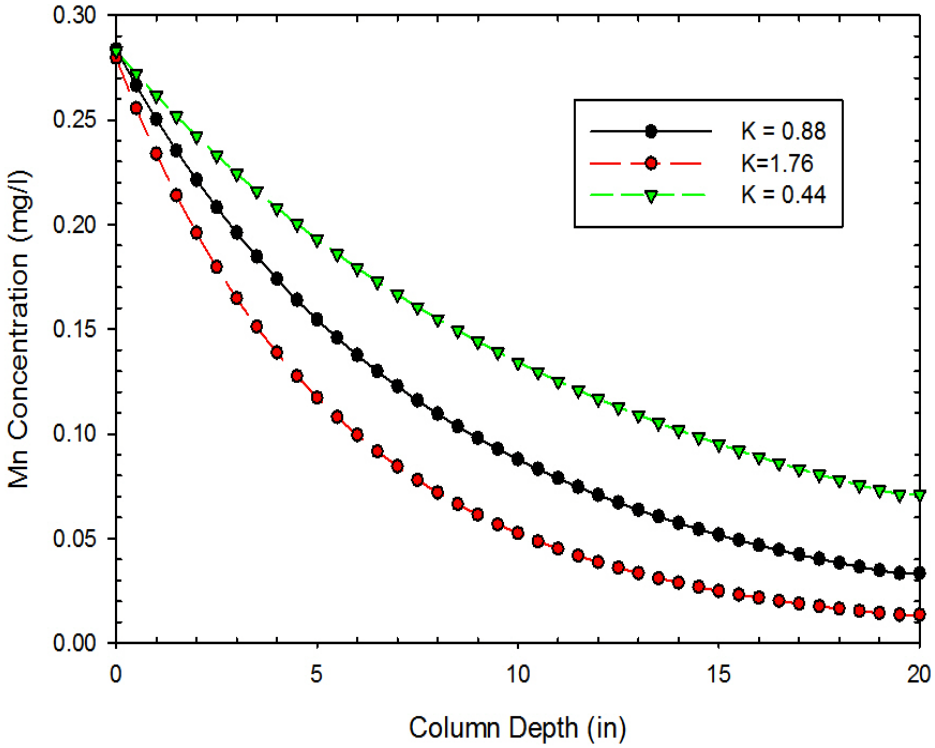

Figure 5-8d.Impact of Freundlich constants: K.

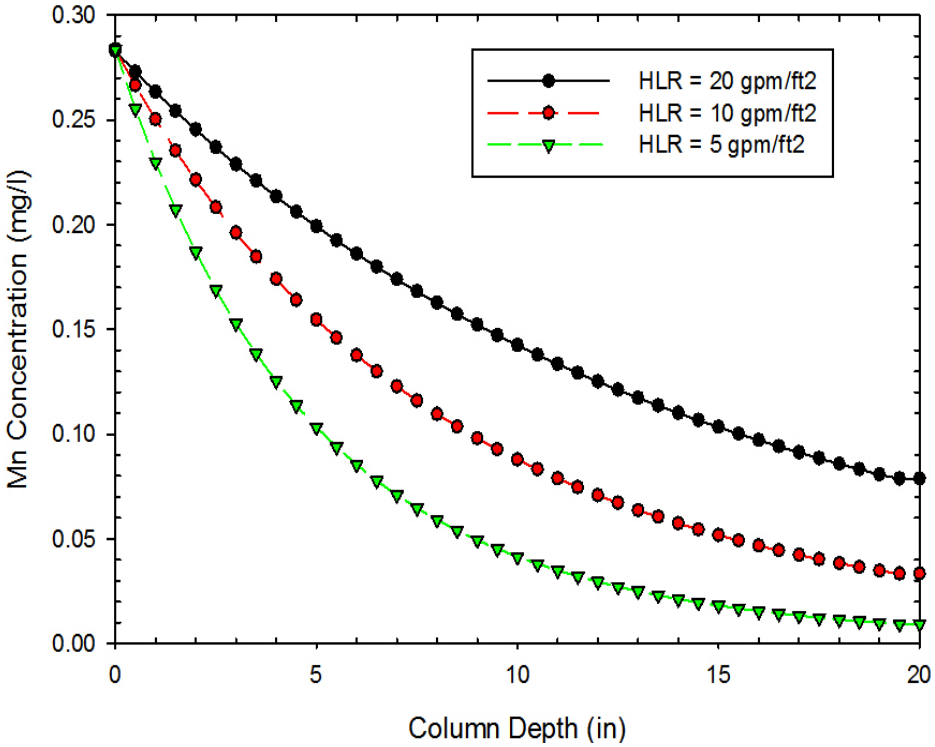

Figure 5-8e. Impact of HLR

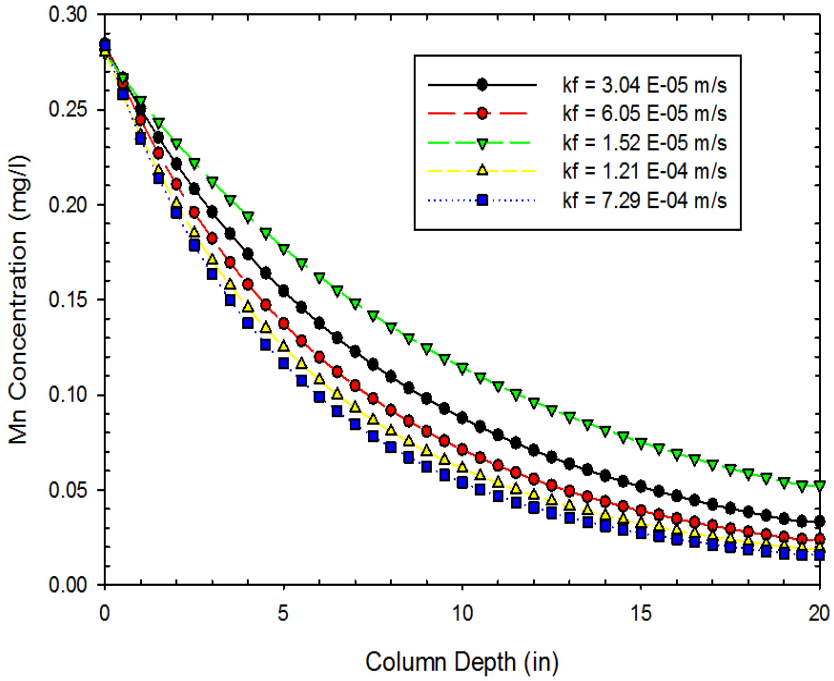

Figure 5-8f. . f) Impact of mass transfer coefficient: kf.

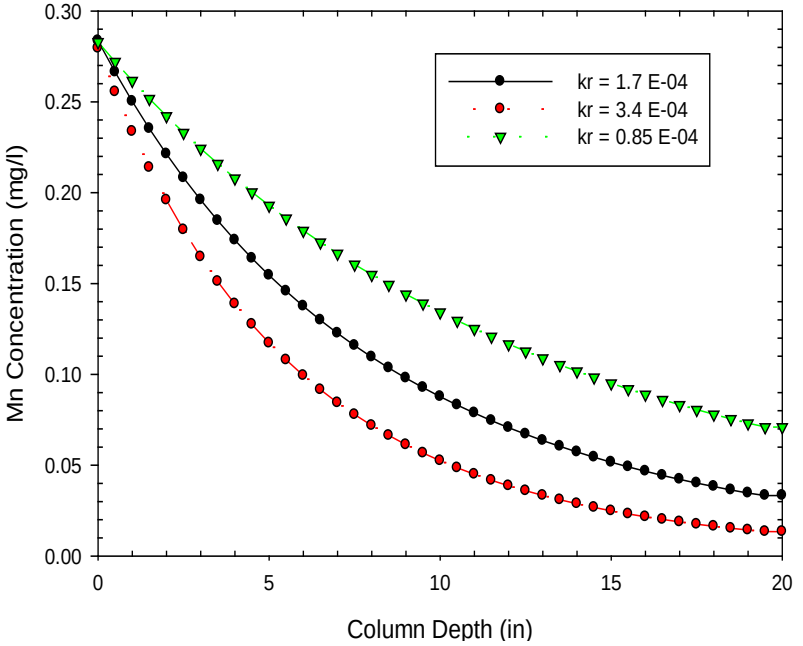

Figure 5-8g. Impact of surface oxidation rate: kr.

Figure 5-8. UM- model sensitivity analysis

The dependence of model results on k'_r and k_f show the important roles of the surface oxidation and mass transfer through film diffusion on manganese removal,

respectively (see Figure 5-8f and Figure 5-8g). These two processes have an interrelated relationship in which the slower process controls the rate of manganese removal. This notion is proven in Figure 5-8f where the value of k_f was increased. The results show that the model manganese profiles at k_f of $1.21x10^{-4}$ m/s and $7.29x10^{-4}$ m/s approximately overlap each other. It is understood that at k_f values of $1.00x10^{-4}$ or greater, surface oxidation controls the rate of the NGE process.

5.4 MODEL RESULTS FOR THE LHWTP SECOND-STAGE PILOT SYSTEM

Profiles of manganese concentration across the depth of the second-stage contactor were collected during LHWTP pilot experiments on 1/13/2010, 7/8/2010, 7/14/2010 and 7/15/2010. The HLR of the second-stage contactor was varied between 2, 5, 10, 15 and 20 gpm/ft^2, and pH of the second-stage contactor was in the range of 6.7-7.3. The objectives of these experiments were to: (1) assess the accuracy of the UM-model at different testing conditions, and (2) determine the best k'_r value to use for the LHWTP field conditions.

Field data and the UM-model results for the LH second-stage contactor manganese profiles at four different HLRs on 7/14/2010 are shown in Figure 5-9. A summary of model results for the 7/14/2010 pilot experiments is shown in Figure 5-10. Overall, the UM-model simulated the manganese versus depth profile well at different HLR with R^2 values in the range of 0.98-0.99. However, the model could not produce best fit k'_r values at HLR of 5 and 2 gpm/ft^2 when the manganese concentration at bed depth of 23 inch and 32 inch was included. This could be due to the mathematical

methods incorporated in the model to solve the mass balance equations (Equation 5-13 to Equation 5-16).

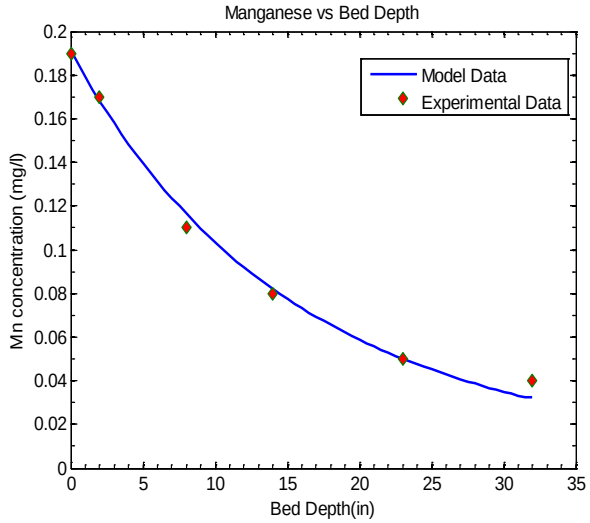

a) Testing condition: HLR = 20 gpm/ft^2, pH = 7. Free-chlorine = 1.3 mg/L.
Result: Fitted k'$_r$ = 1.80E-04 1/s, R^2 = 0.9885

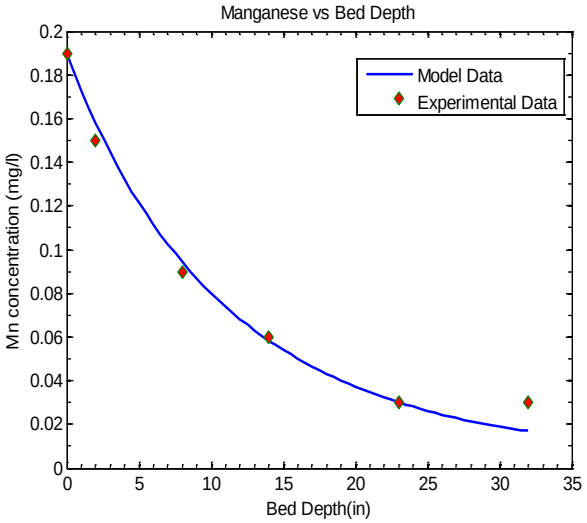

b) Testing condition: HLR = 10 gpm/ft^2, pH = 7. Free-chlorine = 1.3 mg/L
Result: Fitted k'$_r$ = 1.30E-04 1/s, R^2 = 0.9885

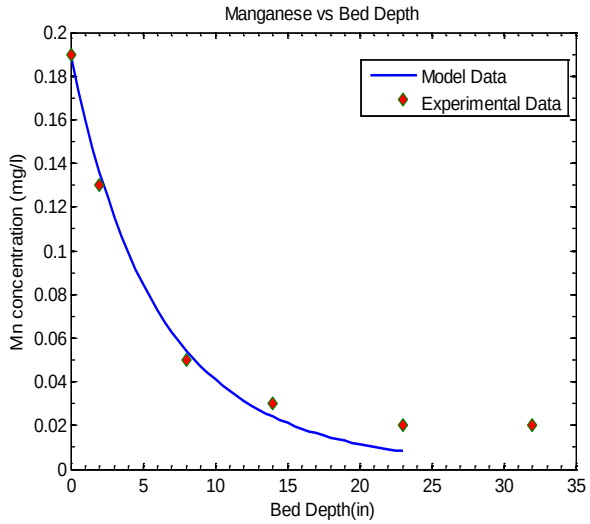

c) Testing condition: HLR =5 gpm/ft^2, pH = 7. Free-chlorine = 1.3 mg/L
Result: Fitted k'$_r$ = 1.40E-04 1/s, R^2 = 0.99

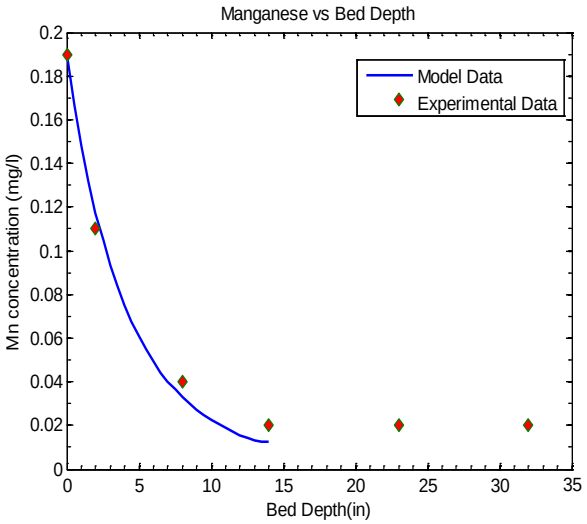

d) Testing condition: HLR = 2 gpm/ft^2, pH = 7. Free-chlorine = 1.3 mg/L
Result: Fitted k'$_r$ = 8.0E-05 1/s, R^2 = 0.98

Figure 5-9. The LHWTP second-stage contactor model results on 7/14/2010 field trip at different HLR.

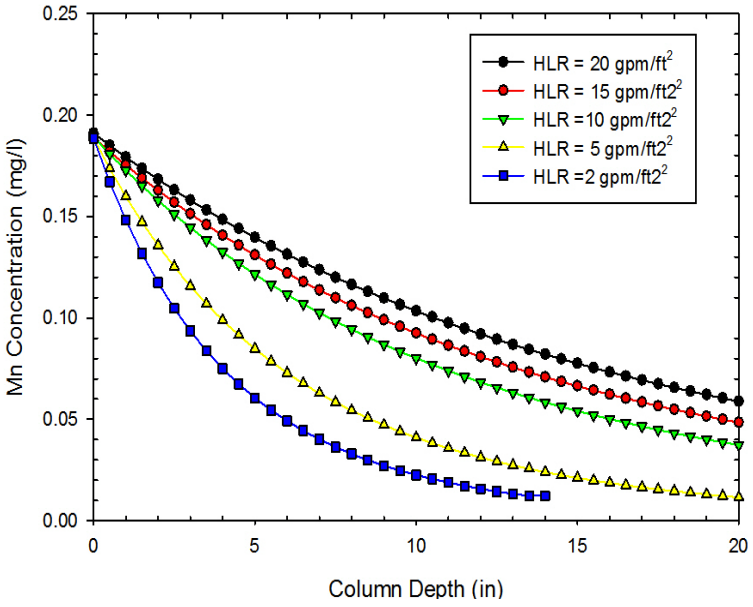

Figure 5-10. Summary of the UM-model results (Figure 5-9) for the LH second-stage contactor on 7/14/2010.

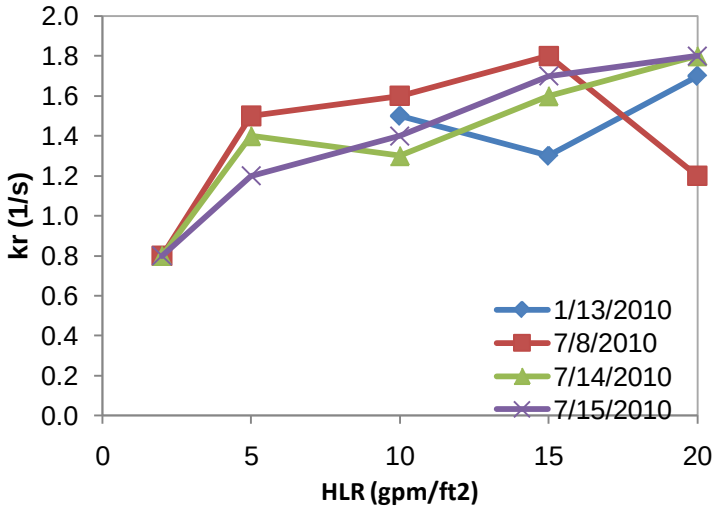

Figure 5-11. UM-model results for the LH second-stage contactor: calculated k'_r vs HLR

The best-fit k'_r values for several LH second-stage contactor profiles are plotted against HLR in Figure 5-11. The best-fitted k'_r varied in the relatively narrow range of 0.8×10^{-4}-1.8×10^{-4} with an average value of 1.4×10^{-4}. These model results are different from the NN pilot-plant results, presented in Figure 5-7a, in which k'_r varied in the range

of $2.9x10^{-4}$ to $5.5x10^{-4}$ with an average value of $4.32x10^{-4}$. The differences might be explained by differences in water quality, such as NOM, or iron, between the two pilot systems which were not fully accounted for in the UM-model. In addition, a tendency of increasing k'_r with increasing of HLR similar to NNWTP model results can be observed in Figure 5-11. Based on these results, the average k'_r value of $1.4x10^{-4}$ s^{-1} is recommended to use in designing operation parameters of the LH second-stage contactor.

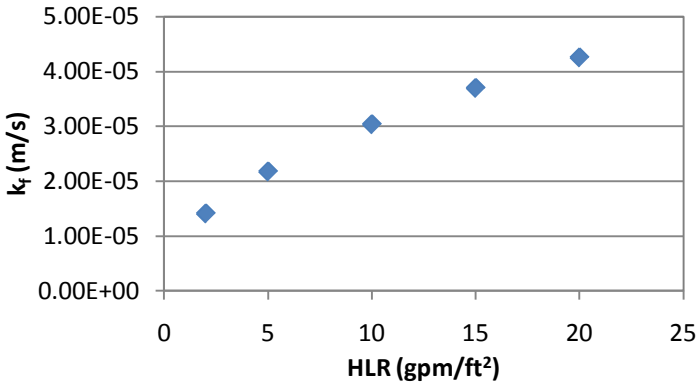

Figure 5-12. UM-model results for the LH second-stage contactor: calculated k_f vs HLR

Figure 5-12 presents calculated k_f at each HLR. As expected, k_f increases correspondingly to the increase of HLR, and ranges from $0.8x10^{-4}$ m s^{-1} to $4.3x10^{-4}$ m s^{-1}. Analysis showed that even at the low HLR of 2 gpm/ft^2, k'_r still controls the rate of manganese removal.

5.5 RECOMMENDATIONS FOR THE SECOND-STAGE CONTACTOR DESIGN AT THE LHWTP

The following design parameters are needed for the second-stage contactor upgrade at the LHWTP: HLR, media bed depth and media type. Based on the previous experimental data, two different designs for the LH upgrade are proposed as follows:

1. $KMnO_4$ dose and influent pH are optimized to convert all of the dissolved iron and part of the dissolved manganese to particulate forms which are removed in the first-stage filter. The second-stage contactor removes the remaining dissolved manganese.
2. $KMnO_4$ dose and influent pH are optimized to oxidize iron only; the dissolved manganese in the raw water is removed in the second-stage contactor.

In the first design, soluble manganese can be decreased to as low as 0.05 mg/L ahead of the second-stage contactor with a $KMnO_4$ dose of 1.25 times the stoichiometric dose and pH of 7.5. The benefits of this design are lower bed depth and higher HLR to achieve the manganese treatment goal, resulting in smaller footprint and less construction cost. However, the disadvantages are a higher $KMnO_4$ dose, resulting in higher O&M cost, and also adding more manganese into the treatment system. Moreover, effluent pH also needs to be readjusted to 7 before entering the distribution system.

Since iron oxidation was effective and rapid under all testing conditions presented in Table 4-1, the advantage of the second design is a lower $KMnO_4$ doses (~ 0.5 times the stoichiometric dose), lower NaOH doses, resulting in lower O&M cost. The risk of adding more manganese into the system is also attenuated. However, with a higher concentration of dissolved manganese (~0.18 mg/L) entering the second-stage column, a lower loading rate and deeper bed depth compared to the first scenario are required to achieve the manganese treatment goal, leading to higher capital cost.

The UM-model was used to evaluate design parameters for the second-stage contactor following the two scenarios. Table 5-4 presents the UM-model initial values.

Notice that dissolved manganese concentrations of the contactor influent are 0.08 mg/L and 0.20 mg/L representing worst-case scenario for the first and second design, respectively.

Table 5-4. The UM model initial values

Parameter	Scenario I	Scenario II
Mn concentration	0.08 mg/L	0.2 mg/L
Free Chlorine residual	1.05 mg/L	1.05 mg/L
pH	7.5	7
Media	Pyrolucite	Pyrolucite
k'_r	$1.4x10^{-4}$ s^{-1}	$1.4x10^{-4}$ s^{-1}

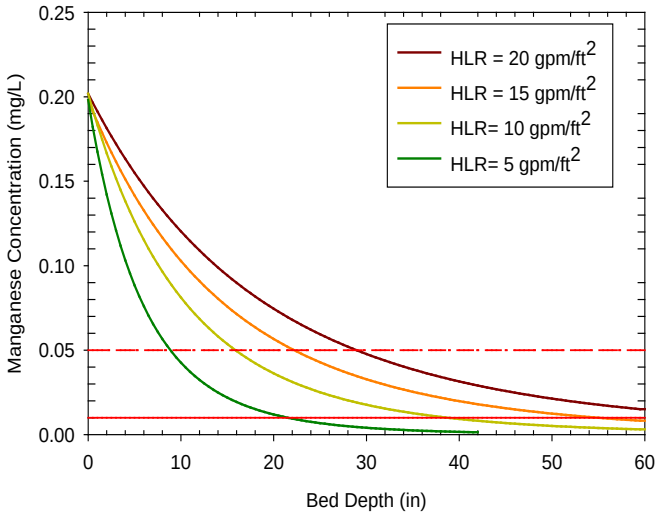

a)

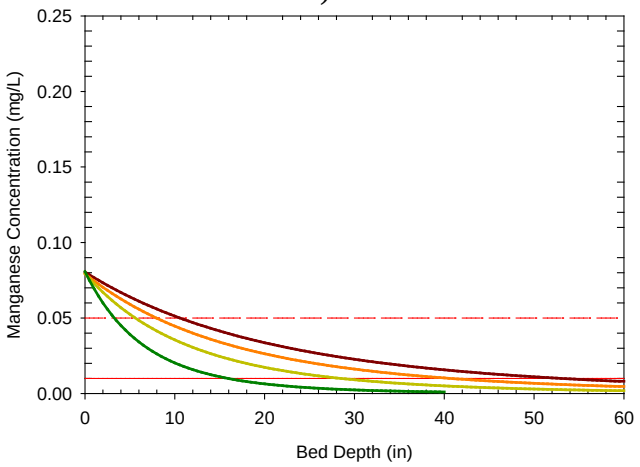

b)

Figure 5-13. UM-model prediction results at different influent dissolved manganese: a) $[Mn]_{inf}$ = 0.20 mg/L. b) $[Mn]_{inf}$ = 0.08 mg/L.

Figure 5-13 shows the predicted results from the UM-model for the two proposed designs. For the first design, with HLR of 20 gpm/ft^2, dissolved manganese starts to decrease below the SMCL level of 0.05 mg/L at a bed depth of 30 inches; however, it is unable to reach the treatment goal level of 0.01 mg/L even at a bed depth of 60 inches. At a HLR of 15 gpm/ft^2, the manganese treatment goal can be obtained at a bed depth of 56 inches. For HLR of 10 gpm/ft^2 and 5 gpm/ft^2, relatively low bed depths of 38 inch and 22 inches, respectively, are adequate to achieve the treatment goal.

For the second design, a similar pattern can be observed. At HLRs of 20 and 15 gpm/ft^2, the predicted results show that the second-stage contactor is unable to reduce manganese concentration to the treatment goal within 40 inches of pyrolucite media. However, at HLR of 10 gpm/ft^2 and 5 gpm/ft^2, the manganese treatment goal can be achieved at bed depth of 28 inch and 16 inch, respectively.

As mentioned in Chapter 2, the three parallel full-scale filters at the LHWTP have a design HLR of 3 gpm/ft^2. From a practical point of view, a second stage contactor, which has the same diameter as full-scale filters and is operated at HLR of 10 gpm/ft^2, is suitable for the LH upgrade. In this case, based on the UM-model results, the bed depths of 42 inches and 32 inches are recommended for the first and second scenario, respectively. These results can be used by AWC to conduct a cost analysis for each design and determine the best option for the LH upgrade.

CHAPTER 6: SUMMARY, CONCLUSIONS and RECOMMENDATIONS

This chapter presents a summary of this research conducted at the LHWTP, along with conclusions drawn from field experiments as well as model results. Finally, recommendations for the LHWTP upgrade and suggestions for future work are also discussed in this chapter.

6.1 Summary

The primary objective of this research was to conduct pilot-scale experiments to determine a possible treatment technology to simultaneously control both manganese and DBP production at the LHWTP. DBP and manganese samples were collected and compared between different treatment designs. In addition, recommended design parameters were also provided based on model results. A pilot treatment system comprised of two stages was installed and operated onsite at the LHWTP. Different designs, and chemical addition orders were tested. The effectiveness of each solution was evaluated based on manganese and DBP results along with other water quality parameters such as UV_{254}, turbidity, NOM and iron concentrations. An existing model which simulates manganese removal as a function of bed depth was modified and used for design calculations of the second-stage contactor. Based on model results, design parameters (HLR, bed depth) of the second-stage contactor were recommended

6.2 Conclusions

Based on the experimental results, the following conclusions can be drawn:

1. Without the NGE process, pre-filter oxidation with $KMnO_4$ followed by coagulation and dual-media filtration can remove approximately 70-83% of dissolved manganese and approximately 92-99% of dissolved iron in the raw water. At the optimum $KMnO_4$ dose of 1.25 times the stoichiometric dose and a pH of 7.5, the lowest manganese concentration in the dual media filter effluent was 0.05 mg/L. The results confirm that this process alone cannot decrease manganese concentration to the desired level of 0.01 mg/L.
2. With a pre-filter chlorine residual of 2 mg/L and OCM, the manganese concentration in filter effluent could be as low as 0.01 mg/L. However, similar to the full-scale plant, 24-hour HAA and THMs for the pilot effluent were approximately 131 µg/L and 116 µg/L, respectively (much higher than MCLs of 60 µg/L and 80 µg/L). A different approach to simultaneously control manganese and DBPs was needed.
3. Use of a second-stage contactor with chlorine addition after the DM filter effectively removes manganese under high HLR via the NGE process. At a HLR of 20 gpm/ft^2 and an influent manganese of 0.16 mg/L, manganese concentrations in the second-stage contactor could be as low as 0.02 mg/L.
4. By removing 1 mg/L of NOM in the DM filter ahead of chlorine addition, DBP concentrations were decreased approximately 80% compared to full-

scale DBP concentrations, and well below the MCL levels. These results, in conjunction with manganese removal results, prove that the two-stage filtration is an appropriate technology for the LHWTP.

5. With R^2 square values in the range of 0.98 to 0.99, the UM-model was able to simulate manganese removal as a function of bed depth along the second-stage contactor. The value of the fitting parameter (k'_r, surface oxidation rate constant) varied in the relatively narrow range of 0.8×10^{-4} ms^{-1} to 1.8×10^{-4} ms^{-1}. An average k'_r value of 1.4×10^{-4} ms^{-1} was used to predict manganese concentration at different bed depths and HLRs.
6. Two different two-stage filtration designs were considered for the LHWTP upgrade. In the first design, $KMnO_4$ dose and influent pH are optimized to convert all of the dissolved iron and part of manganese to particulate forms which are removed in the first-stage filter. In the second design, the $KMnO_4$ dose and influent pH are optimized to oxidize iron only; dissolved manganese of the raw water is treated in the second-stage contactor. Based on the UM-model results, for a HLR of 10 gpm/ft^2, the required bed depths for the first and second designs to achieve the manganese treatment goal of 0.01 mg/L are 42 and 32 inches, respectively. These data could be used to conduct cost analysis and determine the best design for the two-stage filtration system at the LHWTP.

6.3 Recommendations

Research on types of media with lower density for the second-stage contactor should be conducted. If successful, it can result in a lower back wash flow rate, i.e. lower O&M cost. In addition, to reduce the O&M cost, the AWC should also consider using a very low free chlorine dose (less than 2 mg/L) to oxidize dissolved iron only rather than using permanganate which is more expensive. This setup also requires less piping and easier for operators to control since the LHWTP already use free-chlorine as a disinfectant. The disadvantage of adding free chlorine upstream would be higher DBP production, but with such low free chlorine dose, it may be possible for the AWC to satisfy the Stage 1and 2 D/DBPR.

REFERENCES

Agency for Toxic Substances and Disease Registry, 2008. *Toxicological Profile for Manganese* Draft for public comments.,

Benjamin, M.M., 2010. *Water Chemistry* 1st ed., Waveland Pr Inc.

Coffey, B.M., Gallagher, D.L. & Knocke, W.R., 1993. Modeling Soluble Manganese Removal by Oxide-Coated Filter Media. *Journal of Environmental Engineering*, 119(4), 679-694.

David Reckhow, 2006. Analysis of Haloacetic Acids. Lab Manual. University of Massachusetts, Amherst.

Gabelich, C.J. et al., 2006. Sequential manganese desorption and sequestration in anthracite coal and silica sand filter media. *Journal of American Water Works Association*, 98(5), 116-127+12.

Griffin, A., 1960. Significance and Removal of Manganese in Water Supplies. *Journal of American Water Works Association*, (52), 1326-1334.

Hargette, A.C. & Knocke, W.R., 2001. Assessment of Fate of Manganese in Oxide-Coated Filtration Systems. *Journal of Environmental Engineering*, 127(12), 1132-1138.

Islam, A.A., 2010. Manganese Removal By Media Filtration: Release and Complexation. Unpublished PhD Dissertation. University of Massachusetts, Amherst.

Jodellah, A. & Weber Jr., W., 1985. Controlling trihalomethane formation potential by chemical treatment and adsorption. *Journal / American Water Works Association*, 77(10), 95-100.

Knocke, W. et al., 2010. Adsorptive contactors for removal of soluble manganese during drinking water treatment. *Journal American Water Works Association*, 64.

Knocke, W.R., 1990. *Alternative Oxidants for the Removal of Soluble Iron and Manganese*, American Water Works Association.

Knocke, W.R., Hamon, J.R. & Thompson, C.P., 1988. Soluble manganese removal on oxide-coated filter media. *Journal American Water Works Association*, 80(12), 65-70.

Knocke, W.R., Occiano, S.C. & Hungate, R., 1991. Removal of soluble manganese by oxide-coated filter media. Sorption rate and removal mechanism issues. *Journal / American Water Works Association*, 83(8), 64-69.

Kohl, P.M. & Medlar, S.J., 2006. *Occurrence of Manganese in Drinking Water and Manganese Control*, AWWA Reasearch Foundation.

Long, B.W., Hulsey, R.A. & Hoehn, R.C., 1999. Complementary uses of chlorine dioxide and ozone for drinking water treatment. *Ozone: Science and Engineering*, 21(5), 465-476.

Merkle, P.B. et al., 1997. Dynamic Model for Soluble Mn[2+] Removal by Oxide-Coated Filter Media. *Journal of Environmental Engineering*, 123(7), 650-658.

Morgan, J.J. & Stumm, W., 1964. Colloid-chemical properties of manganese dioxide. *Journal of Colloid Science*, 19(4), 347-359.

Morris, R.D. et al., 1992. Chlorination, chlorination by-products, and cancer: a meta-analysis. *American Journal of Public Health*, 82(7), 955-963.

Reckhow, D.A. & Singer, P.C., 1986. Mechanisms Of Organic Halide Formation During Fulvic Acid Chlorination And Implications With Respect To Preozonation. In *Water Chlorination: Chemistry, Environmental Impact and Health Effects, Proceedings of the Fifth Conference.* Water Chlorination: Environmental Impact and Health Effects. Williamsburg, VA, USA: Lewis Publ Inc, pp. 1229-1257.

Roberts, P.V., Cornel, P. & Summers, R.S., 1985. External Mass-Transfer Rate in Fixed-Bed Adsorption. *Journal of Environmental Engineering*, 111(6), 891-905.

Russell, J., 2008. *Control of Manganese, Iron, and Disinfection By-Products for the Mystic Connecticut Water System*. Unpublished MS report. University of Massachusetts ,Amherst.

Sly, L.I., Hodgkinson, M.C. & Arunpairojana, V., 1990. Deposition of manganese in a drinking water distribution system. *Applied and Environmental Microbiology*, 56(3), 628-639.

Subramaniam, A., 2010. *A Pilot-scale Evaluation of Soluble Manganese Removal Using Pyrolucite Media in a High-Rate Adsorptive Contactor*. Unpublished MS report. Virginia Tech University.

Tobiason, J. et al., 2008. Characterization and Performance of Filter Media for Manganese Control. *American Water Works Association Research Foundation*.

U.S. Environmental Protection Agency, 2004. *Drinking Water Health Advisory for Manganese*,

US EPA, 2006. *Federal Register*.

US EPA, 2001. Stage 1 Disinfectants and Disinfection Byproducts Rule: A Quick

Reference Guide.

Xie, Y.F., 2004. *Disinfection byproducts in drinking water: formation, analysis, and control*, CRC Press.

Zuravnsky, L., 2006. *Development of Soluble Manganese Sorptive Contactors for Enhancing Potable Water Treatment Practices*. Unpublished MS report. Virginia Tech University.

APPENDIX

Table 1. Experimental and model data on 01/13/2010

Date	HLR	pH	Chlorine In	Analytical Method	Depth (in)							kf	k'r.10^{-4}	Rsquare
					0	3	6	9	15	20	42			
	(gpm/ft^2)		(mg/L)		(mg/L)	(mg/L)	(mg/L)	(mg/L)	(mg/L)	(mg/L)	(mg/L)	m/s	1/s	--
01/13/10	10	7.3	1.1	ICP-MS	0.240	0.175	0.130	0.090	0.052	0.029		3.04E-05	1.5	0.985
	15	7.3	1.1	ICP-MS	0.250	0.197	0.167	0.138	0.080	0.058		3.70E-05	1.3	0.995
	20	7.3	1.1	ICP-MS	0.282	0.228	0.191	0.160	0.105	0.071		4.26E-05	1.7	0.987

Table 2. Experimental and model data on 07/08/2010

Date	HLR	pH	Chlorine In	Analytical Method	Depth (in)							kf	k'r.10-4	Rsquare
	(gpm/ft^2)		(mg/L)		0	4	10	16	25	34	42	m/s	1/s	---
7/8/2010	20	6.7	1.33	HACH	0.16	0.13	0.10	0.07	0.05	0.03		4.26E-05	1.2	0.997
	15	6.7	1.33	HACH	0.16	0.12	0.08	0.05	0.03	0.02		3.70E-05	1.8	0.9983
	10	6.7	1.33	HACH	0.16	0.110	0.070	0.030	0.020	0.020		3.04E-05	1.6	0.9878
	5	6.7	1.33	HACH	0.16	0.08	0.04	0.02	0.01	0.01		2.17E-05	1.5	0.9940
	2	6.7	1.33	HACH	0.16	0.06	0.03	0.01	0.01	0.01		1.41E-05	0.8	0.9908

Table 3. Experimental and model data on 7/14/2010

Date	HLR	pH	Chlorine In	Analytical Method	Depth (in)							kf	k'r.10-4	Rsquare
					0	2	8	14	23	32	40			
	(gpm/ft^2)		(mg/L)		(mg/L)	(mg/L)	(mg/L)	(mg/L)	(mg/L)	(mg/L)	(mg/L)	**m/s**	1/s	--
7/14/2010	20	7	1.33	HACH	0.19	0.17	0.11	0.08	0.05	0.04		4.26E-05	1.8	0.996
	15	7	1.33	HACH	0.19	0.16	0.10	0.07	0.04	0.03		3.70E-05	1.6	.9965
	10	7	1.33	HACH	0.19	0.15	0.09	0.06	0.03	0.03		3.04E-05	1.3	0.9885
	5	7	1.33	HACH	0.19	0.13	0.05	0.03	0.02	0.02		2.17E-05	1.4	0.9900
	2	7	1.33	HACH	0.19	0.11	0.04	0.02	0.02	0.02		1.41E-05	0.8	0.9907

Table 4 Experimental and model data on 07/15/2010

Date	**HLR**	**pH**	**Chlorine In**	Analytical Method	Depth (in)							kf	k'r.10-4	Rsquare
					0	2	8	14	23	32	**40**			
	(gpm/ft^2)		**(mg/L)**		**(mg/L)**	**(mg/L)**	**(mg/L)**	**(mg/L)**	**(mg/L)**	**(mg/L)**	**(mg/L)**	**m/s**	1/s	--
7/15/2010	20	7	1.33	HACH	0.18	0.14	0.11	0.08	0.05	0.03	0.02	4.26E-05	1.8	0.9919
	15	7	1.33	HACH	0.18	0.15	0.10	0.06	0.04	0.03	0.02	3.70E-05	1.7	0.9902
	10	7	1.33	HACH	0.18	0.15	0.09	0.05	0.03	0.02	0.02	3.04E-05	1.4	0.9973
	5	7	1.33	HACH	0.18	0.13	0.06	0.03	0.01	0.01	0.01	2.17E-05	1.2	0.9997
	2	7	1.33	HACH	0.18	0.10	0.03	0.02	0.02	0.02	0.02	1.41E-05	0.8	0.9926